LOCKHEED MARTIN ENERGY RESEARCH LIBRARIES
3 4456 0514430 4

CENTRAL RESEARCH LIBRARY
DOCUMENT COLLECTION

OAK RIDGE NATIONAL LABORATORY
operated by
UNION CARBIDE CORPORATION
NUCLEAR DIVISION
for the
U.S. ATOMIC ENERGY COMMISSION

ORNL-TM-3519

cy .33

DATE - Sept. 3, 1971

Neutron Physics Division

Calculated Perturbations in Threshold Foil Measurements Due to Neutron Interactions in B_4C Shells

W. E. Ford, III,* and J. S. Gillen*

Abstract

Calculations were made to determine expected perturbation effects to the measured neutron flux in B_4C shielded threshold foils resulting from neutron interactions in the B_4C. Results indicated that there is a significant increase in the measured flux below the source energy of monoenergetic neutron beams due to scattering.

The activities in a series of threshold foils encased within a B_4C shell were calculated for exposure of the shell to monoenergetic 13.57- and 1.01-MeV neutron beams incident at 0° with respect to the shell axis. Calculations were also made to determine if there would be a significant change in the measured threshold foil activities if the detector were inadvertently positioned "upside down" (beam incident at 180°) during an experiment. The difference between the 0° and 180° activities was not sufficient to distinguish which end of the detector was oriented toward the beam.

*Mathematics Division.

OAK RIDGE NATIONAL LABORATORY
CENTRAL RESEARCH LIBRARY
DOCUMENT COLLECTION
LIBRARY LOAN COPY
DO NOT TRANSFER TO ANOTHER PERSON
If you wish someone else to see this document, send in name with document and the library will arrange a loan.
UCN-7969
(3 3-67)

NOTICE This document contains information of a preliminary nature and was prepared primarily for internal use at the Oak Ridge National Laboratory. It is subject to revision or correction and therefore does not represent a final report.

This report was prepared as an account of work sponsored by the United States Government. Neither the United States nor the United States Atomic Energy Commission, nor any of their employees, nor any of their contractors, subcontractors, or their employees, makes any warranty, express or implied, or assumes any legal liability or responsibility for the accuracy, completeness or usefulness of any information, apparatus, product or process disclosed, or represents that its use would not infringe privately owned rights.

ACKNOWLEDGEMENTS

The authors wish to express appreciation to L. R. Williams who performed the GAM-II calculation and to J. H. McNeilly of the Army Nuclear Defense Laboratory at Edgewood Arsenal, Maryland, F. R. Mynatt, R. M. Freestone, Jr., and C. E. Clifford who provided counsel during the course of the study. Virginia Glidewell typed the rough draft and final report.

LOCKHEED MARTIN ENERGY RESEARCH LIBRARIES

3 4456 0514430 4

TABLE OF CONTENTS

Page

ABSTRACT

I. INTRODUCTION 1

II. CALCULATIONS 7

III. RESULTS AND CONCLUSIONS 13

REFERENCES 63

LIST OF FIGURES

Figure		Page
1.	Standard B_4C Shell	2
2.	Miniature B_4C Shell	3
3.	Activation Foil Configuration within the Standard B_4C Shell	4
4.	Total Flux in Standard Shell "Detector" due to 13.57 MeV Beam at 0°	22
5.	Total Flux in Standard Shell "Detector" due to 11.11 MeV Beam at 0°	23
6.	Total Flux in Standard Shell "Detector" due to 9.09 MeV Beam at 0°	24
7.	Total Flux in Standard Shell "Detector" due to 7.45 MeV Beam at 0°	25
8.	Total Flux in Standard Shell "Detector" due to 6.10 MeV Beam at 0°	26
9.	Total Flux in Standard Shell "Detector" due to 4.09 MeV Beam at 0°	27
10.	Total Flux in Standard Shell "Detector" due to 1.84 MeV Beam at 0°	28
11.	Total Flux in Standard Shell "Detector" due to 1.01 MeV Beam at 0°	29
12.	Total Flux in Standard Shell "Detector" due to 0.55 MeV Beam at 0°	30
13.	Total Flux in Standard Shell "Detector" due to 13.57 MeV Beam at 45° and 90°	31
14.	Total Flux in Standard Shell "Detector" due to 11.11 MeV Beam at 45° and 90°	32
15.	Total Flux in Standard Shell "Detector" due to 9.09 MeV Beam at 45° and 90°	33
16.	Total Flux in Standard Shell "Detector" due to 4.09 MeV Beam at 45° and 90°	34
17.	Total Flux in Standard Shell "Detector" due to 1.84 MeV Beam at 45° and 90°	35

Figure Page

18. Total Flux in Standard Shell "Detector" due to 1.01 MeV Beam at 45° and 90° 36
19. Total Flux in Standard Shell "Detector" due to 0.55 MeV Beam at 45° and 90° 37
20. Total Flux in Miniature Shell "Detector" due to 13.57 MeV Beam at 0° 40
21. Total Flux in Miniature Shell "Detector" due to 1.01 MeV Beam at 0° 41
22. Fission Activity in ^{235}U Foil due to 13.57 MeV Beam 51
23. Fission Activity in ^{239}Pu Foil due to 13.57 MeV Beam 52
24. Fission Activity in ^{237}Np Foil due to 13.57 MeV Beam 53
25. Fission Activity in ^{238}U Foil due to 13.57 MeV Beam 54
26. (n,p) Activity in S Foil due to 13.57 MeV Beam 55
27. (n,p) Activity in Mg Foil due to 13.57 MeV Beam 56
28. (n,α) Activity in Aℓ Foil due to 13.57 MeV Beam 57
29. (n,2n') Activity in Zr Foil due to 13.57 MeV Beam 58
30. Fission Activity in ^{235}U Foil due to 1.01 MeV Beam 59
31. Fission Activity in ^{239}Pu Foil due to 1.01 MeV Beam 60
32. Fission Activity in ^{237}Np Foil due to 1.01 MeV Beam 61
33. Fission Activity in ^{238}U Foil due to 1.01 MeV Beam 62

LIST OF TABLES

Table		Page
I.	Composition of the Standard and Miniature Shells	6
II.	Characteristics of the Activation Foils and Cladding Materials	8
III.	Neutron-Energy-Group Structure	9
IV.	Activity Cross Sections for the Threshold Foils	10
V.	Total Flux in the "Detector" within the Standard B_4C Shell for Monoenergetic Beams Incident at 0°	14
VI.	Total Flux in the "Detector" within the Standard B_4C Shell for Monoenergetic Beams Incident at 45°	16
VII.	Total Flux in the "Detector" within the Standard B_4C Shell for Monoenergetic Beams Incident at 90°	18
VIII.	Total Flux in the Unshielded (Void in B_4C Zone) Standard Detector for Monoenergetic Beams Incident at 0°	20
IX.	Total Flux in the "Detector" within the Miniature B_4C Shell for the 13.57 and 1.01 MeV Beams Incident at 0°	39
X.	Activities in the Threshold Foils for 13.57 MeV Beam Incident at 0°	43
XI.	Activities in the Threshold Foils for 13.57 MeV Beam Incident at 180°	45
XII.	Activities in the Threshold Foils for 1.01 MeV Beam Incident at 0°	47
XIII.	Activities in the Threshold Foils for 1.01 MeV Beam Incident at 180°	49

I. Introduction

Boron carbide shielded threshold foil detectors are frequently used for measuring the intermediate and fast-neutron flux in a neutron environment. Since various materials exhibit characteristic neutron-induced reactions above some threshold energy, the disintegration of the resultant radioactive product of the reactions can be measured and related to the intensity and energy spectrum of the neutron environment -- hence the terminology "threshold foils." Boron carbide is used as a shield for threshold foils because the low-neutron-energy absorption cross section of the ^{10}B isotope minimizes the thermal and epithermal components of the neutron flux seen by the foils and thus eliminates undesired low-energy neutron reactions in the foils.* It is known that perturbations are introduced in the measured energy spectrum as a result of scattering and absorption of neutrons in the boron carbide. Simple mathematical expressions using uncollided and single-collision approximations to correct for the perturbations are given in the literature.[1] These approximations are adequate for routine measurements; however, for a precise threshold foil analysis, detailed perturbation corrections are necessary.

Using the Monte Carlo techniques of the O5R neutron transport code, Freestone studied the transport of neutrons through a nearly spherical $^{10}B_4C$ shell.[2] These calculations were made for exposure of the shell to isotropic monoenergetic neutrons, an isotropic fission spectrum source, and a 4-MeV normal beam source. Subsequent to the publication of the afore-mentioned work, considerable interest has evolved in (1) the perturbation effects in threshold foil measurements made with the B_4C shells shown in Figs. 1 and 2, and (2) the activity in the threshold foils shown in Fig. 3 resulting from exposure of the shielded foils to neutron spectra. Hereinafter the larger shell, shown in Fig. 1, is identified as the standard shell and the smaller shell, shown in Fig. 2, is identified as the miniature shell. These shells are currently being used by the Army Nuclear Defense Laboratory for neutron measurements.

*The technique of neutron-flux measurement using threshold foil detectors is described in ref. 1 and many other nuclear engineering texts.

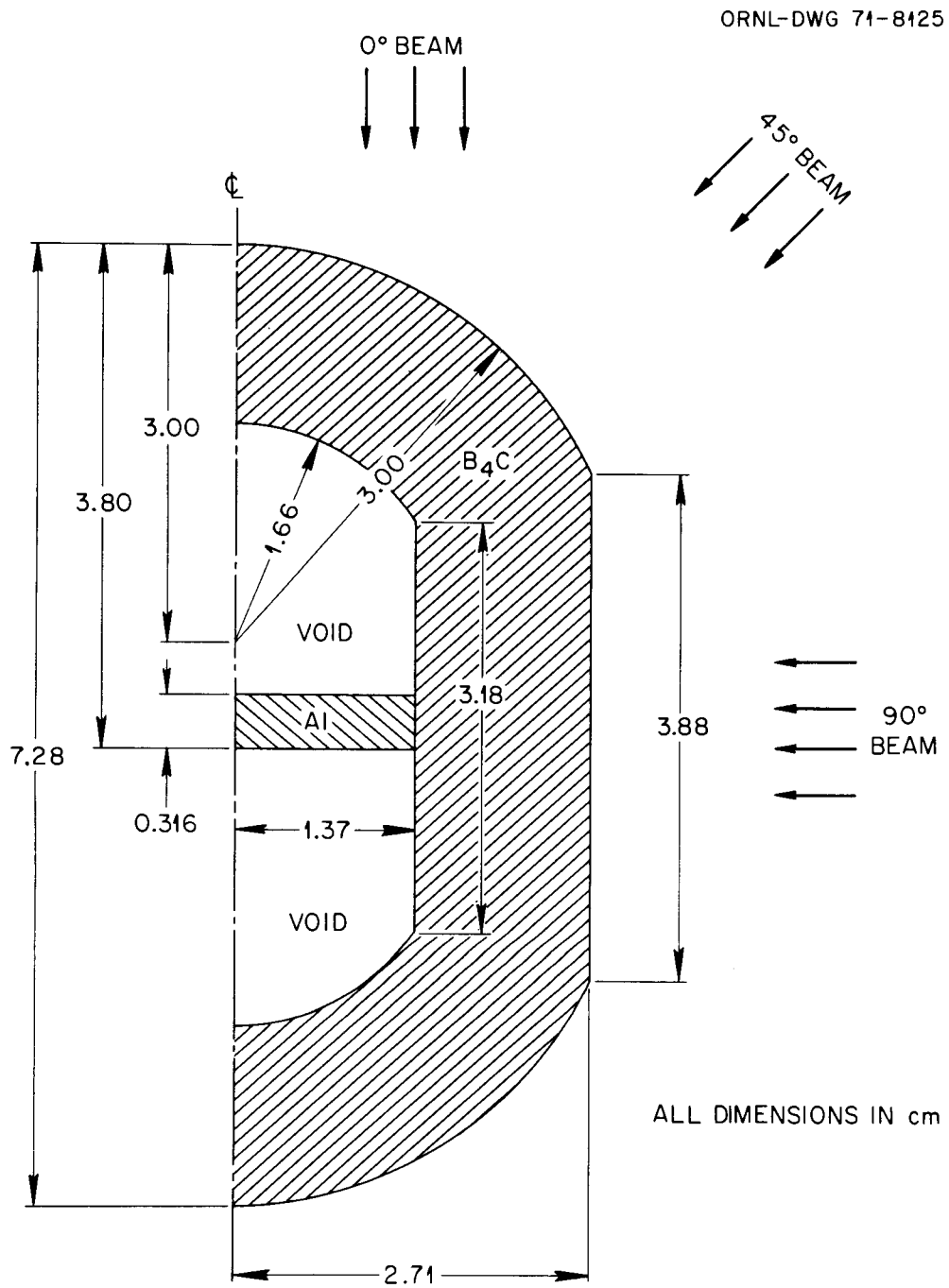

Figure 1. Standard B_4C Shell

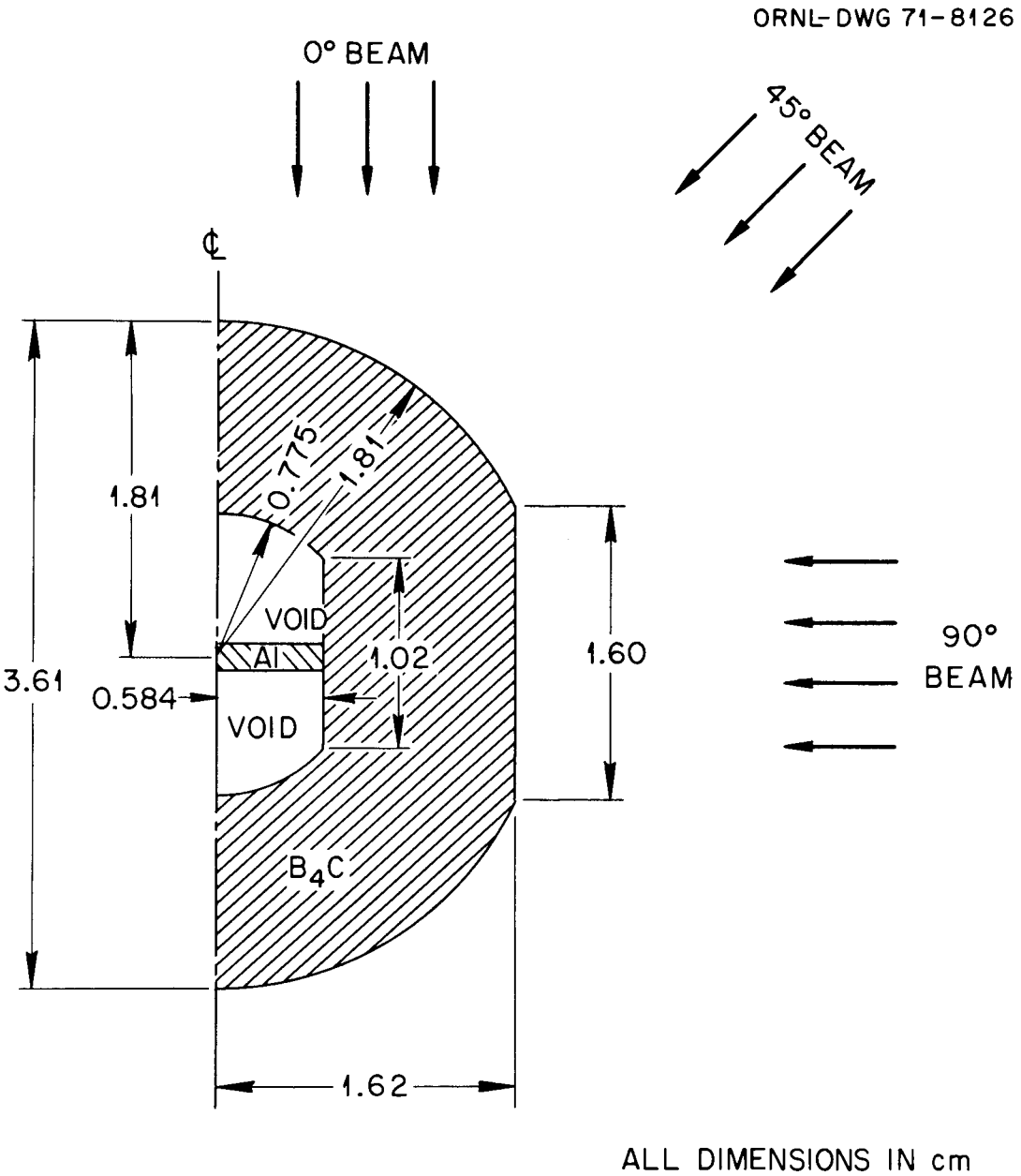

Figure 2. Miniature B_4C Shell

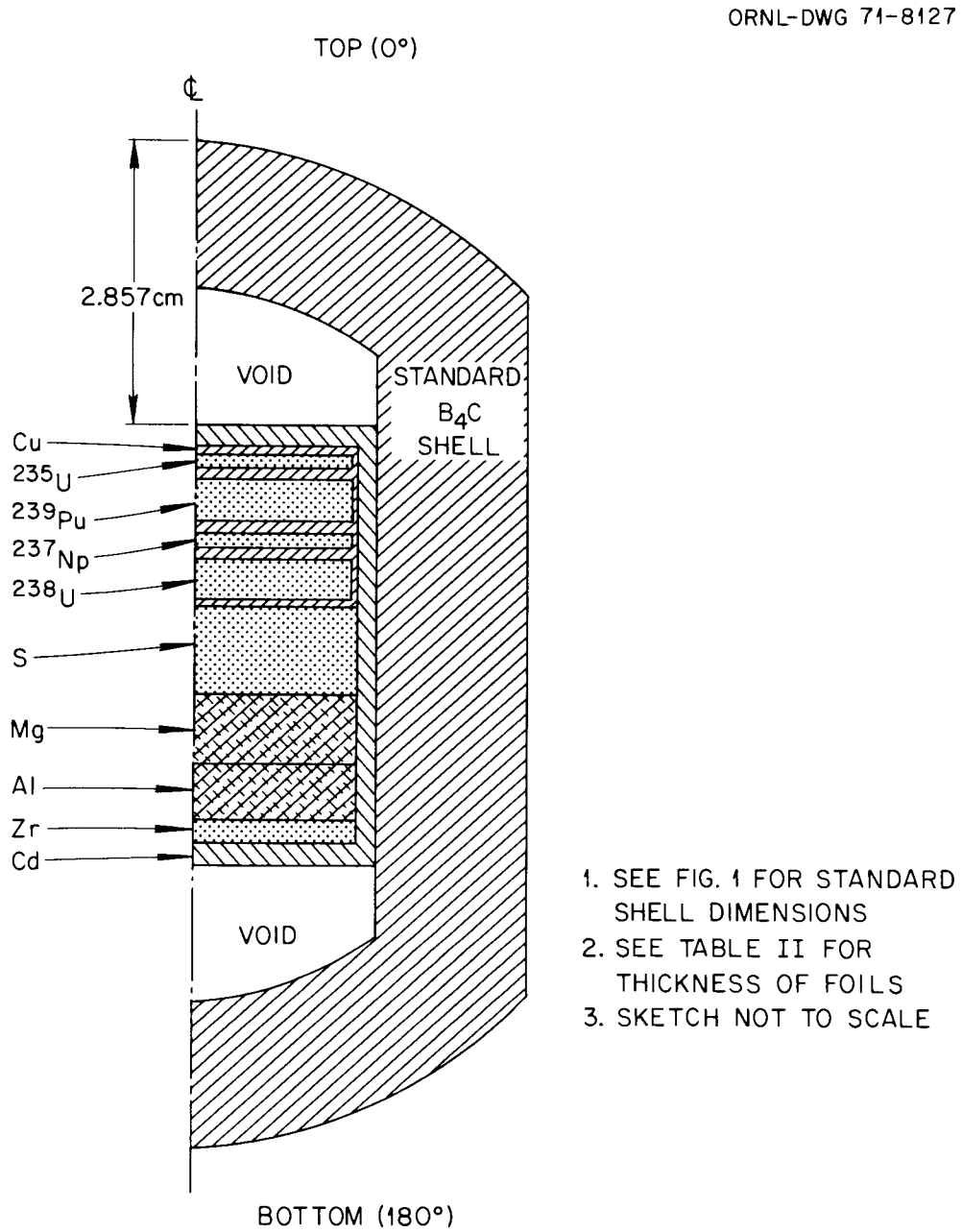

Figure 3. Activation Foil Configuration within the Standard B_4C Shell

The objectives of this study were threefold. First, the expected perturbations induced in neutron energy spectra due to neutron interactions in the B_4C shells were determined by calculating the scalar flux in a simulated series of foils resulting from exposure of the shells to monoenergetic neutron beams and comparing the results with the calculated flux in unshielded foils. Second, the activities in the series of threshold foils shown in Fig. 3 were calculated for exposure of the shielded foils to monoenergetic neutron beams. Due to the symmetric shape of the shells, it is possible to inadvertently place the axis of the detectors 180° out of position during a measurement. Therefore, the third objective was to calculate foil activities resulting from exposure of the detector to monoenergetic neutron beams with the detector in the two possible axial positions in order to determine if it would be possible to distinguish "which end was up" in a neutron flux measurement by comparing the relative value of the foil activities. All transport calculations were made with the two-dimensional discrete ordinates transport code DOT.[3]

For the first objective, threshold foils were simulated by a 0.316-cm-thick aluminum disk (the "detector") located at the midpoint of the axis of each shell. An aluminum density of 2.699 gm/cm^3 was assumed for the "detector." Densities and weight percents of the nuclides in the boron carbide are listed in Table I. The scalar flux in the "detector," shielded with the standard shell, was calculated for exposure of the shell to monoenergetic 13.57-, 11.11-. 9.09-, 7.45-, 6.10-, 4.09-, 1.84-, 1.01-, and 0.55-MeV neutron beams incident at 0° with respect to the shell axis. (Since DOT is a multigroup code, the above energies are midpoint energies of neutron groups.) Flux calculations were also made for the 13.57-, 11.11-, 9.09-, 4.09-, 1.84-, 1.01-, and 0.55-MeV beams incident at 45° and 90°. The scalar flux in the "detector," shielded with the miniature shell, was calculated for exposure of the shell to the 13.57- and 1.01-MeV beams at 0°. For comparison, the flux resulting from exposure of the unshielded (vacuum in B_4C region) "detectors" to the neutron beams incident at 0° was also calculated. These calculations are described in Section II and the results are presented in Section III.

Table I. Composition of the Standard and Miniature Shells

Shell Identification	Density (gm/cm^3)	Nuclide	Weight Percent
Standard	2.25	^{10}B	73.33
		^{11}B	6.42
		C	20.25
Miniature	2.32	^{10}B	73.33
		^{11}B	6.42
		C	20.25

Physical characteristics of the threshold foils and cladding materials shown in Fig. 3 are listed in Table II. Foil activities were calculated for exposure of the standard shell shielded foils to 13.6- and 1.01-MeV neutron beams incident at 0° and 180° with respect to the shell axis. Activities of interest were the fission reaction rate for the ^{235}U, ^{239}Pu, ^{237}Np, and ^{238}U foils; the (n,p) reaction rate for the S and Mg foils; the (n,α) reaction rate for the Al foil; and the (n,2n') reaction rate for the Zr foil. The transport calculations are described in Section II and the results are presented in Section III.

II. Calculations

All transport calculations were made using the 50 neutron-energy-group structure listed in Table III. This group structure consisted of 49 GAM-II broad groups and a thermal group.[4] Using fine group cross-section data from the ORNL GAM-II library, broad group P_3 cross sections for the nuclide of interest were calculated with GAM-II. Thermal cross sections for group 50 were obtained from the "Barn Book"[5-8] and were non 1/v corrected using the following relation:

$$\bar{\sigma}_a = g\ \sigma_a^o\ \sqrt{\pi/4}$$

where g is the "non 1/v" correction factor for the nuclide of interest and σ_a^o is 2200 m/sec absorption cross section.[9] Using microscopic cross sections from the GAM-II calculation and the foil densities and isotropic abundances from Table II, macroscopic activity cross sections were calculated for each foil for use in the transport calculations. These cross sections are listed in Table IV. Although the activity cross sections are identified in Table IV by the primary isotope in the respective foils, the cross sections are actually the cross sections for the foils, e.g.,

$$\Sigma_f^{235U} = N^{234U}\sigma_f^{234U} + N^{235U}\sigma_f^{235U} + N^{236U}\sigma_f^{236U} + N^{238U}\sigma_f^{238U}$$

where N^j is the number density of the j<u>th</u> isotope in the foil. The multi-group ^{235}U fission spectrum from the GAM-II calculation was assumed applicable to all fissile materials in the threshold foils.

Table II. Characteristics of the Activation Foils and Cladding Materials

Foil or* Cladding	Thickness (cm)	Density (gm/cm^3)	Nuclides Present	Isotopic Abundance (%)	Remarks
Cd	0.074	8.65	NE**	100.0	Cladding
Cu	0.0205	8.94	NE	100.0	Cladding
^{235}U	0.051	19.05	^{234}U ^{235}U ^{236}U ^{238}U	1.0 93.2 0.3 5.5	Threshold foil
Cu	0.041	8.94	NE	100.0	Cladding
^{239}Pu	0.150	19.82	^{239}Pu	100.0	Threshold foil
Cu	0.041	8.94	NE	100.0	Cladding
^{237}Np	0.051	1.01	^{237}Np ^{16}O	88.1 11.9	Threshold foil
Cu	0.041	8.94	NE	100.0	Cladding
^{238}U	0.150	19.05	^{238}U	~100.0	Threshold foil
Cu	0.0205	8.94	NE	100.0	Cladding
S	0.320	1.55	^{32}S ^{33}S ^{34}S	95.1 0.7 4.2	Threshold foil
Mg	0.250	1.66	NE	100.0	Threshold foil
Aℓ	0.200	2.63	NE	100.0	Threshold foil
Zr	0.086	6.62	NE	100.0	Threshold foil
Cd	0.074	8.65	NE	100.0	Cladding

*Listed in order shown in Figure 3.

**Natural element.

Table III. Neutron-Energy-Group Structure

Energy Group	Upper Energy (eV)	Energy Interval, ΔE (eV)	Energy Group	Upper Energy (eV)	Energy Interval, ΔE (eV)
1	14.91820(6)*	2.704(6)	26	8.65170(4)	3.404(4)
2	12.21400(6)	2.214(6)	27	5.24752(4)	1.161(4)
3	10.00000(6)	1.813(6)	28	4.08677(4)	9.040(3)
4	8.18731(6)	1.484(6)	29	3.18278(4)	7.040(3)
5	6.70320(6)	1.215(6)	30	2.47875(4)	5.483(3)
6	5.48812(6)	9.948(5)	31	1.93045(4)	4.270(3)
7	4.49329(6)	8.145(5)	32	1.50344(4)	7.933(3)
8	3.67879(6)	6.669(5)	33	7.10175(3)	2.794(3)
9	3.01194(6)	5.460(5)	34	4.30743(3)	9.528(2)
10	2.46597(6)	4.470(5)	35	3.35463(3)	7.420(2)
11	2.01897(6)	3.660(5)	36	2.61259(3)	5.779(2)
12	1.65299(6)	2.996(5)	37	2.03468(3)	4.501(2)
13	1.35335(6)	2.453(5)	38	1.58461(3)	3.505(2)
14	1.10803(6)	2.009(5)	39	1.23410(3)	2.730(2)
15	9.07180(5)	1.644(5)	40	9.61117(2)	5.071(2)
16	7.42736(5)	1.346(5)	41	4.53999(2)	2.395(2)
17	6.08101(5)	1.102(5)	42	2.14454(2)	1.132(2)
18	4.97871(5)	9.025(4)	43	1.01301(2)	5.345(1)
19	4.07622(5)	7.389(4)	44	4.78512(1)	2.525(1)
20	3.33733(5)	6.050(4)	45	2.26033(1)	1.193(1)
21	2.73237(5)	4.953(4)	46	1.06770(1)	5.634
22	2.23708(5)	4.055(4)	47	5.04348	2.661
23	1.83156(5)	3.320(4)	48	2.38237	1.257
24	1.49956(5)	2.718(4)	49	1.12535	0.71136
25	1.22773(5)	3.626(4)	50**	0.41399	0.41399

*Numbers in parentheses indicate power-of-ten multipliers, e.g., 14.91820(6) = 14.91820×10^6.

**Bottom energy of the lowest group is 0.0.

Table IV. Activity Cross Sections for the Threshold Foils

Energy Group	Σ_f^{235U} (cm^{-1})	Σ_f^{239Pu} (cm^{-1})	Σ_f^{237Np} (cm^{-1})	Σ_f^{238U} (cm^{-1})	$\Sigma^{S}_{(n,p)}$ (cm^{-1})	$\Sigma^{Mg}_{(n,p)}$ (cm^{-1})	$\Sigma^{A\ell}_{(n,\alpha)}$ (cm^{-1})	$\Sigma^{Zr}_{(n,2n')}$ (cm^{-1})
1	8.6850(-2)*	1.1419(-1)	5.9228(-3)	4.9249(-2)	8.1932(-3)	8.6153(-3)	7.4747(-3)	3.8184(-2)
2	7.7382(-2)	1.1185(-1)	5.9040(-3)	4.5416(-2)	9.8309(-3)	7.2112(-3)	6.1699(-3)	2.2492(-2)
3	8.1905(-2)	1.1191(-1)	5.8158(-3)	4.6760(-2)	9.8114(-3)	4.2266(-3)	3.9627(-3)	7.5002(-3)
4	7.3057(-2)	1.0572(-1)	5.3549(-3)	4.4113(-2)	9.3903(-3)	1.6719(-3)	1.4829(-3)	5.8300(-4)
5	5.3649(-2)	8.7145(-2)	4.1795(-3)	3.0360(-2)	8.7586(-3)	4.3062(-4)	1.2680(-4)	0.0
6	4.9366(-2)	8.3132(-2)	3.8651(-3)	2.4833(-2)	7.2145(-3)	8.6044(-5)	0.0	0.0
7	5.1816(-2)	8.7373(-2)	4.0455(-3)	2.5073(-2)	8.0012(-3)	3.0807(-7)	0.0	0.0
8	5.4518(-2)	9.0980(-2)	4.1921(-3)	2.4459(-2)	5.5909(-3)	0.0	0.0	0.0
9	5.7550(-2)	9.1553(-2)	4.2759(-3)	2.4852(-2)	2.5488(-3)	0.0	0.0	0.0
10	6.1299(-2)	9.6728(-2)	4.2594(-3)	2.6195(-2)	1.5789(-3)	0.0	0.0	0.0
11	6.0318(-2)	9.9494(-2)	4.1817(-3)	2.2603(-2)	1.1525(-4)	0.0	0.0	0.0
12	5.7526(-2)	9.3128(-2)	4.0340(-3)	1.2484(-2)	6.1263(-6)	0.0	0.0	0.0
13	5.6307(-2)	8.7846(-2)	3.8747(-3)	2.1311(-3)	0.0	0.0	0.0	0.0
14	5.6049(-2)	8.4676(-2)	3.6595(-3)	7.7149(-4)	0.0	0.0	0.0	0.0
15	5.4350(-2)	8.4095(-2)	3.0561(-3)	2.4999(-4)	0.0	0.0	0.0	0.0
16	5.2248(-2)	7.9750(-2)	2.2704(-3)	6.4167(-5)	0.0	0.0	0.0	0.0
17	5.2729(-2)	7.6957(-2)	1.4062(-3)	2.7972(-5)	0.0	0.0	0.0	0.0
18	5.4426(-2)	7.5973(-2)	5.8689(-4)	0.0	0.0	0.0	0.0	0.0
19	5.6624(-2)	7.5598(-2)	2.3799(-4)	0.0	0.0	0.0	0.0	0.0
20	5.8840(-2)	7.5137(-2)	1.5492(-4)	0.0	0.0	0.0	0.0	0.0
21	6.1410(-2)	7.5090(-2)	1.1985(-4)	0.0	0.0	0.0	0.0	0.0
22	6.4121(-2)	7.5033(-2)	9.5652(-5)	0.0	0.0	0.0	0.0	0.0
23	6.6862(-2)	7.4936(-2)	7.8723(-5)	0.0	0.0	0.0	0.0	0.0
24	6.9628(-2)	7.4750(-2)	6.6132(-5)	0.0	0.0	0.0	0.0	0.0
25	7.3503(-2)	7.4562(-2)	5.3671(-5)	0.0	0.0	0.0	0.0	0.0
26	8.1238(-2)	7.5595(-2)	4.0660(-5)	0.0	0.0	0.0	0.0	0.0
27	9.1287(-2)	7.8395(-2)	3.3687(-5)	0.0	0.0	0.0	0.0	0.0
28	9.8471(-2)	8.0568(-2)	3.0825(-5)	0.0	0.0	0.0	0.0	0.0
29	1.0679(-1)	8.2898(-2)	2.9521(-5)	0.0	0.0	0.0	0.0	0.0
30	1.1857(-1)	9.2703(-2)	3.1014(-5)	0.0	0.0	0.0	0.0	0.0
31	1.2737(-1)	9.5703(-2)	3.6405(-5)	0.0	0.0	0.0	0.0	0.0
32	1.4075(-1)	9.9353(-2)	4.7754(-5)	0.0	0.0	0.0	0.0	0.0
33	1.8158(-1)	1.1103(-1)	7.8836(-5)	0.0	0.0	0.0	0.0	0.0
34	2.3345(-1)	1.3363(-1)	1.0179(-4)	0.0	0.0	0.0	0.0	0.0
35	2.5057(-1)	1.7204(-1)	1.1745(-4)	0.0	0.0	0.0	0.0	0.0

Table IV. (Cont'd.)

Energy Group	Σ_f^{235U} (cm^{-1})	Σ_f^{239Pu} (cm^{-1})	Σ_f^{237Np} (cm^{-1})	Σ_f^{238U} (cm^{-1})	$\Sigma^{S}_{(n,p)}$ (cm^{-1})	$\Sigma^{Mg}_{(n,p)}$ (cm^{-1})	$\Sigma^{A\ell}_{(n,\alpha)}$ (cm^{-1})	$\Sigma^{Zr}_{(n,2n')}$ (cm^{-1})
36	2.7883(-1)	1.4687(-1)	1.3553(-4)	0.0	0.0	0.0	0.0	0.0
37	3.1135(-1)	1.6943(-1)	1.5638(-4)	0.0	0.0	0.0	0.0	0.0
38	3.4583(-1)	2.8665(-1)	1.8045(-4)	0.0	0.0	0.0	0.0	0.0
39	3.9727(-1)	3.0880(-1)	2.1492(-4)	0.0	0.0	0.0	0.0	0.0
40	5.2148(-1)	3.8180(-1)	2.8035(-4)	0.0	0.0	0.0	0.0	0.0
41	7.3295(-1)	6.1137(-1)	4.3309(-4)	0.0	0.0	0.0	0.0	0.0
42	9.7069(-1)	9.8349(-1)	6.5929(-4)	0.0	0.0	0.0	0.0	0.0
43	1.3849	2.4340	9.9115(-4)	0.0	0.0	0.0	0.0	0.0
44	1.9294	7.7082(-1)	6.8113(-4)	0.0	0.0	0.0	0.0	0.0
45	2.3646	5.1070	2.0571(-10)	0.0	0.0	0.0	0.0	0.0
46	2.6725	1.9998	1.6970(-9)	0.0	0.0	0.0	0.0	0.0
47	7.2473(-1)	4.9521(-1)	2.2055(-7)	0.0	0.0	0.0	0.0	0.0
48	9.8030(-1)	9.9502(-1)	1.5026(-5)	0.0	0.0	0.0	0.0	0.0
49	3.1719	4.4731	8.1919(-6)	0.0	0.0	0.0	0.0	0.0
50	2.2828(+1)	3.5207(+1)	4.1820(-5)	0.0	0.0	0.0	0.0	0.0

*Numbers in parenthesis indicate power-of-ten multiplies, e.g., 8.6850(-2) = 8.6850×10^{-2}

Characteristics of the transport calculations of the flux distribution in the "detector" were as follows:

Code used: DOT

Order of Legendre expansion of scattering cross sections: P_2

Total number of angles in quadrature set: 100 for the 0° beam, 70 for the 45° and 90° beams

Geometry: r-z

Total number of radial intervals: 18

Number of radial intervals in "detector" zone: 8

Total number of axial intervals: 48

Number of axial intervals in "detector" zone: 2

Left boundary condition: reflected

Right boundary condition: vacuum for top boundary source

Top boundary condition: vacuum for right boundary source

Bottom boundary condition: vacuum

Number groups of upscatter allowed: 0

Total boundary source normalization factor: 1.0

General convergence epsilon: 1.0×10^{-4}

A DOT calculation was made for each beam energy and angle of interest.

Characteristics of the transport calculations of the activities in the threshold foils were as follows:

Code used: DOT

Order of Legendre expansion of scattering cross sections: P_3

Total number of radial intervals: 21

Total number of axial intervals: 78

Left boundary conditions: reflected

Right boundary condition: vacuum

Top boundary condition: source

Bottom boundary condition: vacuum

Number of groups of upscatter allowed: 0

Total boundary source normalization factor: 1.0

General convergence epsilon: 1.0×10^{-4}

A DOT calculation was made for each beam energy and angle of interest.

III. Results and Conclusions

Results of the perturbation studies are presented in both tabular and graphic form. The total flux in the standard B_4C shelled "detector" times the volume of the "detector," ØV, is listed in Tables V, VI, and VII for the monoenergetic beams incident at 0°, 45°, and 90° respectively. The quantity ØV is defined as follows:

$$(\emptyset V)_i = \sum_{j,k}^{\text{Al zone}} \phi_{i,j,k} V_{j,k}$$

where ϕ is the scalar flux, V is the volume of an interval, and i, j, and k are the indices for the ith energy group, jth radial interval, and kth axial interval, respectively. ØV for an unshielded "detector" exposed to the neutron beams incident at 0° is listed in Table VIII.

The data from Tables V-VIII were normalized to an incident flux of unity and plotted as histograms in Figs. 4-19.* The normalization factor used with ØV for the 0° results in Table V and VIII was obtained from the following expression:

$$N^o = \frac{1.0}{\sum_{i=1}^{3} \phi_i W_i}$$

where W_i = weight of angle i in the 100 angle quadrature set (defined in the discrete ordinates sense)

ϕ_i = normalized top boundary angular flux

$$= \frac{SO1}{\pi r^2 \cdot \sum_{j=1}^{3} |W_j \cos\alpha_j| \, S_j}$$

where

SO1 = normalization factor used in the transport calculation (1.0)

πr^2 = area of a plane perpendicular to the shell axis (23.04 cm^2)

*Since the neutron source was input to DOT in the appropriate angles of the quadrature set used for the 0°, 45°, and 90° beams, normalization to a unit flux implies a parallel beam with units of 1 neutron/cm^2·sec.

Table V. Total Flux in the "Detector" Within the Standard B_4C Shell for Monoenergetic Beams Incident at 0°

Energy Group	ØV (neutrons cm/sec/source neutron)								
	Average Energy of Beam (MeV)								
	13.57	11.11	9.09	7.45	6.10	4.09	1.84	1.01	0.55
1	7.03176(-2)*	0.0	0.0	0.0	0.0	0.0	0.0	0.0	0.0
2	3.16212(-3)	7.02487(-2)	0.0	0.0	0.0	0.0	0.0	0.0	0.0
3	1.08842(-3)	3.21285(-3)	7.02100(-2)	0.0	0.0	0.0	0.0	0.0	0.0
4	6.65074(-4)	1.24000(-3)	3.25559(-3)	6.95449(-2)	0.0	0.0	0.0	0.0	0.0
5	6.57968(-4)	6.96723(-4)	1.40082(-3)	3.58706(-3)	6.88921(-2)	0.0	0.0	0.0	0.0
6	6.44884(-4)	7.66634(-4)	6.19364(-4)	1.62065(-3)	3.59919(-3)	0.0	0.0	0.0	0.0
7	6.12108(-4)	6.84306(-4)	7.60014(-4)	6.43595(-4)	1.81612(-3)	6.71526(-2)	0.0	0.0	0.0
8	5.60260(-4)	5.79190(-4)	8.40648(-4)	5.13766(-4)	6.87890(-4)	4.91018(-3)	0.0	0.0	0.0
9	5.03901(-4)	5.12346(-4)	5.99456(-4)	6.03542(-4)	5.42321(-4)	3.37977(-3)	0.0	0.0	0.0
10	4.41427(-4)	4.39896(-4)	4.40144(-4)	6.11478(-4)	4.00480(-4)	1.00691(-3)	0.0	0.0	0.0
11	3.60273(-4)	3.54792(-4)	3.36667(-4)	5.11198(-4)	3.21836(-4)	6.33243(-4)	6.37788(-2)	0.0	0.0
12	2.86968(-4)	2.77790(-4)	2.52681(-4)	3.32378(-4)	3.59228(-4)	3.57214(-4)	6.78658(-3)	0.0	0.0
13	2.23974(-4)	2.13443(-4)	1.91152(-4)	2.24405(-4)	3.25261(-4)	2.60417(-4)	3.02929(-3)	0.0	0.0
14	1.76192(-4)	1.65631(-4)	1.46820(-4)	1.65051(-4)	2.65467(-4)	2.10516(-4)	1.18889(-3)	6.13712(-2)	0.0
15	1.32891(-4)	1.23459(-4)	1.08623(-4)	1.19778(-4)	2.07167(-4)	1.69512(-4)	7.87162(-4)	8.24289(-3)	0.0
16	1.02381(-4)	9.40659(-5)	8.21729(-5)	9.01956(-5)	1.66468(-4)	1.07135(-4)	3.83713(-4)	4.04122(-3)	0.0
17	7.68857(-5)	6.98011(-5)	6.01089(-5)	6.54385(-5)	1.14197(-4)	6.93115(-5)	1.83855(-4)	1.78474(-3)	5.08282(-2)
18	5.73761(-5)	5.15257(-5)	4.37854(-5)	4.69543(-5)	6.93827(-5)	2.47587(-5)	8.08560(-5)	9.29174(-4)	8.55175(-3)
19	4.40764(-5)	3.91811(-5)	3.28205(-5)	3.50092(-5)	4.81935(-5)	2.07234(-5)	4.74770(-5)	4.53131(-4)	4.76000(-3)
20	3.16840(-5)	2.79330(-5)	2.31604(-5)	2.45735(-5)	3.16292(-5)	1.79292(-5)	2.78980(-5)	2.22050(-4)	2.45477(-3)
21	2.32695(-5)	2.04017(-5)	1.68173(-5)	1.78014(-5)	2.21358(-5)	1.54558(-5)	1.67150(-5)	1.13524(-4)	1.37454(-3)
22	1.61495(-5)	1.40970(-5)	1.15731(-5)	1.22501(-5)	1.48376(-5)	1.18902(-5)	1.02696(-5)	6.73389(-5)	6.32517(-4)
23	1.07848(-5)	9.39111(-6)	7.69219(-6)	8.17785(-6)	9.75719(-6)	8.09509(-6)	6.59178(-6)	4.48397(-5)	2.91182(-4)
24	8.07471(-6)	7.02177(-6)	5.73900(-6)	6.14836(-6)	7.24559(-6)	5.99409(-6)	4.96576(-6)	3.29016(-5)	1.51537(-4)
25	7.27223(-6)	6.31793(-6)	5.17085(-6)	5.56408(-6)	6.48360(-6)	5.53172(-6)	4.44443(-6)	1.28665(-5)	7.85999(-5)
26	5.02205(-6)	4.37268(-6)	3.60357(-6)	3.90149(-6)	4.53816(-6)	4.14499(-6)	3.36265(-6)	5.02469(-6)	2.62478(-5)
27	1.03785(-6)	9.05270(-7)	7.50180(-7)	8.16500(-7)	9.56795(-7)	9.63059(-7)	4.97183(-7)	7.42218(-6)	2.60739(-6)
28	5.80071(-7)	5.08513(-7)	4.25315(-7)	4.66385(-7)	5.52272(-7)	6.00602(-7)	2.61229(-7)	4.99568(-6)	8.74672(-7)
29	4.16839(-7)	3.68149(-7)	3.11919(-7)	3.45033(-7)	4.13546(-7)	4.89603(-7)	1.81415(-7)	3.75686(-6)	3.62416(-7)
30	2.09987(-7)	1.86858(-7)	1.60200(-7)	1.79269(-7)	2.18684(-7)	2.86267(-7)	8.90317(-8)	1.93438(-6)	8.46161(-8)
31	1.23331(-7)	1.10710(-7)	9.60464(-8)	1.08926(-7)	1.35176(-7)	1.93789(-7)	5.19891(-8)	1.18657(-6)	2.50850(-8)
32	1.45944(-7)	1.32897(-7)	1.17198(-7)	1.36555(-7)	1.75265(-7)	2.95913(-7)	6.08608(-8)	1.47144(-6)	9.14979(-9)
33	1.92611(-8)	1.99429(-8)	1.90870(-8)	2.46933(-8)	3.35627(-8)	8.03898(-8)	9.48713(-9)	2.79948(-7)	1.56153(-10)
34	3.41193(-9)	3.15773(-9)	4.30393(-9)	5.64257(-9)	8.21106(-9)	2.48973(-8)	2.20120(-9)	6.97740(-8)	6.95496(-12)
35	2.19881(-9)	1.99403(-9)	1.80510(-9)	2.56990(-9)	5.08062(-9)	1.85273(-8)	1.40498(-9)	4.55759(-8)	1.50216(-12)

Table V. (Cont'd.)

Energy Group	ØV (neutrons cm/sec/source neutron)								
	Average Energy of Beam (MeV)								
	13.57	11.11	9.09	7.45	6.10	4.09	1.84	1.01	0.55
36	1.44462(-9)	1.32716(-9)	1.21417(-9)	1.73893(-9)	2.97772(-9)	1.88585(-8)	8.98767(-10)	3.01529(-8)	3.00943(-13)
37	7.82974(-10)	8.69970(-10)	8.38039(-10)	1.21528(-9)	2.08776(-9)	9.90487(-9)	5.77005(-10)	2.01002(-8)	5.71980(-14)
38	5.16068(-10)	5.73617(-10)	5.85863(-10)	8.59719(-10)	1.48697(-9)	7.47291(-9)	3.75820(-10)	1.35982(-8)	1.02060(-14)
39	3.63825(-10)	4.00327(-10)	4.16478(-10)	6.13103(-10)	1.06349(-9)	5.67842(-9)	2.48229(-10)	9.34389(-9)	1.70915(-15)
40	5.99618(-10)	6.51904(-10)	6.87974(-10)	9.79085(-10)	1.70356(-9)	1.02158(-8)	3.67333(-10)	1.44742(-8)	2.88658(-16)
41	2.31015(-10)	2.47761(-10)	2.69268(-10)	3.44377(-10)	5.73955(-10)	4.66790(-9)	1.32253(-10)	5.53435(-9)	5.47858(-18)
42	9.42694(-11)	1.00002(-10)	1.10997(-10)	1.32815(-10)	2.10008(-10)	1.72492(-9)	5.52331(-11)	2.32495(-9)	7.40470(-20)
43	2.88503(-11)	3.01525(-11)	3.24945(-11)	4.19790(-11)	5.88870(-11)	1.37571(-10)	2.47993(-11)	1.03309(-9)	7.18813(-22)
44	3.37470(-12)	3.64497(-12)	3.02926(-12)	6.43699(-12)	1.27348(-11)	2.59701(-12)	1.14217(-11)	4.73056(-10)	5.05950(-24)
45	9.82129(-13)	1.07195(-12)	8.78952(-13)	1.95830(-12)	3.94565(-12)	6.06910(-13)	3.05780(-12)	1.01591(-10)	2.64426(-26)
46	2.71768(-13)	3.02774(-13)	2.45258(-13)	5.85755(-13)	1.20386(-12)	1.44100(-13)	6.59337(-13)	7.04936(-12)	1.06015(-28)
47	1.03915(-13)	1.12740(-13)	9.24610(-14)	2.03121(-13)	4.13100(-13)	6.76667(-14)	3.09287(-13)	3.22494(-12)	3.33916(-31)
48	4.12994(-14)	4.35935(-14)	3.62158(-14)	7.24288(-14)	1.45218(-13)	3.19467(-14)	1.46017(-13)	1.52233(-12)	8.78070(-34)
49	2.00887(-14)	2.05986(-14)	1.73496(-14)	3.11058(-14)	6.11527(-14)	1.80719(-14)	8.26003(-14)	8.61156(-13)	2.09107(-36)
50	2.66231(-17)	2.73484(-17)	2.30431(-17)	4.16163(-17)	8.16720(-17)	2.41772(-17)	1.09457(-16)	1.13807(-15)	2.80144(-39)
SUM	8.02186(-2)	7.98612(-2)	7.94556(-2)	7.87950(-2)	7.79134(-2)	7.83735(-2)	7.63415(-2)	7.73414(-2)	6.91529(-2)

*Numbers in parenthesis indicate power-of-ten multipliers, e.g., 7.03176(-2) = 7.03176×10^{-2}

Table VI. Total Flux in the "Detector" Within the Standard B_4C Shell for Monoenergetic Beam Incident at 45°

Energy Group	ØV (neutrons-cm/sec/source neutron)						
	Average Energy of Beam (MeV)						
	13.57	11.11	9.09	4.09	1.84	1.01	0.55
1	3.55212(-2)*	0.0	0.0	0.0	0.0	0.0	0.0
2	1.74378(-3)	3.55111(-2)	0.0	0.0	0.0	0.0	0.0
3	6.28192(-4)	1.79332(-3)	3.55549(-2)	0.0	0.0	0.0	0.0
4	3.75146(-4)	7.15319(-4)	1.83973(-3)	0.0	0.0	0.0	0.0
5	3.69198(-4)	3.92638(-4)	8.07904(-4)	0.0	0.0	0.0	0.0
6	3.60747(-4)	4.31417(-4)	3.46977(-4)	0.0	0.0	0.0	0.0
7	3.41766(-4)	3.83588(-4)	4.26501(-4)	3.37990(-2)	0.0	0.0	0.0
8	3.12464(-4)	3.23035(-4)	4.73597(-4)	2.88303(-3)	0.0	0.0	0.0
9	2.80963(-4)	2.85320(-4)	3.34795(-4)	1.98759(-3)	0.0	0.0	0.0
10	2.46350(-4)	2.44878(-4)	2.44037(-4)	5.92100(-4)	0.0	0.0	0.0
11	2.01047(-4)	1.97289(-4)	1.85818(-4)	3.52522(-4)	3.18539(-2)	0.0	0.0
12	1.60270(-4)	1.54440(-4)	1.39159(-4)	1.93897(-4)	4.10310(-3)	0.0	0.0
13	1.25175(-4)	1.18648(-4)	1.05119(-4)	1.38365(-4)	1.86950(-3)	0.0	0.0
14	9.85686(-5)	9.21096(-5)	8.07151(-5)	1.10560(-4)	7.19103(-4)	3.04911(-2)	0.0
15	7.43909(-5)	6.86715(-5)	5.96984(-5)	8.83780(-5)	4.47899(-4)	5.16923(-3)	0.0
16	5.73529(-5)	5.23447(-5)	4.51674(-5)	5.62309(-5)	2.16575(-4)	2.56839(-3)	0.0
17	4.31131(-5)	3.88748(-5)	3.30523(-5)	3.65614(-5)	1.04954(-4)	1.11611(-3)	2.46294(-2)
18	3.22002(-5)	2.87183(-5)	2.40614(-5)	1.38878(-5)	4.78817(-5)	5.65206(-4)	5.79886(-3)
19	2.47650(-5)	2.18644(-5)	1.80744(-5)	1.15101(-5)	2.82060(-5)	2.78304(-4)	3.27841(-3)
20	1.78151(-5)	1.55995(-5)	1.27630(-5)	9.80162(-6)	1.66634(-5)	1.36417(-4)	1.63995(-3)
21	1.30897(-5)	1.13986(-5)	9.27087(-6)	8.36388(-6)	1.00384(-5)	6.96068(-5)	8.90071(-4)
22	9.08642(-6)	7.87766(-6)	6.38088(-6)	6.40670(-6)	6.18096(-6)	3.97532(-5)	4.13434(-4)
23	6.06753(-6)	5.24719(-6)	4.24006(-6)	4.36390(-6)	3.97807(-6)	2.51939(-5)	1.90113(-4)
24	4.54178(-6)	3.92191(-6)	3.16140(-6)	3.22330(-6)	3.00462(-6)	1.78958(-5)	9.85309(-5)
25	4.08867(-6)	3.52653(-6)	2.84594(-6)	2.97567(-6)	2.69929(-6)	7.26557(-6)	5.09171(-5)
26	2.82111(-6)	2.43784(-6)	1.98038(-6)	2.22773(-6)	2.04967(-6)	2.84380(-6)	1.69800(-5)
27	5.82733(-7)	5.04404(-7)	4.12005(-7)	5.17159(-7)	3.00416(-7)	3.72682(-6)	1.68444(-6)
28	3.25187(-7)	2.82859(-7)	2.33231(-7)	3.22120(-7)	1.57342(-7)	2.49732(-6)	5.64616(-7)
29	2.33521(-7)	2.04602(-7)	1.70897(-7)	2.62342(-7)	1.09321(-7)	1.87589(-6)	2.33897(-7)
30	1.17556(-7)	1.03782(-7)	8.77295(-8)	1.53240(-7)	5.36567(-8)	9.65549(-7)	5.45994(-8)
31	6.89656(-8)	6.14191(-8)	5.25525(-8)	1.03463(-7)	3.13281(-8)	5.91938(-7)	1.61823(-8)
32	8.15130(-8)	7.36590(-8)	6.41163(-8)	1.57296(-7)	3.66617(-8)	7.33965(-7)	5.90122(-9)
33	1.06364(-8)	1.09610(-8)	1.03776(-8)	4.24192(-8)	5.71114(-9)	1.39599(-7)	1.00692(-10)
34	1.92864(-9)	1.78098(-9)	2.33229(-9)	1.30904(-8)	1.32447(-9)	3.48176(-8)	4.48451(-12)
35	1.24285(-9)	1.12509(-9)	1.01296(-9)	9.71570(-9)	8.44693(-10)	2.27583(-8)	9.68565(-13)

Table VI. (Cont'd.)

Energy Group	ØV (neutrons-cm/sec/source neutron)						
	Average Energy of Beam (MeV)						
	13.57	11.11	9.09	4.09	1.84	1.01	0.55
36	8.16030(-10)	7.48530(-10)	6.82087(-10)	7.24890(-9)	5.39938(-10)	1.50677(-8)	1.94035(-13)
37	4.40264(-10)	4.90024(-10)	4.71044(-10)	5.17796(-9)	3.46350(-10)	1.00519(-8)	3.68786(-14)
38	2.89729(-10)	3.22540(-10)	3.29139(-10)	3.89857(-9)	2.25376(-10)	6.80617(-9)	6.58025(-15)
39	2.04116(-10)	2.24900(-10)	2.33859(-10)	2.95751(-9)	1.48706(-10)	4.68086(-9)	1.10195(-15)
40	3.36141(-10)	3.65877(-10)	3.86077(-10)	5.30839(-9)	2.19701(-10)	7.26138(-9)	1.86108(-16)
41	1.29360(-10)	1.38840(-10)	1.50981(-10)	2.42036(-9)	7.88814(-11)	2.78215(-9)	3.53204(-18)
42	5.27296(-11)	5.59581(-11)	6.21858(-11)	9.00342(-10)	3.28924(-11)	1.17064(-8)	4.77363(-20)
43	1.61389(-11)	1.68592(-11)	1.81700(-11)	8.00868(-11)	1.47579(-11)	5.20644(-10)	4.63371(-22)
44	1.90266(-12)	2.05408(-12)	1.69410(-12)	1.38430(-12)	6.79457(-12)	2.38517(-10)	3.26128(-24)
45	5.54214(-13)	6.04801(-13)	4.92187(-13)	3.17236(-13)	1.79727(-12)	5.22465(-11)	1.70431(-26)
46	1.53588(-13)	1.71173(-13)	1.37718(-13)	7.50368(-14)	3.74635(-13)	4.38254(-12)	6.83227(-29)
47	5.86216(-14)	6.35801(-14)	5.17408(-14)	3.52343(-14)	1.75666(-13)	2.01790(-12)	2.15226(-31)
48	2.32557(-14)	2.45203(-14)	2.01944(-14)	1.66347(-14)	8.29338(-14)	9.52577(-13)	5.65896(-34)
49	1.12912(-14)	1.15532(-14)	9.63833(-15)	9.41005(-15)	4.69143(-14)	5.38857(-13)	1.34737(-36)
50	1.49536(-17)	1.53283(-17)	1.27941(-17)	1.25786(-17)	6.20933(-17)	7.11111(-16)	1.80469(-39)
SUM	4.10555(-2)	4.09048(-2)	4.07610(-2)	4.03026(-2)	3.94364(-2)	4.04979(-2)	3.70093(-2)

*Numbers in parenthesis indicate power-of-ten multipliers, e.g., 3.55212(-2) = 3.55212×10^{-2}

Table VII. Total Flux in the "Detector" Within the Standard B_4C Shell for Monoenergetic Beams Incident at 90°

Energy Group	ØV (neutrons-cm/sec/source neutron)						
	Average Energy of Beam (MeV)						
	13.57	11.11	9.09	4.09	1.84	1.01	0.55
1	3.98400(-2)*	0.0	0.0	0.0	0.0	0.0	0.0
2	1.99766(-3)	3.97519(-2)	0.0	0.0	0.0	0.0	0.0
3	7.17343(-4)	2.05957(-3)	3.98068(-2)	0.0	0.0	0.0	0.0
4	4.28660(-4)	8.16442(-4)	2.12498(-3)	0.0	0.0	0.0	0.0
5	4.21698(-4)	4.48527(-4)	9.21476(-4)	0.0	0.0	0.0	0.0
6	4.11887(-4)	4.92993(-4)	3.95928(-4)	0.0	0.0	0.0	0.0
7	3.90028(-4)	4.38044(-4)	4.87071(-4)	3.78500(-2)	0.0	0.0	0.0
8	3.56522(-4)	3.68530(-4)	5.41650(-4)	3.34459(-3)	0.0	0.0	0.0
9	3.20631(-4)	3.25455(-4)	3.82212(-4)	2.27732(-3)	0.0	0.0	0.0
10	2.81126(-4)	2.79225(-4)	2.78162(-4)	6.81527(-4)	0.0	0.0	0.0
11	2.29441(-4)	2.24926(-4)	2.11742(-4)	3.98881(-4)	3.54103(-2)	0.0	0.0
12	1.82888(-4)	1.76039(-4)	1.58326(-4)	2.19184(-4)	4.77928(-3)	0.0	0.0
13	1.42848(-4)	1.35235(-4)	1.19547(-4)	1.56043(-4)	2.17133(-3)	0.0	0.0
14	1.12501(-4)	1.04993(-4)	9.17820(-5)	1.24593(-4)	8.38470(-4)	3.44672(-2)	0.0
15	8.49042(-5)	7.82716(-5)	6.78721(-5)	9.95018(-5)	5.12809(-4)	6.10452(-3)	0.0
16	6.54722(-5)	5.96721(-5)	5.13532(-5)	6.34207(-5)	2.47535(-4)	3.02188(-3)	0.0
17	4.92258(-5)	4.43251(-5)	3.75849(-5)	4.12841(-5)	1.20251(-4)	1.31731(-3)	2.80991(-2)
18	3.67715(-5)	3.27501(-5)	2.73678(-5)	1.58891(-5)	5.53293(-5)	6.60297(-4)	6.98482(-3)
19	2.82859(-5)	2.49395(-5)	2.05632(-5)	1.31457(-5)	3.26110(-5)	3.25262(-4)	3.95194(-3)
20	2.03490(-5)	1.77951(-5)	1.45225(-5)	1.11564(-5)	1.92982(-5)	1.59209(-4)	1.97712(-3)
21	1.49542(-5)	1.30052(-5)	1.05507(-5)	9.50110(-6)	1.16368(-5)	8.11741(-5)	1.06290(-3)
22	1.03805(-5)	8.98790(-6)	7.26183(-6)	7.27163(-6)	7.17243(-6)	4.60635(-5)	4.92860(-4)
23	6.93082(-6)	5.98599(-6)	4.82490(-6)	4.95301(-6)	4.62006(-6)	2.89775(-5)	2.26135(-4)
24	5.18789(-6)	4.47387(-6)	3.59701(-6)	3.65577(-6)	3.49219(-6)	2.04806(-5)	1.16992(-4)
25	4.67063(-6)	4.02288(-6)	3.23792(-6)	3.37534(-6)	3.13921(-6)	8.36749(-6)	6.03180(-5)
26	3.22307(-6)	2.78100(-6)	2.25290(-6)	2.52635(-6)	2.38509(-6)	3.27875(-6)	2.00904(-5)
27	6.65910(-7)	5.75495(-7)	4.68766(-7)	5.86505(-7)	3.50083(-7)	4.21111(-6)	1.99094(-6)
28	3.71294(-7)	3.22463(-7)	2.65170(-7)	3.65159(-7)	1.83297(-7)	2.81969(-6)	6.67015(-7)
29	2.66841(-7)	2.33387(-7)	1.94372(-7)	2.97369(-7)	1.27519(-7)	2.11745(-6)	2.76274(-7)
30	1.34381(-7)	1.18419(-7)	9.98093(-8)	1.73699(-7)	6.26348(-8)	1.09024(-6)	6.44760(-8)
31	7.88353(-8)	7.00769(-8)	5.97838(-8)	1.17206(-7)	3.65782(-8)	6.68352(-7)	1.91059(-8)
32	9.31815(-8)	8.40392(-8)	7.29435(-8)	1.78001(-7)	4.28135(-8)	8.28721(-7)	6.96595(-9)
33	1.21310(-8)	1.24821(-8)	1.17872(-8)	4.79093(-8)	6.66838(-9)	1.57579(-7)	1.18838(-10)
34	2.20990(-9)	2.03849(-9)	2.64612(-9)	1.47719(-8)	1.54647(-9)	3.93095(-8)	5.29227(-12)
35	1.42399(-9)	1.28744(-9)	1.15695(-9)	1.09571(-8)	9.85967(-10)	2.56982(-8)	1.14299(-12)

Table VII. (Cont'd.)

Energy Group	ØV (neutrons-cm/sec/source neutron)						
	Average Energy of Beam (MeV)						
	13.57	11.11	9.09	4.09	1.84	1.01	0.55
36	9.34782(-10)	8.56339(-10)	7.79145(-10)	8.17065(-9)	6.30036(-10)	1.70171(-8)	2.28969(-13)
37	5.03107(-10)	5.60241(-10)	5.38102(-10)	5.83562(-9)	4.03965(-10)	1.13541(-8)	4.35170(-14)
38	3.30838(-10)	3.68429(-10)	3.75903(-10)	4.39172(-9)	2.62729(-10)	7.68902(-9)	7.76451(-15)
39	2.33022(-10)	2.56799(-10)	2.67028(-10)	3.33041(-9)	1.73236(-10)	5.28860(-9)	1.30026(-15)
40	3.83725(-10)	4.17695(-10)	4.40792(-10)	5.97455(-9)	2.55672(-10)	8.20677(-9)	2.19593(-16)
41	1.47661(-10)	1.58481(-10)	1.72370(-10)	2.72275(-9)	9.16259(-11)	3.14556(-9)	4.16747(-18)
42	6.01827(-11)	6.38626(-11)	7.09937(-11)	1.01425(-9)	3.81752(-11)	1.32398(-9)	5.63232(-20)
43	1.84214(-11)	1.92388(-11)	2.07366(-11)	9.20179(-11)	1.71244(-11)	5.88945(-10)	5.46715(-22)
44	2.17465(-12)	2.34746(-12)	1.93171(-12)	1.56379(-12)	7.88327(-12)	2.69883(-10)	3.84783(-24)
45	6.33544(-13)	6.91338(-13)	5.61328(-13)	3.56963(-13)	2.07780(-12)	5.93559(-11)	2.01081(-26)
46	1.75620(-13)	1.95742(-13)	1.57131(-13)	8.43874(-14)	4.28650(-13)	5.16014(-12)	8.06095(-29)
47	6.70035(-14)	7.26653(-14)	5.89982(-14)	3.96247(-14)	2.00968(-13)	2.37856(-12)	2.53931(-31)
48	2.65705(-14)	2.80083(-14)	2.30124(-14)	1.87075(-14)	9.48790(-14)	1.12284(-12)	6.67662(-34)
49	1.28956(-14)	1.31887(-14)	1.09758(-14)	1.05826(-14)	5.36716(-14)	6.35170(-13)	1.58966(-36)
50	1.70726(-17)	1.74952(-17)	1.45650(-17)	1.41354(-17)	7.10004(-17)	8.37205(-16)	2.12920(-39)
SUM	4.61651(-2)	4.59202(-2)	4.57713(-2)	4.53295(-2)	4.42204(-2)	4.62560(-2)	4.29953(-2)

*Numbers in parenthesis indicate power-of-ten multipliers, e.g., 3.98400(-2) = 3.98400×10^{-2}

Table VIII. Total Flux in the Unshielded (Void in B_4C Zone) Standard Shell "Detector" for Monoenergetic Beams Incident at 0°

Energy Group	ØV (neutrons-cm/sec/source neutron)								
	Average Energy of Beam (MeV)								
	13.57	11.11	9.09	7.45	6.10	4.09	1.84	1.01	0.55
1	7.96709(-2)*	0.0	0.0	0.0	0.0	0.0	0.0	0.0	0.0
2	4.53873(-4)	7.97187(-2)	0.0	0.0	0.0	0.0	0.0	0.0	0.0
3	9.39940(-5)	4.56942(-4)	7.97694(-2)	0.0	0.0	0.0	0.0	0.0	0.0
4	1.27467(-4)	1.13742(-4)	4.28665(-4)	7.98061(-2)	0.0	0.0	0.0	0.0	0.0
5	1.55219(-4)	1.44506(-4)	1.33307(-4)	3.97309(-4)	7.98194(-2)	0.0	0.0	0.0	0.0
6	1.69735(-4)	1.65996(-4)	1.59786(-4)	1.51940(-4)	3.93002(-4)	0.0	0.0	0.0	0.0
7	1.70159(-4)	1.73267(-4)	1.74393(-4)	1.72659(-4)	1.69728(-4)	8.02367(-2)	0.0	0.0	0.0
8	1.59614(-4)	1.67972(-4)	1.75342(-4)	1.80757(-4)	1.84429(-4)	7.54956(-4)	0.0	0.0	0.0
9	1.40653(-4)	1.52084(-4)	1.63588(-4)	1.74349(-4)	1.84086(-4)	2.70078(-4)	0.0	0.0	0.0
10	1.19098(-4)	1.31616(-4)	1.45047(-4)	1.58817(-4)	1.73220(-4)	2.58143(-5)	0.0	0.0	0.0
11	9.62666(-5)	1.08299(-4)	1.21742(-4)	1.36280(-4)	1.52329(-4)	1.42189(-4)	8.13567(-2)	0.0	0.0
12	7.52051(-5)	8.58272(-5)	9.80365(-5)	1.11727(-4)	1.27587(-4)	2.08661(-4)	1.29596(-3)	0.0	0.0
13	5.69106(-5)	6.57515(-5)	7.61352(-5)	8.80874(-5)	1.01939(-4)	1.97346(-4)	1.89890(-5)	0.0	0.0
14	4.28718(-5)	4.99994(-5)	5.85076(-5)	6.84969(-5)	8.02437(-5)	1.78170(-4)	6.97274(-5)	8.15676(-2)	0.0
15	3.10427(-5)	3.64728(-5)	4.30385(-5)	5.08644(-5)	6.02010(-5)	1.51681(-4)	2.52273(-4)	1.38935(-3)	0.0
16	2.28292(-5)	2.69867(-5)	3.20639(-5)	3.81913(-5)	4.57279(-5)	8.90615(-5)	1.67168(-4)	3.84860(-5)	0.0
17	1.60370(-5)	1.90614(-5)	2.27861(-5)	2.73268(-5)	3.29632(-5)	5.34554(-5)	6.14381(-5)	8.44867(-7)	8.22709(-2)
18	1.12147(-5)	1.33871(-5)	1.60803(-5)	1.93870(-5)	2.35370(-5)	5.88334(-6)	3.90871(-6)	2.07989(-8)	2.02988(-3)
19	8.01273(-6)	9.59566(-6)	1.15683(-5)	1.40057(-5)	1.70878(-5)	7.12754(-6)	1.49905(-6)	7.48161(-10)	7.11866(-5)
20	5.43508(-6)	6.52485(-6)	7.88884(-6)	9.58260(-6)	1.17322(-5)	9.52779(-6)	1.00032(-6)	1.95210(-11)	1.83091(-6)
21	3.86012(-6)	4.64153(-6)	5.62257(-6)	6.84529(-6)	8.40857(-6)	9.56930(-6)	6.14900(-8)	7.48008(-13)	6.95517(-8)
22	2.62594(-6)	3.16103(-6)	3.83436(-6)	4.67625(-6)	5.76012(-6)	7.70665(-6)	3.12405(-8)	1.64356(-5)	1.96605(-9)
23	1.74801(-6)	2.10546(-6)	2.55620(-6)	3.12102(-6)	3.85372(-6)	5.14109(-6)	3.37690(-8)	2.53036(-5)	5.62570(-11)
24	1.32437(-6)	1.59697(-6)	1.94115(-6)	2.37300(-6)	2.93408(-6)	3.84942(-5)	3.19388(-8)	2.46068(-5)	3.99242(-12)
25	1.22328(-6)	1.47664(-6)	1.79712(-6)	2.20011(-6)	2.72499(-6)	3.53664(-6)	1.68572(-8)	5.17686(-6)	7.45292(-14)
26	8.93365(-7)	1.07870(-6)	1.31342(-6)	1.60904(-6)	1.99505(-6)	2.71502(-6)	1.31329(-8)	1.92699(-6)	4.92356(-15)
27	1.88249(-7)	2.27404(-7)	2.77060(-7)	3.39731(-7)	4.21857(-7)	6.42165(-7)	8.30520(-9)	9.19492(-6)	2.55388(-17)
28	1.10444(-7)	1.33345(-7)	1.62394(-7)	1.99063(-7)	2.47198(-7)	4.10607(-7)	5.40678(-9)	6.17615(-6)	7.57767(-19)
29	8.44246(-8)	1.01854(-7)	1.23958(-7)	1.51858(-7)	1.88540(-7)	3.43254(-7)	4.18947(-9)	4.55442(-6)	9.35838(-20)
30	4.41135(-8)	5.31507(-8)	6.46077(-8)	7.90641(-8)	9.81292(-8)	2.04195(-7)	2.22437(-9)	2.31023(-6)	3.87959(-22)
31	2.70578(-8)	3.25654(-8)	3.95450(-8)	4.83482(-8)	5.99744(-8)	1.42445(-7)	1.40066(-9)	1.41937(-6)	1.80683(-24)
32	3.34251(-8)	4.01347(-8)	4.86217(-8)	5.93099(-8)	7.33828(-8)	2.27502(-7)	1.84650(-9)	1.77022(-6)	1.19257(-26)
33	6.46487(-9)	7.71233(-9)	9.28316(-9)	1.12531(-8)	1.38594(-8)	6.80969(-8)	4.12535(-10)	3.51213(-7)	5.71995(-30)
34	4.12063(-10)	4.50839(-10)	2.21664(-9)	2.67237(-9)	3.27992(-9)	2.16805(-8)	1.11999(-10)	8.72017(-8)	1.20300(-32)
35	2.79216(-10)	2.99501(-10)	3.37478(-10)	3.65116(-10)	1.42495(-9)	1.64849(-8)	7.79045(-11)	5.70114(-8)	1.24768(-34)

Table VIII. (Cont'd.)

Energy Group	ØV (neutrons-cm/sec/source neutron)								
	Average Energy of Beam (MeV)								
	13.57	11.11	9.09	7.45	6.10	4.09	1.84	1.01	0.55
36	1.94981(-10)	2.09124(-10)	2.23634(-10)	2.37453(-10)	2.18368(-10)	1.25221(-8)	5.46322(-11)	3.74831(-8)	1.29346(-36)
37	1.38384(-10)	1.48309(-10)	1.58340(-10)	1.67915(-10)	1.89980(-10)	8.99171(-9)	3.88804(-11)	2.49933(-8)	1.34100(-38)
38	1.00413(-10)	1.07496(-10)	1.14623(-10)	1.21386(-10)	1.37295(-10)	6.90844(-9)	2.80564(-11)	1.69186(-8)	1.39020(-40)
39	7.37449(-11)	7.88689(-11)	8.40043(-11)	8.88512(-11)	1.00516(-10)	5.32692(-9)	2.05014(-11)	1.16318(-8)	1.44118(-42)
40	1.26670(-10)	1.35279(-10)	1.43859(-10)	1.51886(-10)	1.71875(-10)	9.77485(-9)	3.49582(-11)	1.80205(-8)	1.50621(-44)
41	5.14171(-11)	5.51511(-11)	5.89014(-11)	6.24204(-11)	6.58664(-11)	4.55773(-9)	1.50864(-11)	6.88745(-9)	3.43007(-47)
42	2.21363(-11)	2.37863(-11)	2.54515(-11)	2.70249(-11)	2.85551(-11)	1.61294(-9)	6.80947(-12)	2.89070(-9)	7.83803(-50)
43	6.65385(-12)	7.26237(-12)	7.90327(-12)	8.54667(-12)	9.19680(-12)	2.03582(-11)	3.14591(-12)	1.28461(-9)	1.79753(-52)
44	4.44514(-13)	5.18292(-13)	6.06474(-13)	7.10200(-13)	8.32813(-13)	1.91629(-12)	1.47020(-12)	5.88720(-10)	4.11219(-55)
45	1.17612(-13)	1.37640(-13)	1.61694(-13)	1.90144(-13)	2.24017(-13)	5.29368(-13)	5.54092(-13)	1.17403(-10)	9.39727(-58)
46	2.65201(-14)	3.11561(-14)	3.67603(-14)	4.34395(-14)	5.14922(-14)	1.29438(-13)	2.14531(-13)	1.43556(-12)	2.14656(-60)
47	1.24603(-14)	1.46390(-14)	1.72730(-14)	2.04124(-14)	2.41978(-14)	6.08632(-14)	1.01217(-13)	5.58350(-13)	4.90238(-63)
48	5.88446(-15)	6.91337(-15)	8.15728(-15)	9.63989(-15)	1.14276(-14)	2.87431(-14)	4.78015(-14)	2.63423(-13)	1.11946(-65)
49	3.32923(-15)	3.91149(-15)	4.61527(-15)	5.45412(-15)	6.46556(-15)	1.62624(-14)	2.70453(-14)	1.49040(-13)	2.55893(-68)
50	4.45613(-18)	5.23512(-18)	6.17678(-18)	7.29909(-18)	8.65231(-18)	2.17617(-17)	3.61893(-17)	1.99518(-16)	3.48397(-71)
SUM	8.16378(-2)	8.16603(-2)	8.16543(-2)	8.16266(-2)	8.16035(-2)	8.23644(-2)	8.32284(-2)	8.30951(-2)	8.43737(-2)

*Numbers in parenthesis indicate power-of-ten multipliers, e.g., 7.96709(-2) = 7.96709×10^{-2}

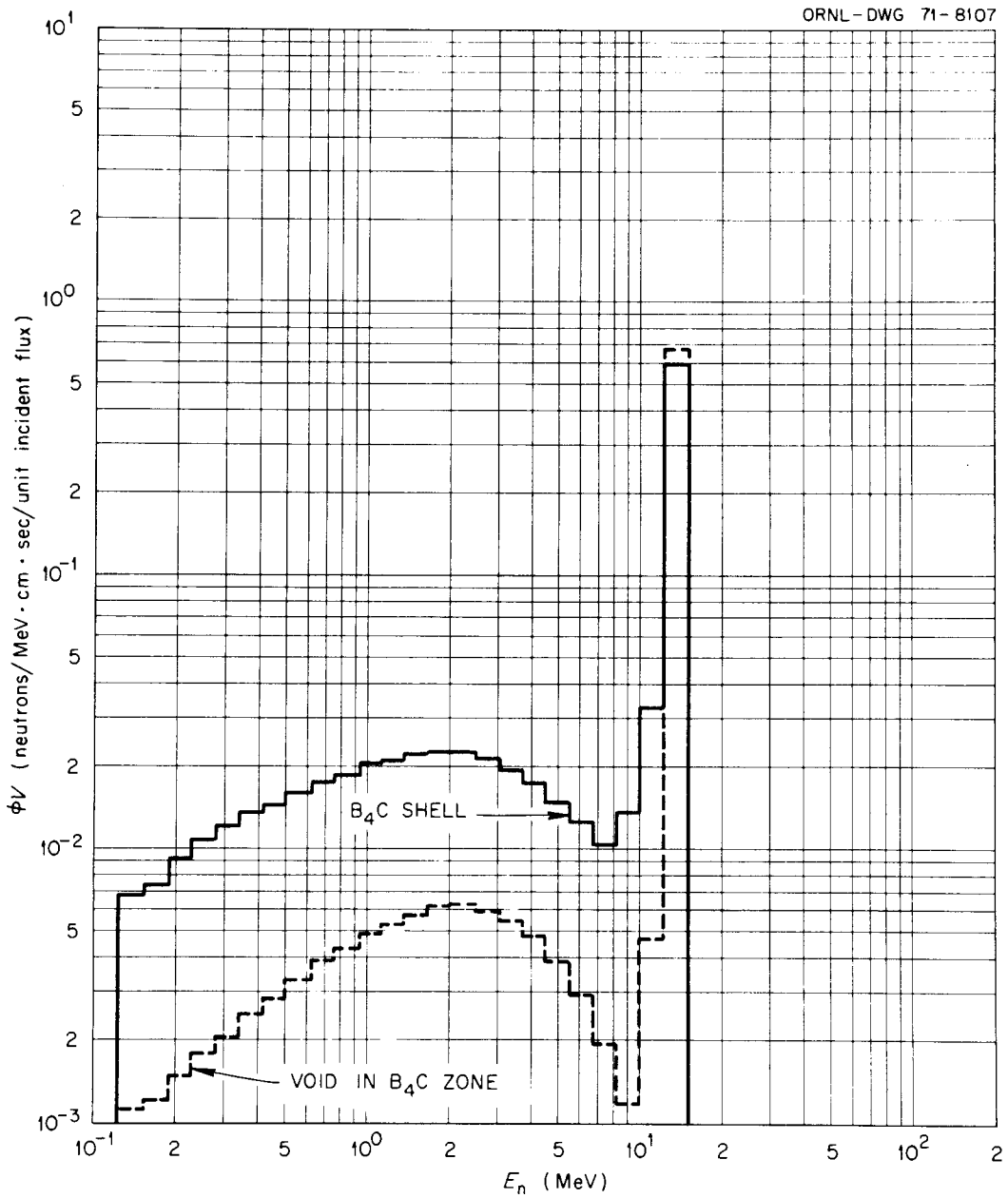

Figure 4. Total Flux in Standard Shell "Detector" due to 13.57 MeV Beam at 0°

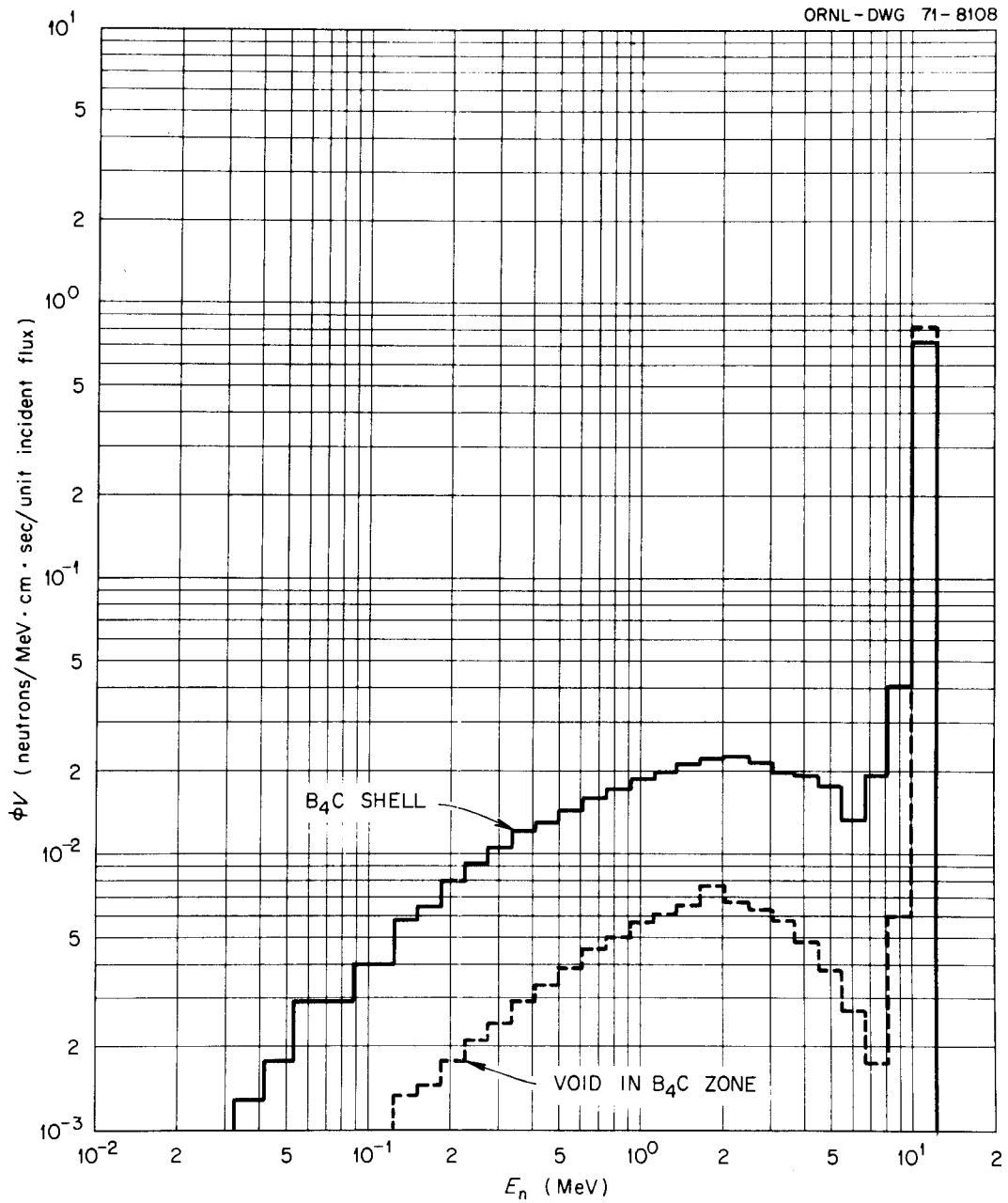

Figure 5. Total Flux in Standard Shell "Detector" due to 11.11 MeV Beam at 0°

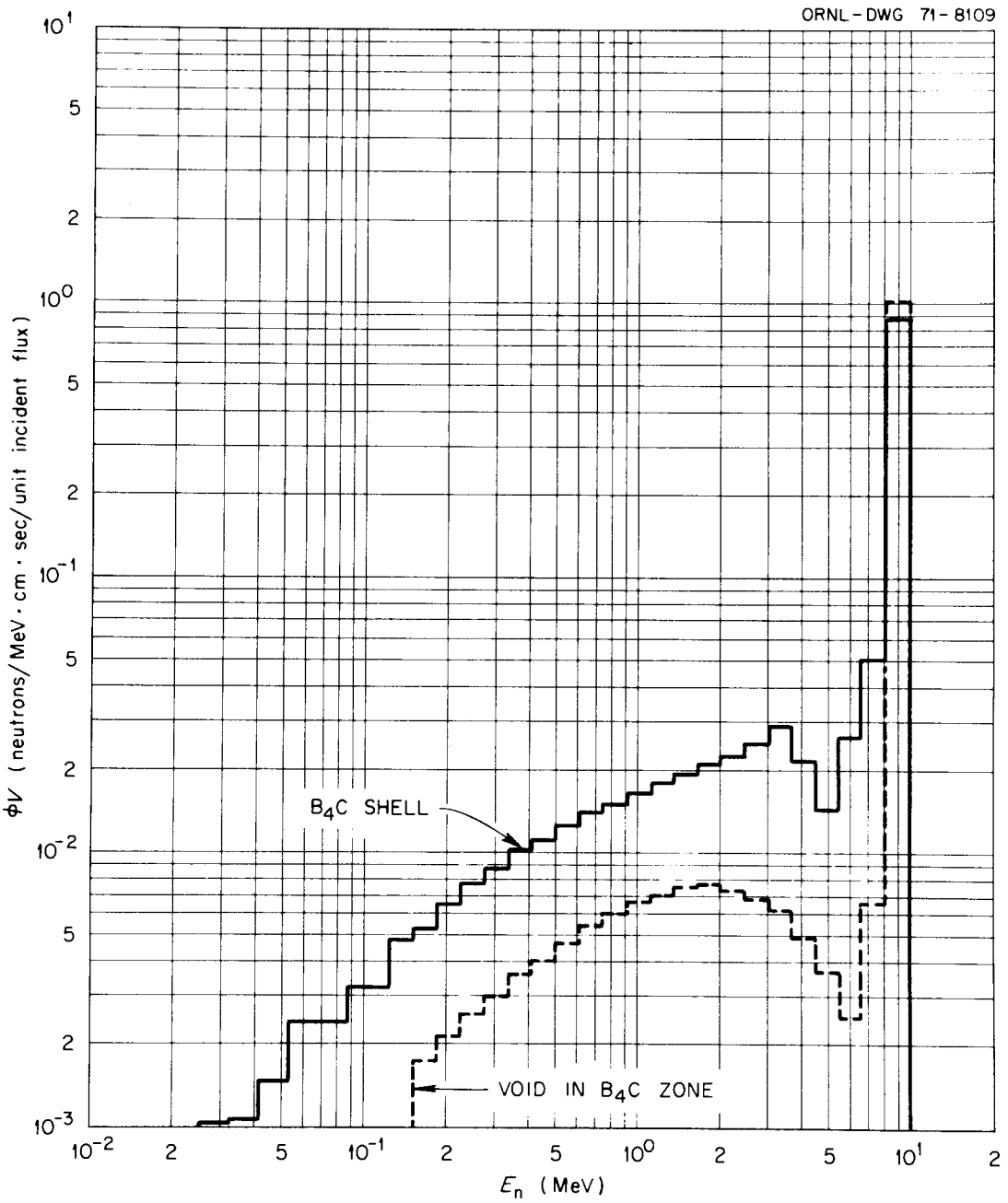

Figure 6. Total Flux in Standard Shell "Detector" due to 9.09 MeV Beam at 0°

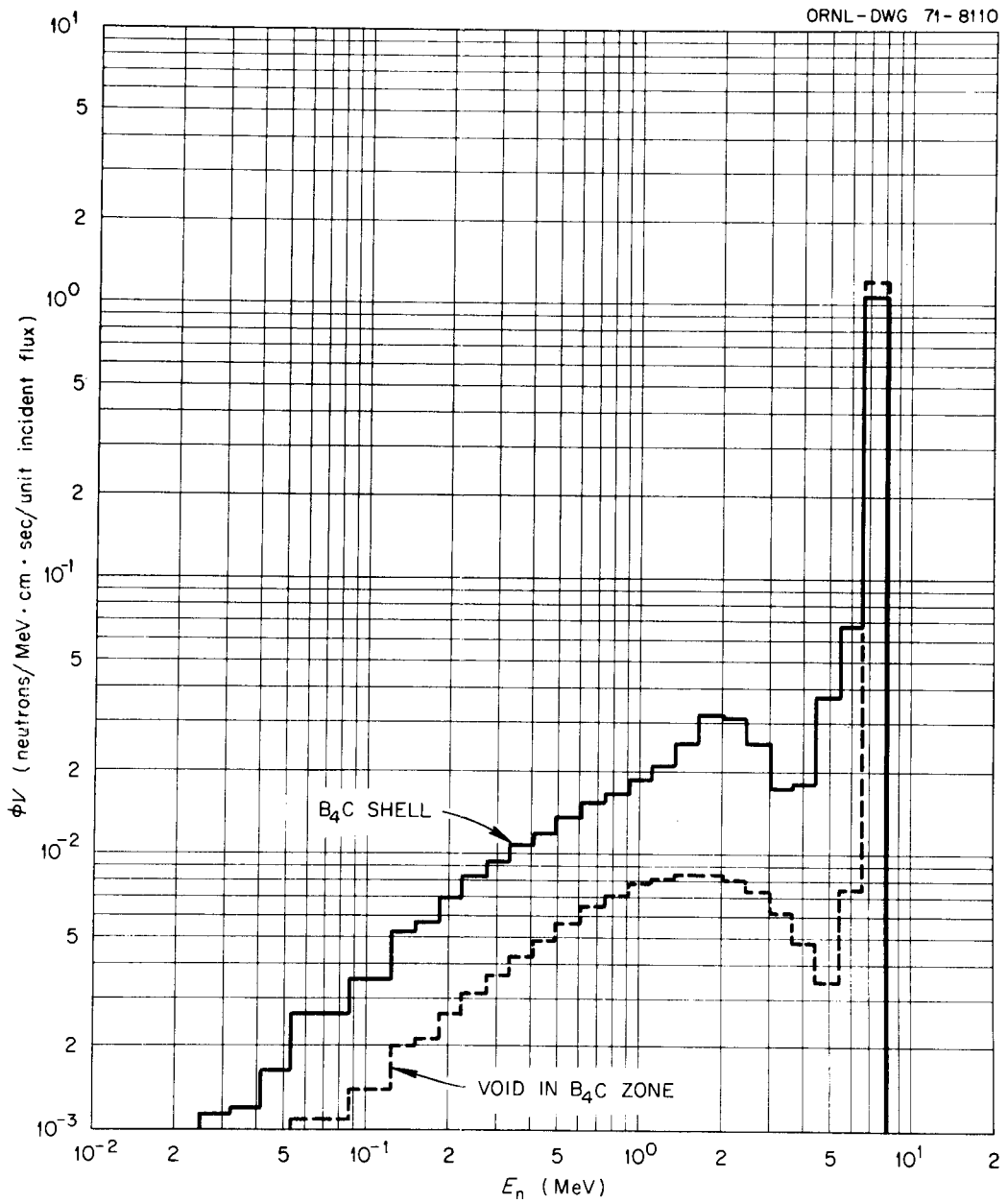

Figure 7. Total Flux in Standard Shell "Detector" due to 7.45 MeV Beam at 0°

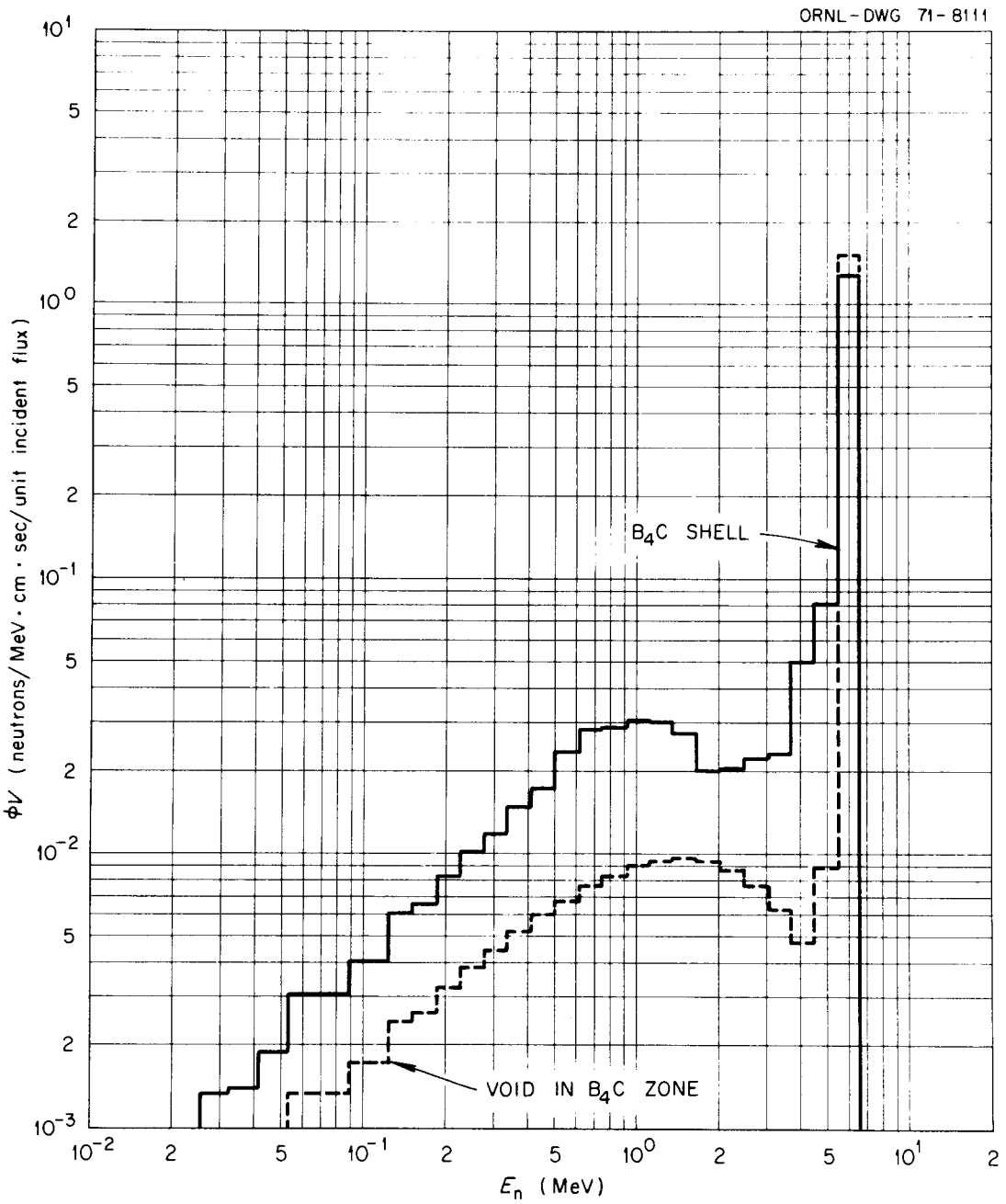

Figure 8. Total Flux in Standard Shell "Detector" due to 6.10 MeV Beam at 0°

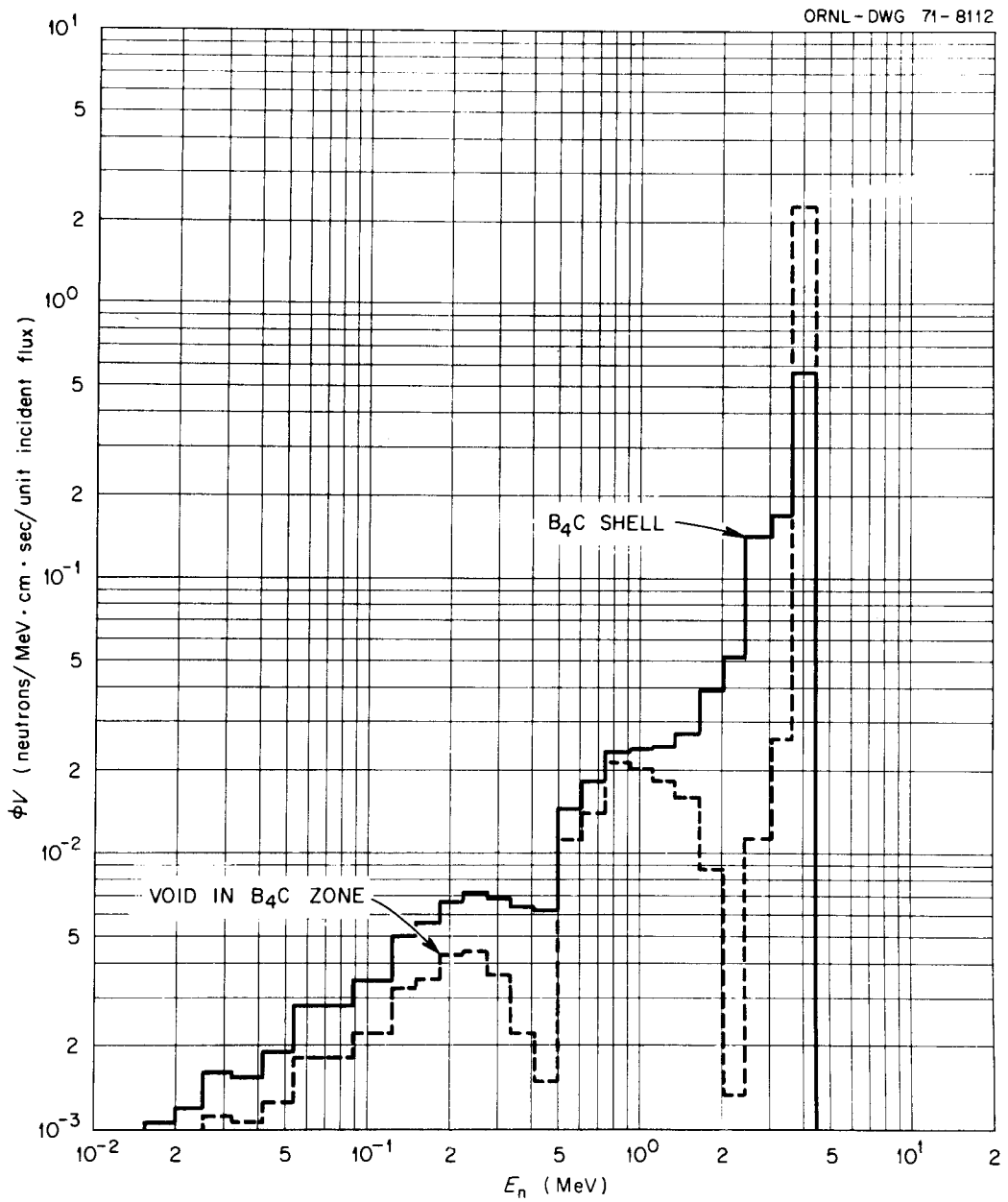

Figure 9. Total Flux in Standard Shell "Detector" due to 4.09 MeV Beam at 0°

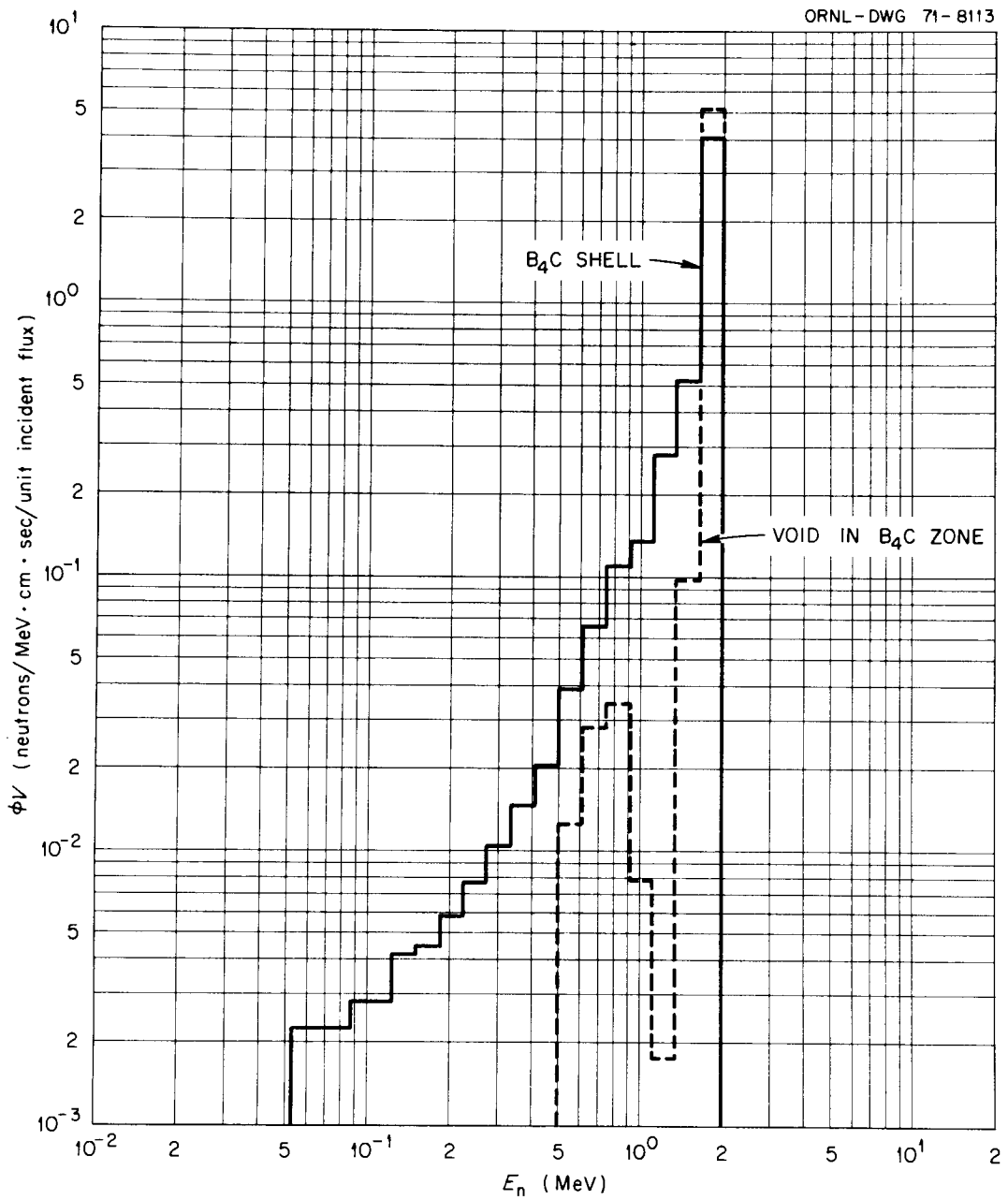

Figure 10. Total Flux in Standard Shell "Detector" due to 1.84 MeV Beam at 0°

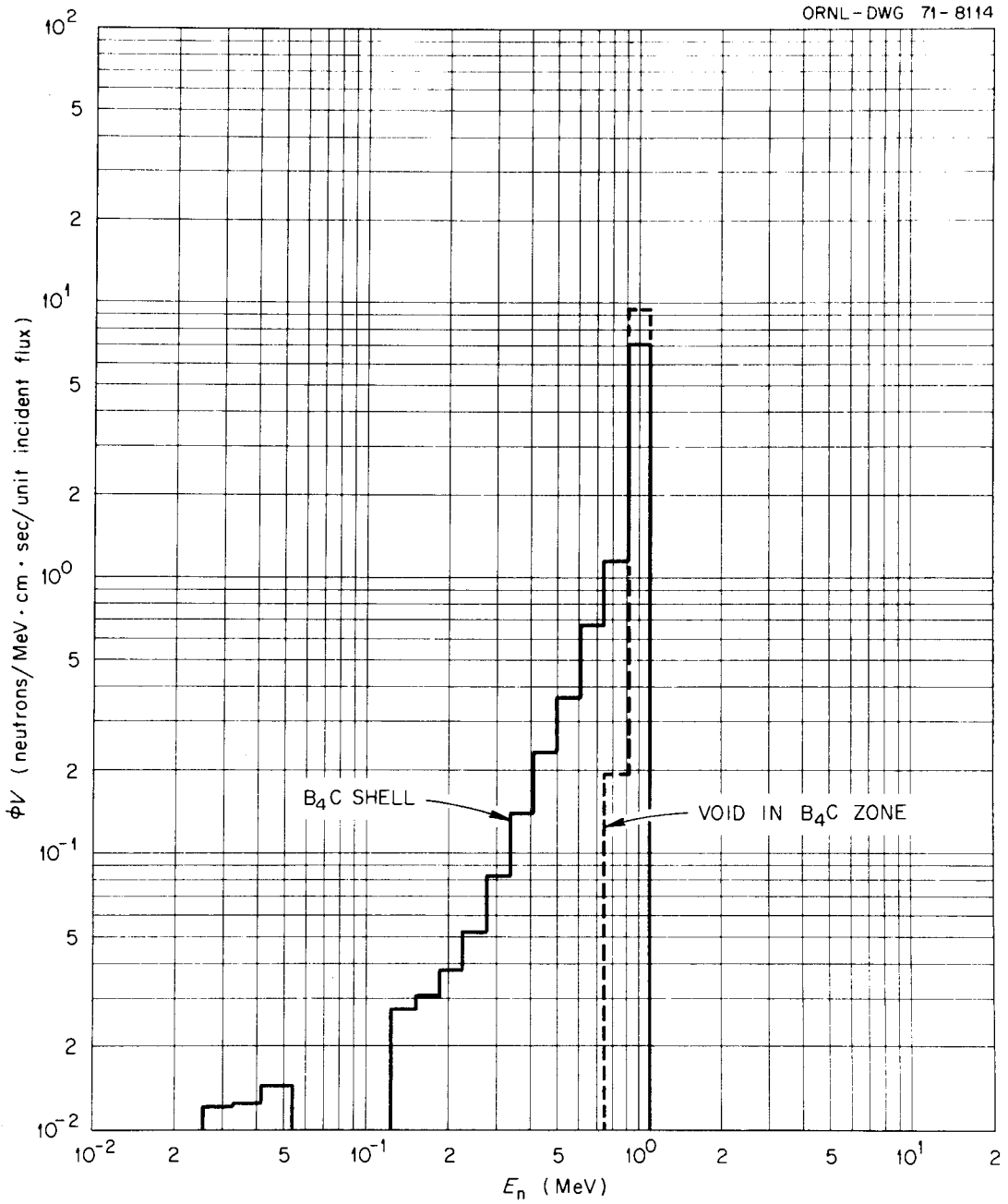

Figure 11. Total Flux in Standard Shell "Detector" due to 1.01 MeV Beam at 0°

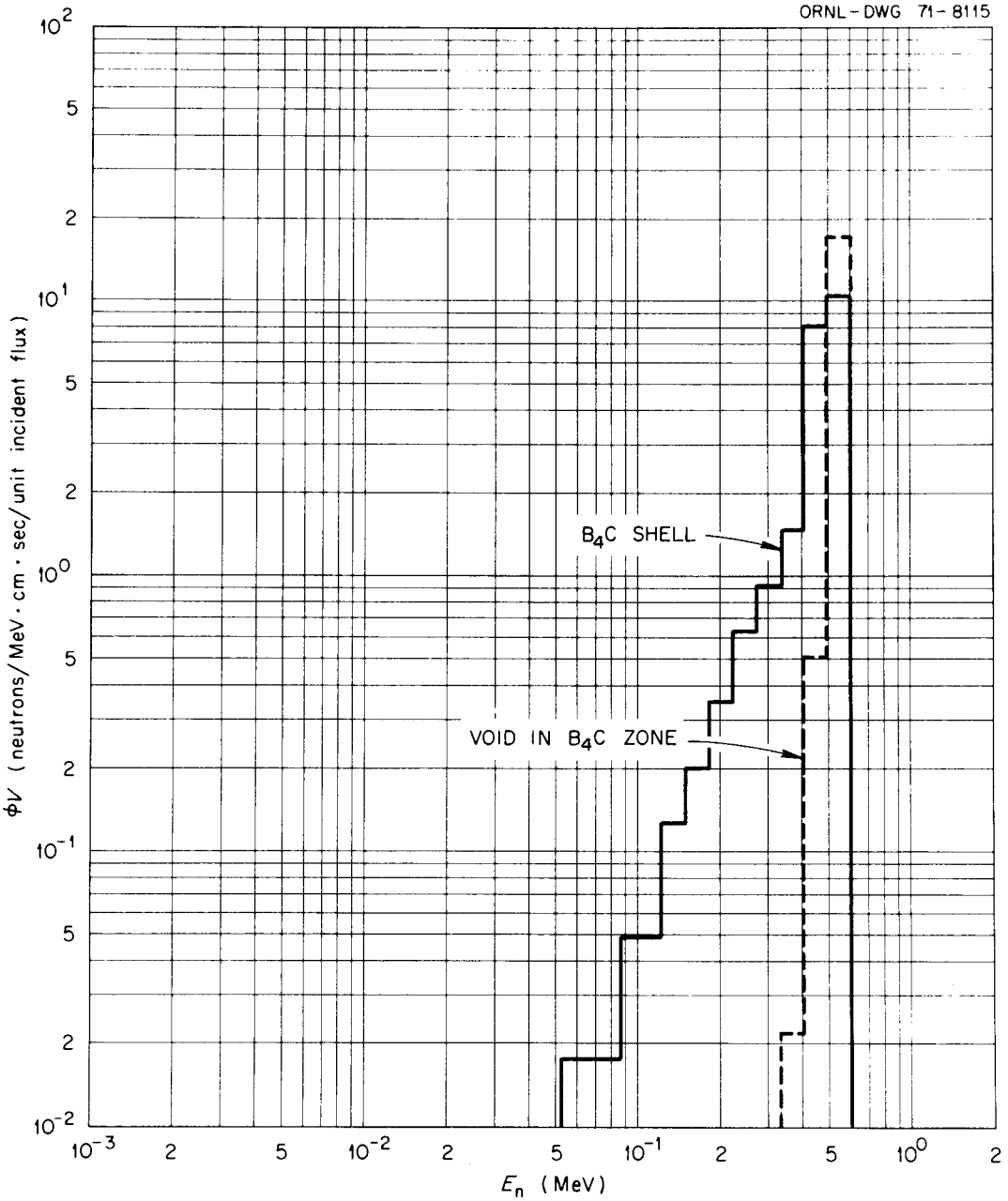

Figure 12. Total Flux in Standard Shell "Detector" due to 0.55 MeV Beam at 0°

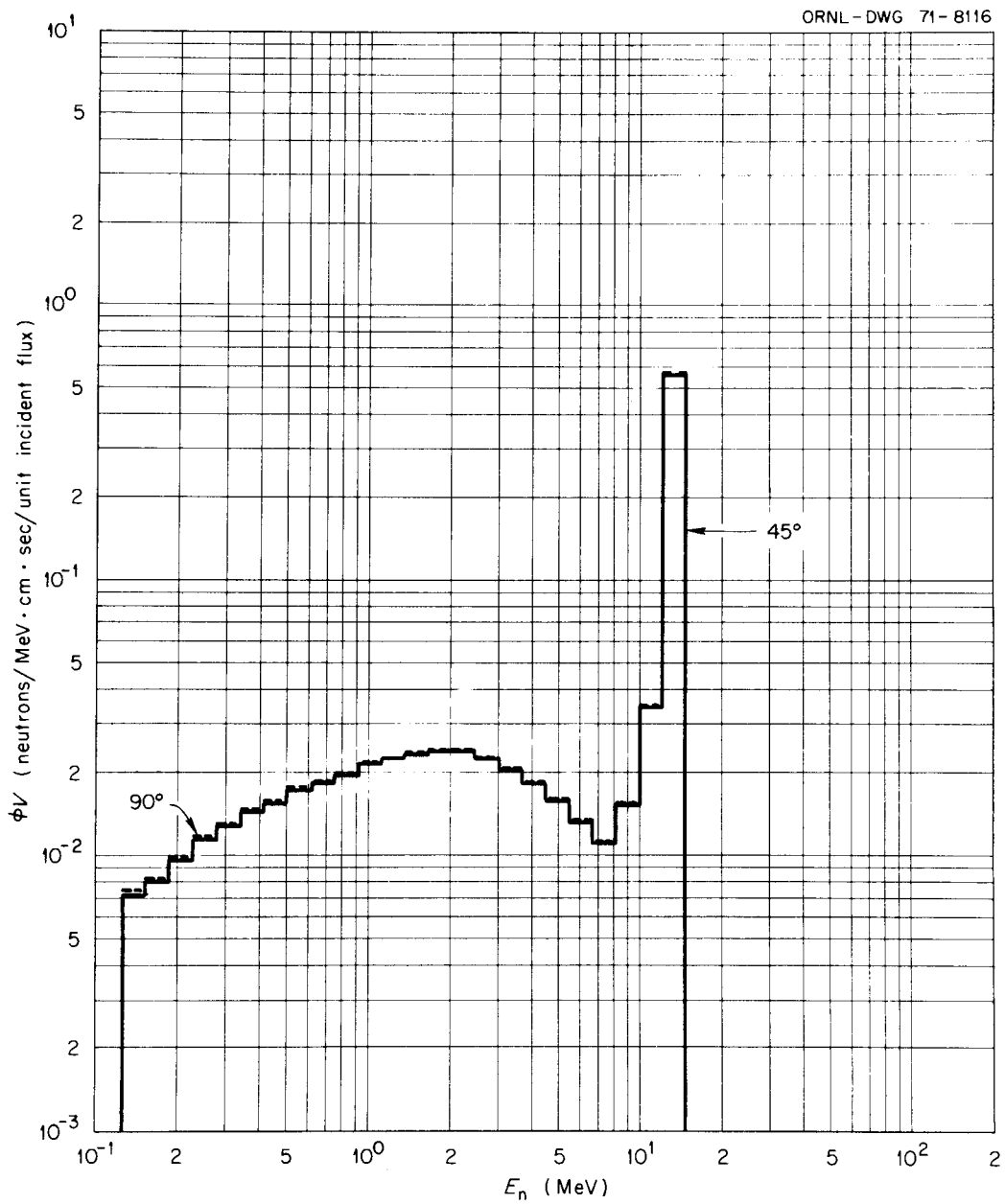

Figure 13. Total Flux in Standard Shell "Detector" due to 13.57 MeV Beam at 45° and 90°

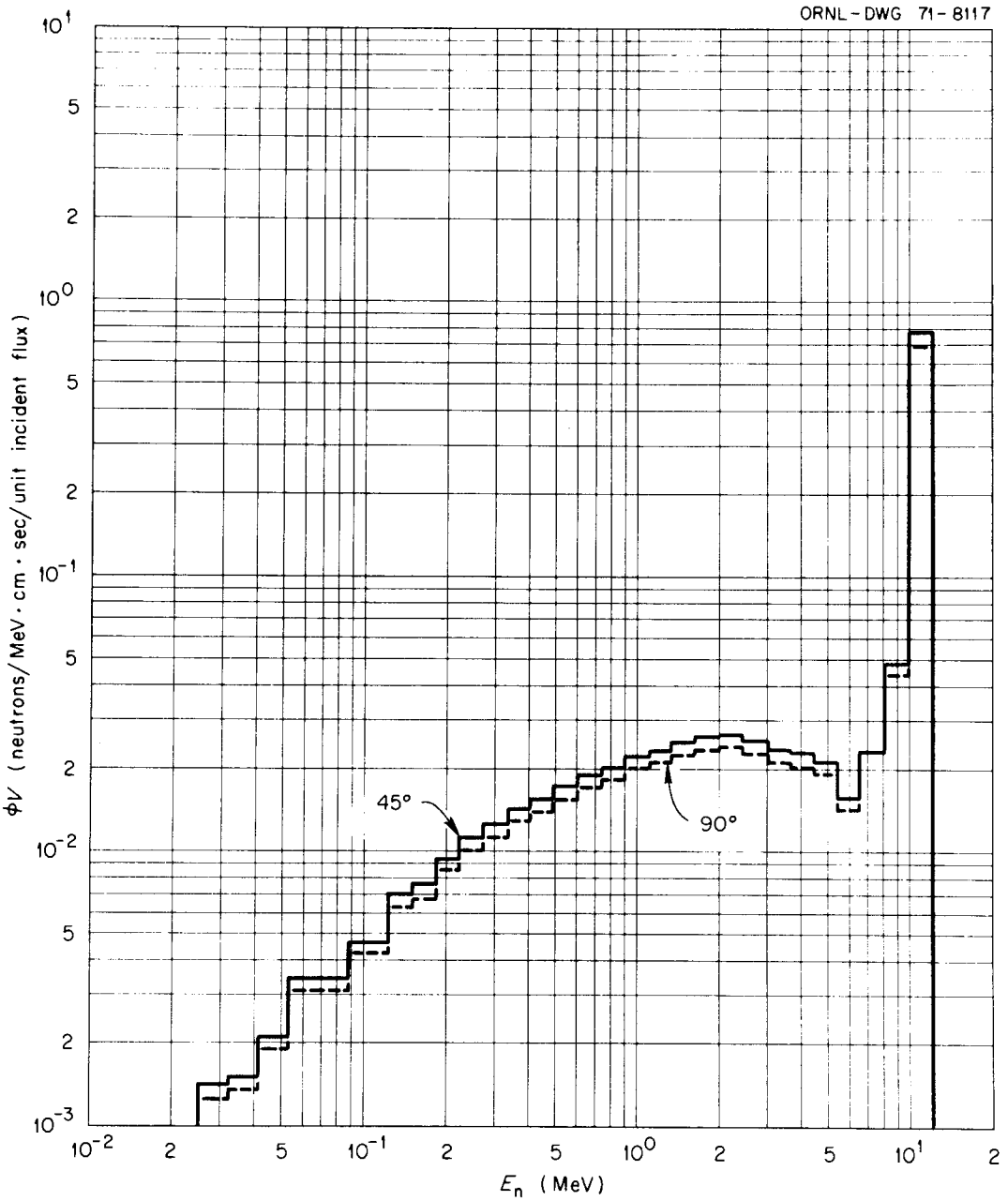

Figure 14. Total Flux in Standard Shell "Detector" due to 11.11 MeV Beam at 45° and 90°

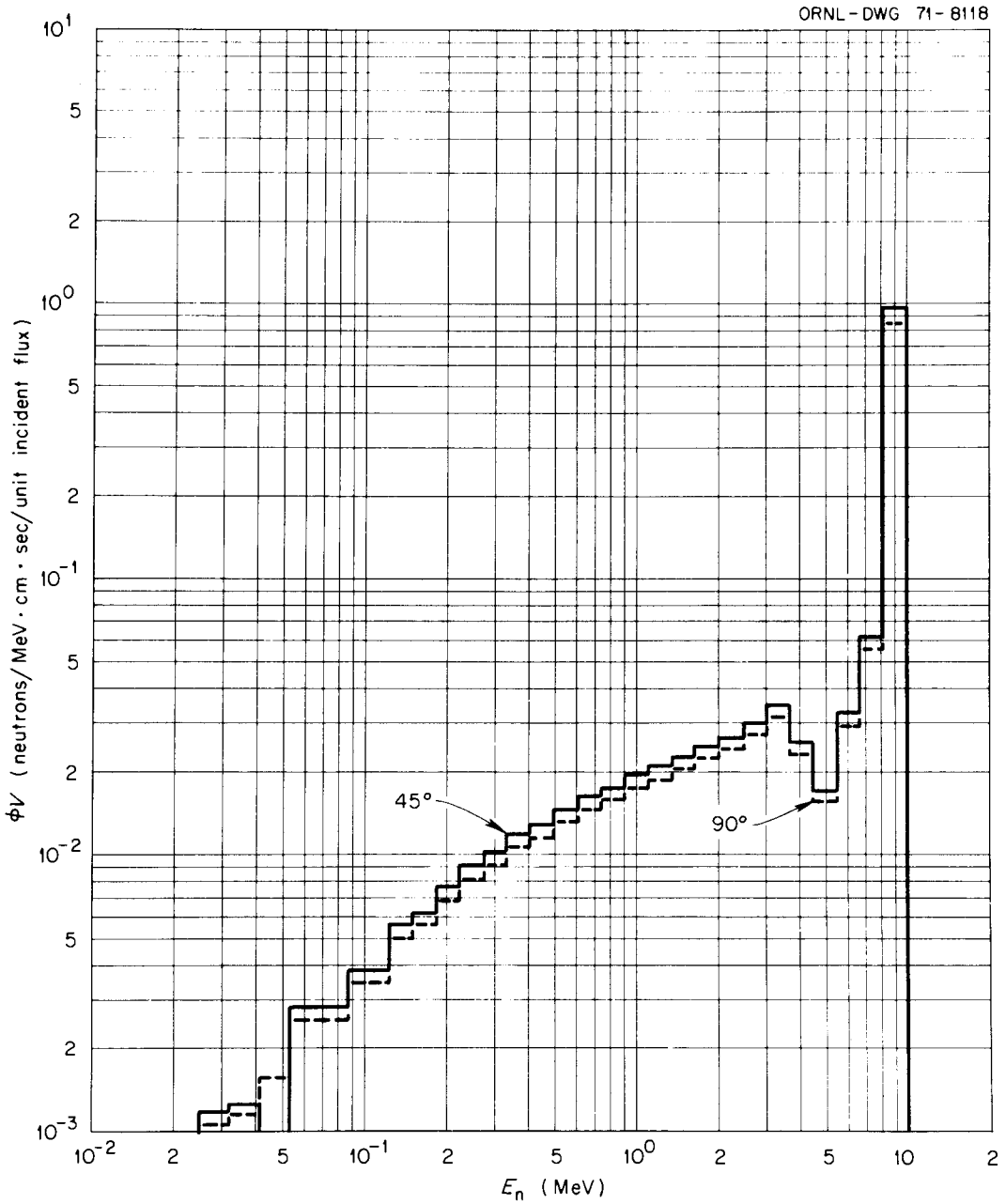

Figure 15. Total Flux in Standard Shell "Detector" due to 9.09 MeV Beam at 45° and 90°

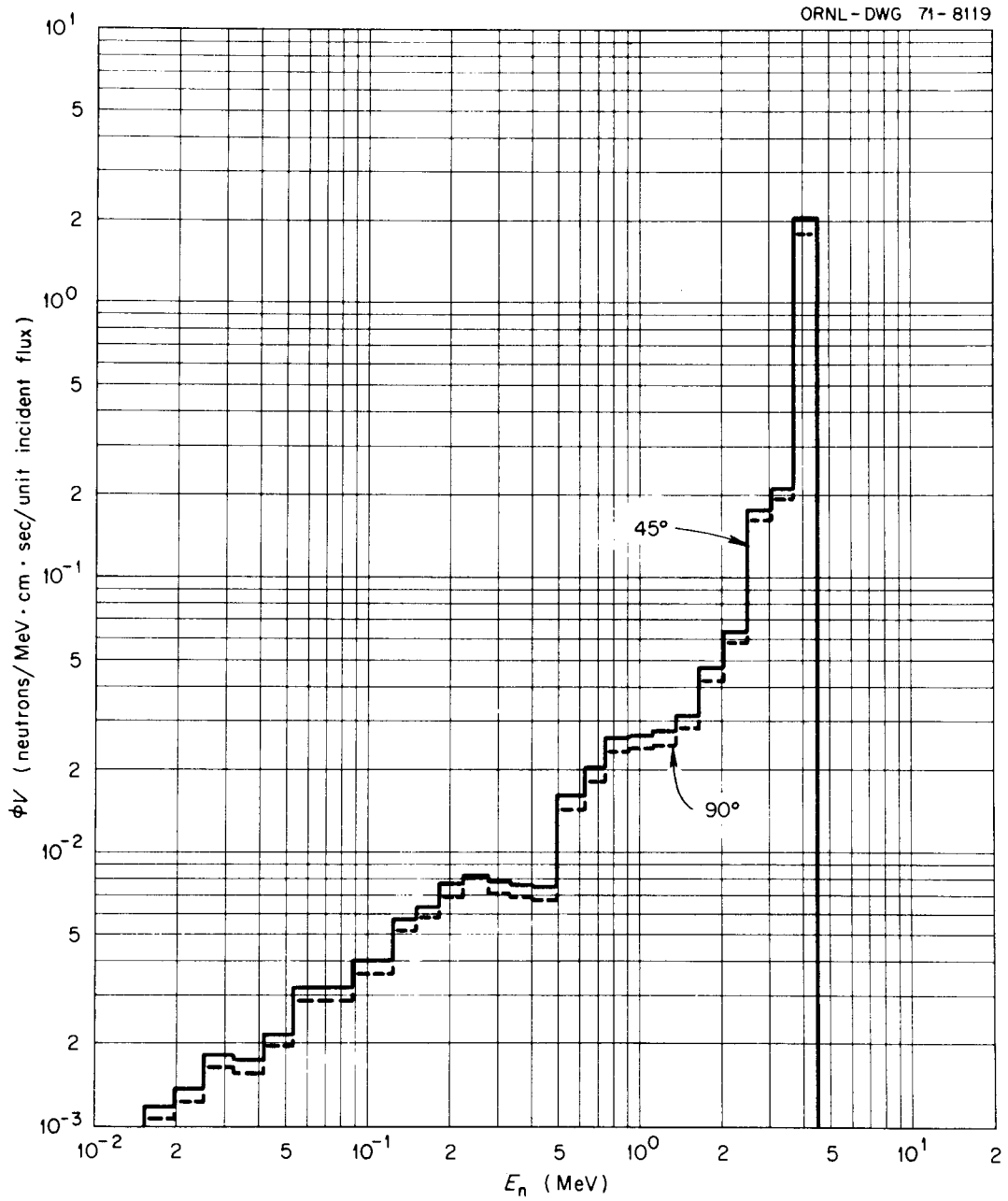

Figure 16. Total Flux in Standard Shell "Detector" due to 4.09 MeV Beam at 45° and 90°

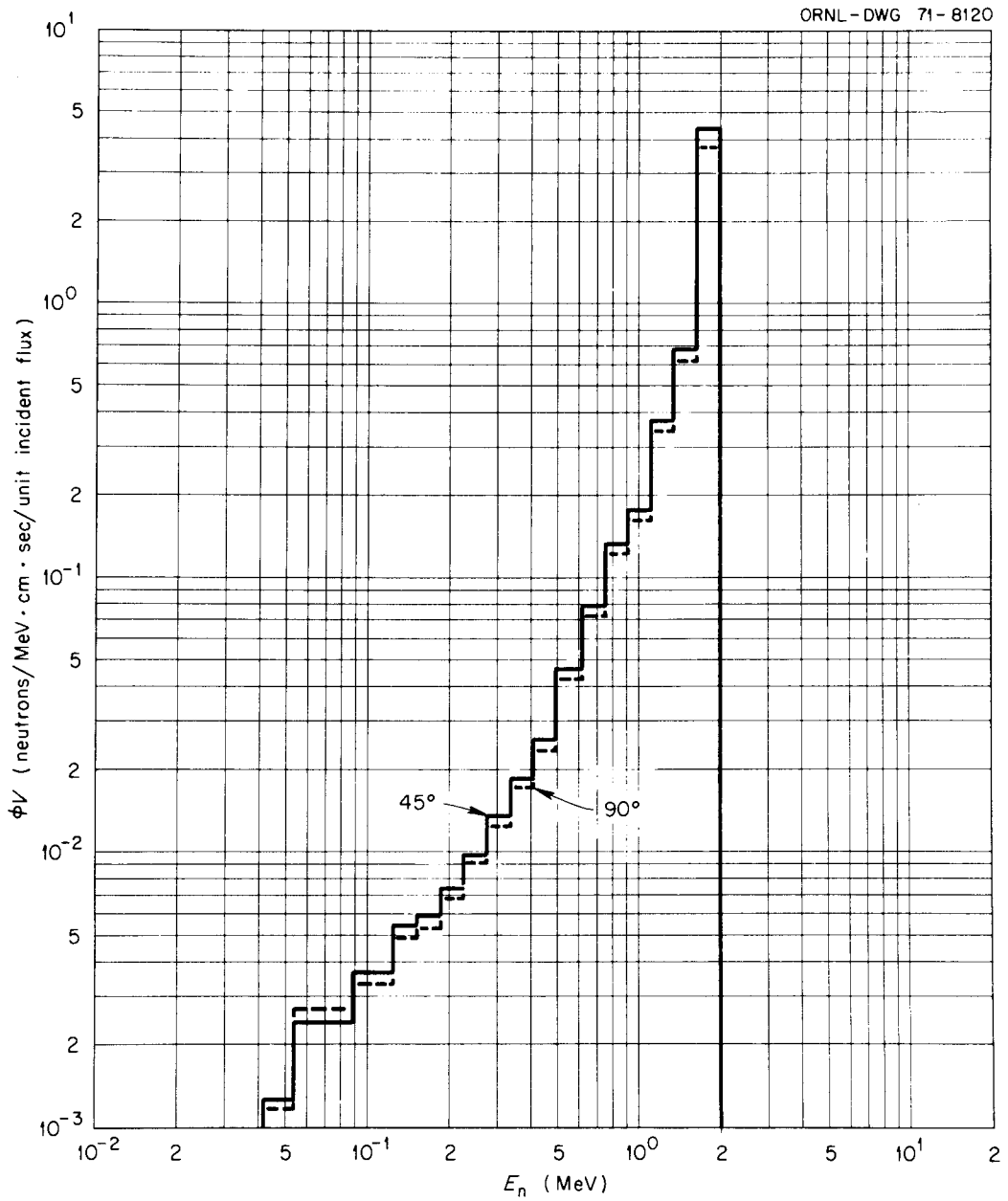

Figure 17. Total Flux in Standard Shell "Detector" due to 1.84 MeV Beam at 45° and 90°

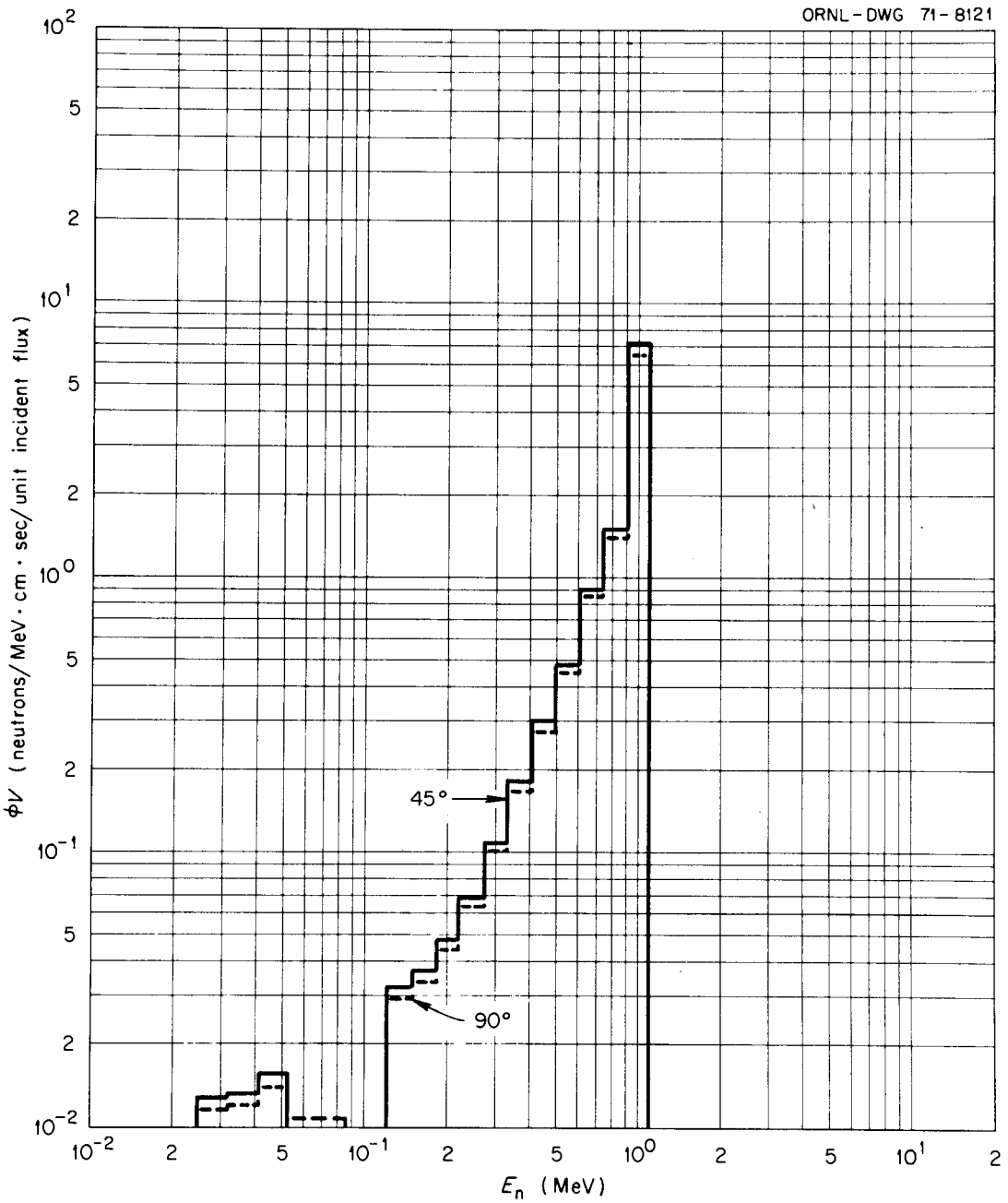

Figure 18. Total Flux in Standard Shell "Detector" due to 1.01 MeV Beam at 45° and 90°

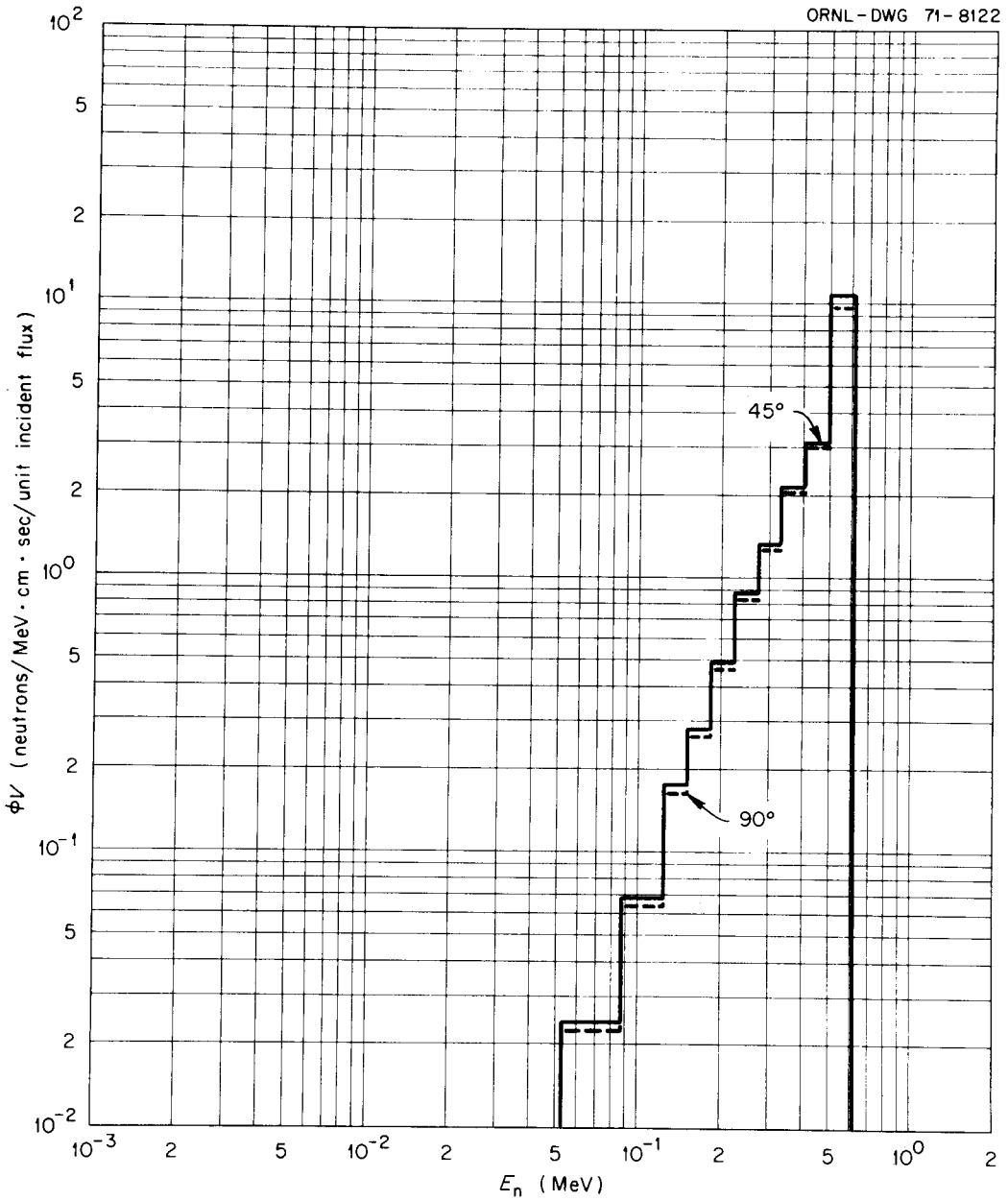

Figure 19. Total Flux in Standard Shell "Detector" due to 0.55 MeV Beam at 45° and 90°

α_j = appropriate angles in the 100 angle quadrature set

S_j = top boundary source input to DOT for angle j
($S_1 = S_2 = S_3 = 1.0$).

Note that the 0° source was described by inputing the source in the first three angles of the quadrature set -- the most downward directed angles. The normalization factor for the 0° case was 23.03. The normalization factors for the 45° and 90° cases were 38.71 and 43.84, respectively.

ØV for the "detector" in the miniature shell and for the unshielded "detector" are listed in Table IX. These results are for the 13.57- and 1.01-MeV beams incident at 0°. The factor to normalize the data in Table IX to an incident flux of unity was 8.23. The normalized data are plotted in Figs. 20 and 21.

The shape of the curves in Figs. 4-21 is due to the neutron interactions in the Al "detectors." However, the difference in the intensities of the shielded and unshielded spectra in Figs. 4-12 and 20-21 is due to the scattering of neutrons in the B_4C shell and the resultant neutrons of energies below the beam energy which strike the "detector." These lower energy neutrons in the shielded beam produce an increase in the intensity of the ØV spectrum below the beam energy. The change in the ØV spectra as a function of beam direction is negligible.

For the threshold foil calculations, the quantity of interest was the activity in each foil, A_r. This activity is defined as:

$$A_{r,k} = \Sigma_{r,k} \sum_{i,j,k}^{\text{Foil, energy}} \phi_{i,j,k} V_{i,j}$$

where

$\Sigma_{r,k}$ = the macroscopic cross section for reaction r for energy group k (given in Table IV, p. 10),

$\phi_{i,j,k}$ = the scalar flux in the axial interval i, radial interval j, and energy group k, per incident source neutron,

$V_{i,j}$ = the volume of the ith-axial interval, jth-radial interval.

Table IX. Total Flux in the "Detector" Within the Miniature B_4C Shell for the 13.57 and 1.01 MeV Beams Incident at 0°

Energy Group	ØV (neutrons-cm/sec/source neutron)			
	13.57 MeV	1.01 MeV	13.57 MeV*	1.01 MeV*
1	3.67043(-2)**	0.0	4.05361(-2)	0.0
2	1.33346(-3)	0.0	1.72455(-4)	0.0
3	4.67795(-4)	0.0	3.50845(-5)	0.0
4	2.71344(-4)	0.0	4.77826(-5)	0.0
5	2.70150(-4)	0.0	5.81421(-5)	0.0
6	2.63515(-4)	0.0	6.35697(-5)	0.0
7	2.47687(-4)	0.0	6.37226(-5)	0.0
8	2.24340(-4)	0.0	5.96686(-5)	0.0
9	1.98948(-4)	0.0	5.25465(-5)	0.0
10	1.71369(-4)	0.0	4.43464(-5)	0.0
11	1.39129(-4)	0.0	3.57931(-5)	0.0
12	1.10134(-4)	0.0	2.79336(-5)	0.0
13	8.55256(-5)	0.0	2.11481(-5)	0.0
14	6.64425(-5)	3.32543(-2)	1.58415(-5)	4.11513(-2)
15	4.98476(-5)	4.19998(-3)	1.15220(-5)	5.11104(-4)
16	3.78475(-5)	1.89152(-3)	8.40720(-6)	1.07184(-5)
17	2.81381(-5)	6.55490(-4)	5.92016(-6)	1.78202(-7)
18	2.07617(-5)	2.94535(-4)	4.14849(-6)	3.33602(-9)
19	1.55983(-5)	1.18352(-4)	2.94049(-6)	9.08764(-11)
20	1.11062(-5)	5.02419(-5)	2.00784(-6)	1.80555(-12)
21	8.00491(-6)	2.18353(-5)	1.41014(-6)	5.24173(-14)
22	5.52672(-6)	1.43024(-5)	9.62420(-7)	6.16518(-6)
23	3.70789(-6)	1.17495(-5)	6.47689(-7)	9.58501(-6)
24	2.71023(-6)	9.49638(-6)	4.77913(-7)	9.08715(-6)
25	2.53059(-6)	3.11856(-6)	4.54476(-7)	1.92601(-6)
26	1.72010(-6)	1.22546(-6)	3.19125(-7)	6.87843(-7)
27	3.67681(-7)	2.89873(-6)	6.85466(-8)	3.44397(-6)
28	2.12009(-7)	2.03816(-6)	4.17012(-8)	2.39330(-6)
29	1.46523(-7)	1.42121(-6)	2.94495(-8)	1.62925(-6)
30	7.76665(-8)	7.54057(-7)	1.58064(-8)	8.52189(-7)
31	4.62411(-8)	4.63484(-7)	9.68301(-9)	5.24307(-7)
32	5.54622(-8)	5.76545(-7)	1.18881(-8)	6.53602(-7)
33	7.24364(-9)	1.11560(-7)	2.28550(-9)	1.30725(-7)
34	1.26242(-9)	2.76991(-8)	1.13021(-10)	3.22695(-8)
35	8.04495(-10)	1.80591(-8)	7.63760(-11)	2.10565(-8)
36	5.22544(-10)	1.19504(-8)	5.33423(-11)	1.38420(-8)
37	2.50064(-10)	7.96737(-9)	3.78638(-11)	9.22880(-9)
38	1.59289(-10)	5.39110(-9)	2.74792(-11)	6.24664(-9)
39	1.11558(-10)	3.70455(-9)	2.01839(-11)	4.29425(-9)
40	1.84391(-10)	5.73765(-9)	3.46738(-11)	6.65153(-9)
41	7.11648(-11)	2.19161(-9)	1.40752(-11)	2.54175(-9)
42	2.88684(-11)	9.20552(-10)	6.05972(-12)	1.06667(-9)
43	8.83763(-12)	4.08980(-10)	1.81872(-12)	4.73992(-10)
44	1.12555(-12)	1.87265(-10)	1.19755(-13)	2.17222(-10)
45	3.33961(-13)	4.00236(-11)	3.19073(-14)	4.31072(-11)
46	9.53662(-14)	2.63729(-12)	7.20955(-15)	3.89307(-13)
47	3.52913(-14)	1.20535(-12)	3.39198(-15)	1.50584(-13)
48	1.35429(-14)	5.68778(-13)	1.60202(-15)	7.10655(-14)
49	6.34537(-15)	3.21684(-13)	9.06493(-16)	4.02117(-14)
50	6.42923(-18)	3.24716(-16)	9.14040(-19)	4.05477(-17)
SUM	4.07425(-2)	4.05344(-2)	4.12735(-2)	4.17104(-2)

*Unshielded detector (void in B_4C zone).

**Numbers in parenthesis indicate power-of-ten multipliers, e.g., 3.67043(-2) = 3.67043×10^{-2}

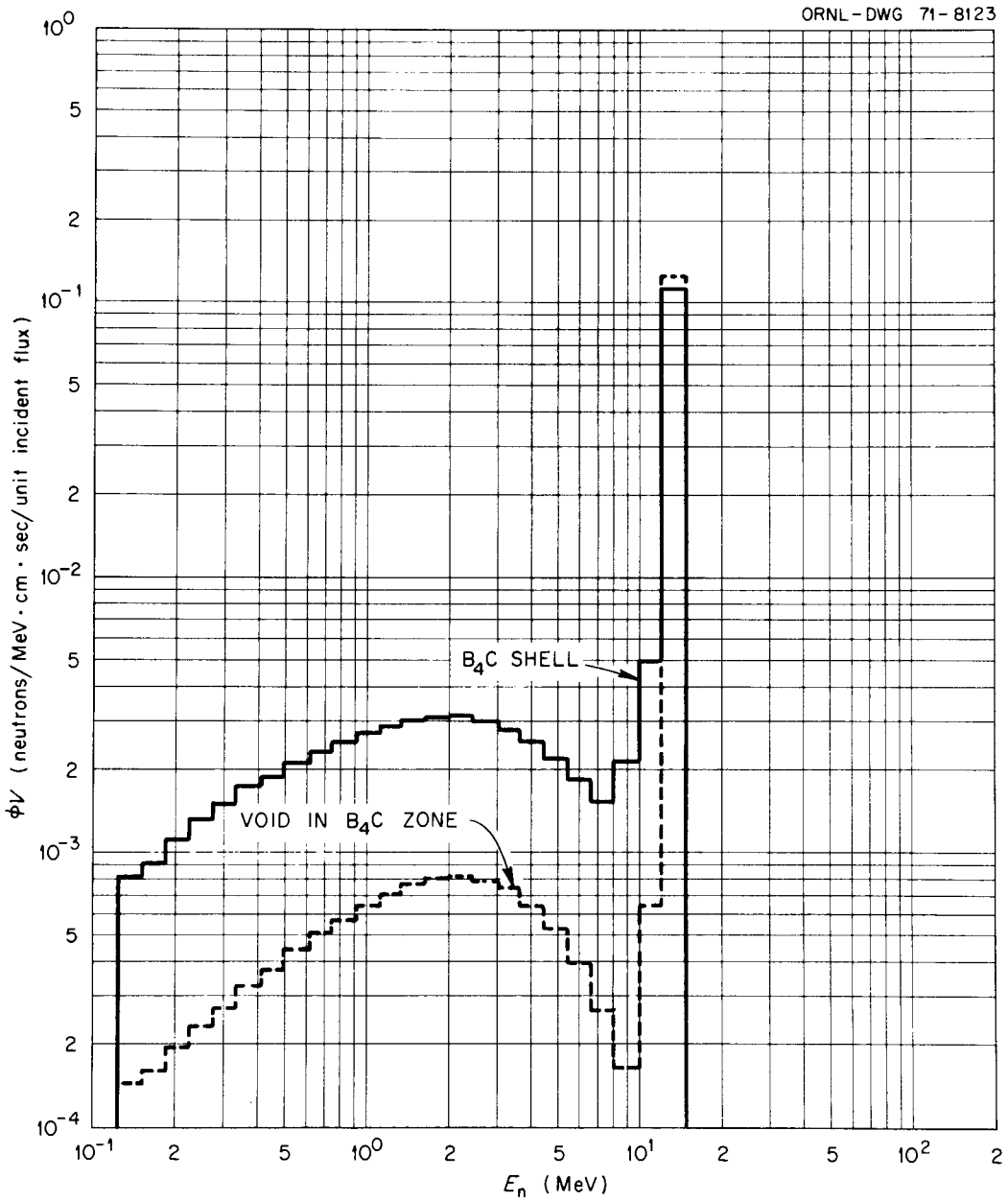

Figure 20. Total Flux in Miniature Shell "Detector" due to 13.57 MeV Beam at 0°

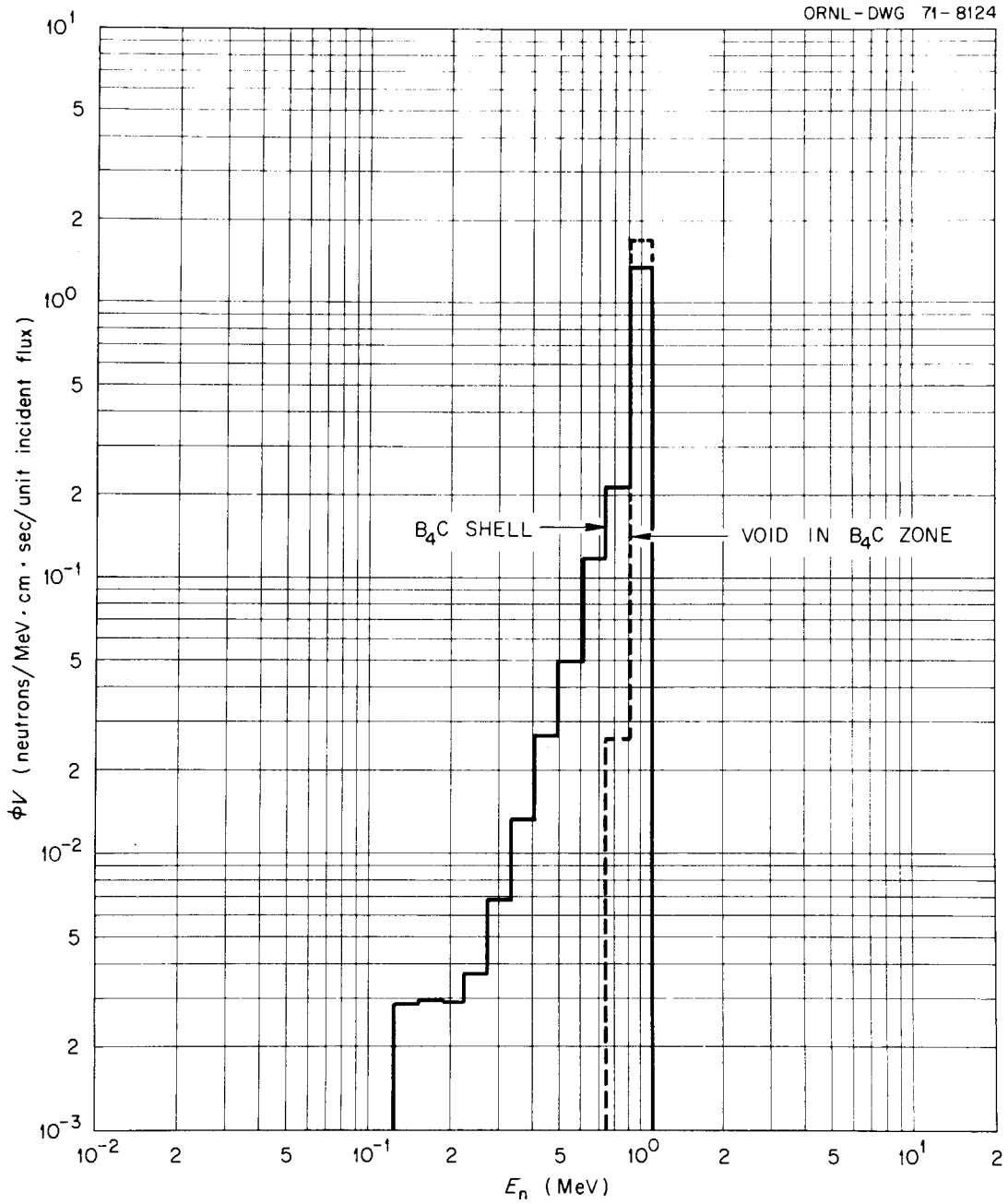

Figure 21. Total Flux in Miniature Shell "Detector" due to 1.01 MeV Beam at 0°

The calculated activities in the threshold foils, positioned as shown in Fig. 3, are listed in Table X for the 13.57-MeV beam incident at 0°. Likewise, the activities for the 13.57-MeV beam at 180°, for the 1.01-MeV beam at 0°, and for the 1.01-MeV beam at 180° are listed in Tables XI, XII, and XIII, respectively. The activities in the various foils are plotted in Figs. 22 through 29 for the 13.57-MeV beam. Both the 0° and 180° beam results are plotted in these figures. Likewise, the activities for the 1.01-MeV beam are plotted in Figs. 30 through 33. The activities plotted in Figs. 22-33 have been normalized to a unit incident flux by multiplying the activities in Tables X-XIII by the 0°, standard shell normalization factor (23.03).

The difference in the shape or magnitude of the 0° and the 180° activities is insufficient to provide a means of determining which end of the detector was up during a measurement.

Table X. Activities in the Threshold Foils for 13.57-MeV Beams Incident at 0°

Energy Group	Activity (reactions/sec/source neutron)							
	A_f^{235U}	A_f^{239Pu}	A_f^{237Np}	A_f^{238U}	$A^{S}_{(n,p)}$	$A^{Mg}_{(n,p)}$	$A^{Al}_{(n,\alpha)}$	$A^{Zr}_{(n,2n')}$
1	8.47315(-4)*	3.19906(-3)	5.55541(-5)	1.33270(-3)	4.85819(-4)	3.96797(-4)	2.71507(-4)	5.85640(-4)
2	3.09105(-5)	1.29871(-4)	2.31843(-6)	5.21388(-5)	2.54235(-5)	1.51266(-5)	1.03167(-5)	1.54589(-5)
3	1.14680(-5)	4.58840(-5)	8.10679(-7)	1.91079(-5)	8.86662(-6)	2.94995(-6)	2.21970(-6)	1.77981(-6)
4	6.38444(-6)	2.69338(-5)	4.65099(-7)	1.11345(-5)	5.22275(-6)	7.24844(-7)	5.27313(-7)	8.68971(-8)
5	4.95121(-6)	2.34343(-5)	3.84202(-7)	8.04943(-6)	5.07302(-6)	1.94489(-7)	4.75824(-8)	0.0
6	4.93750(-6)	2.41533(-5)	3.83938(-7)	7.06967(-6)	4.44797(-6)	4.13896(-8)	0.0	0.0
7	5.56661(-6)	2.71074(-5)	4.27768(-7)	7.56673(-6)	5.16842(-6)	1.55061(-10)	0.0	0.0
8	6.15140(-6)	2.95440(-5)	4.63356(-7)	7.69583(-6)	3.69322(-6)	0.0	0.0	0.0
9	6.74108(-6)	3.08843(-5)	4.92031(-7)	8.16113(-6)	1.71640(-6)	0.0	0.0	0.0
10	7.17851(-6)	3.27842(-5)	4.95598(-7)	8.76019(-6)	1.05337(-6)	0.0	0.0	0.0
11	6.70249(-6)	3.22596(-5)	4.70195(-7)	7.37066(-6)	7.23166(-8)	0.0	0.0	0.0
12	5.85425(-6)	2.79449(-5)	4.25301(-7)	3.86046(-6)	3.50090(-9)	0.0	0.0	0.0
13	5.12209(-6)	2.38609(-5)	3.75621(-7)	6.14796(-7)	0.0	0.0	0.0	0.0
14	4.44501(-6)	2.03005(-5)	3.17857(-7)	2.02110(-7)	0.0	0.0	0.0	0.0
15	3.63724(-6)	1.72188(-5)	2.29998(-7)	5.73624(-8)	0.0	0.0	0.0	0.0
16	2.89938(-6)	1.36660(-5)	1.44625(-7)	1.25926(-8)	0.0	0.0	0.0	0.0
17	2.36750(-6)	1.07404(-5)	7.34789(-8)	4.53333(-9)	0.0	0.0	0.0	0.0
18	1.93897(-6)	8.46294(-6)	2.45778(-8)	0.0	0.0	0.0	0.0	0.0
19	1.57664(-6)	6.62031(-6)	7.87702(-9)	0.0	0.0	0.0	0.0	0.0
20	1.24026(-6)	4.99618(-6)	3.90331(-9)	0.0	0.0	0.0	0.0	0.0
21	9.66686(-7)	3.74762(-6)	2.27383(-9)	0.0	0.0	0.0	0.0	0.0
22	7.31662(-7)	2.72362(-6)	1.32278(-9)	0.0	0.0	0.0	0.0	0.0
23	5.43117(-7)	1.94158(-6)	7.78776(-10)	0.0	0.0	0.0	0.0	0.0
24	3.98947(-7)	1.37130(-6)	4.64695(-10)	0.0	0.0	0.0	0.0	0.0
25	4.49149(-7)	1.46511(-6)	4.05949(-10)	0.0	0.0	0.0	0.0	0.0
26	3.27881(-7)	9.88378(-7)	2.05520(-10)	0.0	0.0	0.0	0.0	0.0
27	8.59748(-8)	2.39574(-7)	3.99183(-11)	0.0	0.0	0.0	0.0	0.0
28	5.69644(-8)	1.51901(-7)	2.25967(-11)	0.0	0.0	0.0	0.0	0.0
29	3.68112(-8)	9.35908(-8)	1.30120(-11)	0.0	0.0	0.0	0.0	0.0
30	2.64623(-8)	6.83159(-8)	8.98055(-12)	0.0	0.0	0.0	0.0	0.0
31	1.67396(-8)	4.16168(-8)	6.23180(-12)	0.0	0.0	0.0	0.0	0.0
32	2.23340(-8)	5.23653(-8)	9.92376(-12)	0.0	0.0	0.0	0.0	0.0
33	4.73765(-9)	9.71884(-9)	2.79021(-12)	0.0	0.0	0.0	0.0	0.0
34	1.46226(-9)	2.82825(-9)	8.74401(-13)	0.0	0.0	0.0	0.0	0.0
35	9.16934(-10)	2.12014(-9)	5.90496(-13)	0.0	0.0	0.0	0.0	0.0

Table X (Cont'd.)

Energy Group	Activity (reactions/sec/source neutron)							
	A_f^{235U}	A_f^{239Pu}	A_f^{237Np}	A_f^{U}	$A^{S}_{(n,p)}$	$A^{Mg}_{(n,p)}$	$A^{Al}_{(n,\alpha)}$	$A^{Zr}_{(n,2n')}$
36	5.31334(-10)	9.40345(-10)	3.51281(-13)	0.0	0.0	0.0	0.0	0.0
37	6.20177(-10)	1.17148(-9)	4.55804(-13)	0.0	0.0	0.0	0.0	0.0
38	2.66977(-10)	7.53742(-10)	2.03475(-13)	0.0	0.0	0.0	0.0	0.0
39	1.77019(-10)	4.82749(-10)	1.48838(-13)	0.0	0.0	0.0	0.0	0.0
40	2.26393(-10)	5.45831(-10)	1.70625(-13)	0.0	0.0	0.0	0.0	0.0
41	9.03503(-11)	2.52582(-10)	8.15935(-14)	0.0	0.0	0.0	0.0	0.0
42	3.11199(-11)	1.09342(-10)	3.65594(-14)	0.0	0.0	0.0	0.0	0.0
43	1.17439(-11)	6.29264(-11)	1.63681(-14)	0.0	0.0	0.0	0.0	0.0
44	6.19494(-12)	8.29891(-12)	4.09402(-15)	0.0	0.0	0.0	0.0	0.0
45	1.47789(-12)	7.42107(-12)	2.91395(-22)	0.0	0.0	0.0	0.0	0.0
46	5.08215(-13)	1.24964(-12)	6.52162(-22)	0.0	0.0	0.0	0.0	0.0
47	1.13780(-13)	2.78924(-13)	5.24653(-20)	0.0	0.0	0.0	0.0	0.0
48	6.37845(-14)	2.17327(-13)	1.50999(-18)	0.0	0.0	0.0	0.0	0.0
49	4.29212(-14)	1.59846(-13)	2.51891(-19)	0.0	0.0	0.0	0.0	0.0
50	1.07770(-16)	4.92222(-16)	2.91346(-21)	0.0	0.0	0.0	0.0	0.0
SUM	9.71055(-4)	3.74862(-3)	6.38740(-5)	1.47451(-3)	5.46559(-4)	4.15834(-4)	2.84618(-4)	6.02965(-4)

*Numbers in parenthesis indicate power-of-ten multiplier, e.g., 8.47315(-4) = 8.47315×10^{-4}

Table XI. Activities in the Threshold Foils for 13.57-MeV Beam Incident at 180°

Energy Group	Activity (reactions/sec/source neutron)							
	A_f^{235U}	A_f^{239Pu}	A_f^{237Np}	A_f^{238U}	$A^{S}_{(n,p)}$	$A^{Mg}_{(n,p)}$	$A^{Al}_{(n,\alpha)}$	$A^{Zr}_{(n,2n')}$
1	7.63402(-4)*	3.03196(-3)	5.45725(-5)	1.35460(-3)	5.18762(-4)	4.20032(-4)	2.93224(-4)	6.46927(-4)
2	2.84870(-5)	1.23456(-4)	2.25419(-6)	5.18775(-5)	2.62271(-5)	1.52775(-5)	1.07958(-5)	1.68814(-5)
3	1.06766(-5)	4.27439(-5)	7.61960(-7)	1.81453(-5)	8.88971(-6)	3.06132(-6)	2.38267(-6)	1.93870(-6)
4	5.82692(-6)	2.51522(-5)	4.43748(-7)	1.08406(-5)	5.36476(-6)	7.58987(-7)	5.67589(-7)	9.51617(-8)
5	4.53180(-6)	2.19714(-5)	3.68059(-7)	7.86235(-6)	5.21834(-6)	2.03288(-7)	5.10547(-8)	0.0
6	4.53129(-6)	2.26831(-5)	3.68105(-7)	6.89981(-6)	4.56770(-6)	4.31916(-8)	0.0	0.0
7	5.11243(-6)	2.54698(-5)	4.10268(-7)	7.38109(-6)	5.30256(-6)	1.61672(-10)	0.0	0.0
8	5.65506(-6)	2.77781(-5)	4.44619(-7)	7.50477(-6)	3.78506(-6)	0.0	0.0	0.0
9	6.21156(-6)	2.90848(-5)	4.72652(-7)	7.95942(-6)	1.75659(-6)	0.0	0.0	0.0
10	6.63164(-6)	3.09405(-5)	4.76981(-7)	8.55455(-6)	1.07724(-6)	0.0	0.0	0.0
11	6.20616(-6)	3.05049(-5)	4.53343(-7)	7.20636(-6)	7.39072(-8)	0.0	0.0	0.0
12	5.43329(-6)	2.64778(-5)	4.10819(-7)	3.77971(-6)	3.57714(-9)	0.0	0.0	0.0
13	4.76601(-6)	2.26571(-5)	3.63515(-7)	6.02753(-7)	0.0	0.0	0.0	0.0
14	4.14742(-6)	1.93210(-5)	3.08220(-7)	1.98446(-7)	0.0	0.0	0.0	0.0
15	3.40123(-6)	1.64166(-5)	2.23301(-7)	5.63585(-8)	0.0	0.0	0.0	0.0
16	2.71828(-6)	1.30561(-5)	1.40623(-7)	1.23845(-8)	0.0	0.0	0.0	0.0
17	2.22388(-6)	1.02758(-5)	7.15127(-8)	4.46106(-9)	0.0	0.0	0.0	0.0
18	1.82418(-6)	8.10472(-6)	2.39305(-8)	0.0	0.0	0.0	0.0	0.0
19	1.48637(-6)	6.35043(-6)	7.67776(-9)	0.0	0.0	0.0	0.0	0.0
20	1.17016(-6)	4.79421(-6)	3.80434(-9)	0.0	0.0	0.0	0.0	0.0
21	9.13492(-7)	3.60057(-6)	2.21792(-9)	0.0	0.0	0.0	0.0	0.0
22	6.92044(-7)	2.61878(-6)	1.29096(-9)	0.0	0.0	0.0	0.0	0.0
23	5.13954(-7)	1.86747(-6)	7.60171(-10)	0.0	0.0	0.0	0.0	0.0
24	3.77756(-7)	1.31961(-6)	4.53732(-10)	0.0	0.0	0.0	0.0	0.0
25	4.25176(-7)	1.40946(-6)	3.96249(-10)	0.0	0.0	0.0	0.0	0.0
26	3.10536(-7)	9.51583(-7)	2.00722(-10)	0.0	0.0	0.0	0.0	0.0
27	8.14214(-8)	2.30694(-7)	3.89993(-11)	0.0	0.0	0.0	0.0	0.0
28	5.38870(-8)	1.46112(-7)	2.20497(-11)	0.0	0.0	0.0	0.0	0.0
29	3.48143(-8)	9.00746(-8)	1.27109(-11)	0.0	0.0	0.0	0.0	0.0
30	2.50058(-8)	6.56437(-8)	8.75057(-12)	0.0	0.0	0.0	0.0	0.0
31	1.58212(-8)	4.00121(-8)	6.07786(-12)	0.0	0.0	0.0	0.0	0.0
32	2.11079(-8)	5.03458(-8)	9.67806(-12)	0.0	0.0	0.0	0.0	0.0
33	4.48091(-9)	9.35441(-9)	2.72430(-12)	0.0	0.0	0.0	0.0	0.0
34	1.38365(-9)	2.72172(-9)	8.53066(-13)	0.0	0.0	0.0	0.0	0.0
35	8.67485(-10)	2.04090(-9)	5.76477(-13)	0.0	0.0	0.0	0.0	0.0

Table XI (Cont'd.)

Energy Group	Activity (reactions/sec/source neutron)							
	A_f^{235U}	A_f^{239Pu}	A_f^{237Np}	A_f^{238U}	$A^{S}_{(n,p)}$	$A^{Mg}_{(n,p)}$	$A^{Al}_{(n,\alpha)}$	$A^{Zr}_{(n,2n')}$
36	4.99944(-10)	9.03065(-10)	3.42753(-13)	0.0	0.0	0.0	0.0	0.0
37	5.86271(-10)	1.12204(-9)	4.40781(-13)	0.0	0.0	0.0	0.0	0.0
38	2.53718(-10)	7.28019(-10)	1.98871(-13)	0.0	0.0	0.0	0.0	0.0
39	1.68718(-10)	4.67336(-10)	1.45643(-13)	0.0	0.0	0.0	0.0	0.0
40	2.13477(-10)	5.22894(-10)	1.64978(-13)	0.0	0.0	0.0	0.0	0.0
41	8.52609(-11)	2.42072(-10)	7.88618(-14)	0.0	0.0	0.0	0.0	0.0
42	2.94590(-11)	1.04833(-10)	3.53446(-14)	0.0	0.0	0.0	0.0	0.0
43	1.10129(-11)	5.98216(-11)	1.57077(-14)	0.0	0.0	0.0	0.0	0.0
44	5.81299(-12)	7.89008(-12)	3.93279(-15)	0.0	0.0	0.0	0.0	0.0
45	1.38044(-12)	7.07003(-12)	2.81434(-22)	0.0	0.0	0.0	0.0	0.0
46	4.78388(-13)	1.19509(-12)	6.31392(-22)	0.0	0.0	0.0	0.0	0.0
47	1.06867(-13)	2.63730(-13)	4.97283(-20)	0.0	0.0	0.0	0.0	0.0
48	5.98563(-14)	2.05146(-13)	1.42947(-18)	0.0	0.0	0.0	0.0	0.0
49	4.02408(-14)	1.50656(-13)	2.38851(-19)	0.0	0.0	0.0	0.0	0.0
50	1.01132(-16)	4.57307(-16)	2.70451(-21)	0.0	0.0	0.0	0.0	0.0
SUM	8.77911(-4)	3.55160(-3)	6.25850(-5)	1.49349(-3)	5.81027(-4)	4.39375(-4)	3.07020(-4)	6.65842(-4)

*Numbers in parenthesis indicate power-of-ten multipliers, e.g., 7.63402(-4) = 7.63402×10^{-4}

Table XII. Activities in the Threshold Foils for 1.01 MeV Beam Incident at 0°

Energy Group	Activity (reactions/sec/source neutron)							
	A_f^{235U}	A_f^{239Pu}	A_f^{237Np}	A_f^{238U}	$A^{S}_{(n,p)}$	$A^{Mg}_{(n,p)}$	$A^{A\ell}_{(n,\alpha)}$	$A^{Zr}_{(n,2n')}$
1	0.0	0.0	0.0	0.0	0.0	0.0	0.0	0.0
2	0.0	0.0	0.0	0.0	0.0	0.0	0.0	0.0
3	0.0	0.0	0.0	0.0	0.0	0.0	0.0	0.0
4	0.0	0.0	0.0	0.0	0.0	0.0	0.0	0.0
5	0.0	0.0	0.0	0.0	0.0	0.0	0.0	0.0
6	0.0	0.0	0.0	0.0	0.0	0.0	0.0	0.0
7	0.0	0.0	0.0	0.0	0.0	0.0	0.0	0.0
8	0.0	0.0	0.0	0.0	0.0	0.0	0.0	0.0
9	0.0	0.0	0.0	0.0	0.0	0.0	0.0	0.0
10	0.0	0.0	0.0	0.0	0.0	0.0	0.0	0.0
11	0.0	0.0	0.0	0.0	0.0	0.0	0.0	0.0
12	0.0	0.0	0.0	0.0	0.0	0.0	0.0	0.0
13	0.0	0.0	0.0	0.0	0.0	0.0	0.0	0.0
14	5.04975(-04)*	2.18865(-03)	3.14529(-05)	1.89547(-05)	0.0	0.0	0.0	0.0
15	7.04604(-05)	3.13827(-04)	3.83956(-06)	9.05014(-07)	0.0	0.0	0.0	0.0
16	3.13222(-05)	1.42069(-04)	1.36522(-06)	1.12252(-07)	0.0	0.0	0.0	0.0
17	1.55173(-05)	6.57645(-05)	3.96149(-07)	2.24326(-08)	0.0	0.0	0.0	0.0
18	9.62938(-06)	3.88623(-05)	9.58141(-08)	0.0	0.0	0.0	0.0	0.0
19	5.73820(-06)	2.23964(-05)	2.38003(-08)	0.0	0.0	0.0	0.0	0.0
20	3.53245(-06)	1.36227(-05)	9.91753(-09)	0.0	0.0	0.0	0.0	0.0
21	2.37513(-06)	9.18507(-06)	5.30366(-09)	0.0	0.0	0.0	0.0	0.0
22	1.44861(-06)	5.36809(-06)	2.34612(-09)	0.0	0.0	0.0	0.0	0.0
23	9.65403(-07)	3.43055(-06)	1.22916(-09)	0.0	0.0	0.0	0.0	0.0
24	6.97915(-07)	2.41419(-06)	7.73161(-10)	0.0	0.0	0.0	0.0	0.0
25	9.36119(-07)	3.12458(-06)	8.53957(-10)	0.0	0.0	0.0	0.0	0.0
26	7.52064(-07)	2.33561(-06)	4.89135(-10)	0.0	0.0	0.0	0.0	0.0
27	2.41630(-07)	7.11260(-07)	1.24942(-10)	0.0	0.0	0.0	0.0	0.0
28	1.78112(-07)	5.01909(-07)	7.86549(-11)	0.0	0.0	0.0	0.0	0.0
29	1.38697(-07)	3.77409(-07)	5.66314(-11)	0.0	0.0	0.0	0.0	0.0
30	1.47299(-07)	4.07377(-07)	5.81685(-11)	0.0	0.0	0.0	0.0	0.0
31	1.02814(-07)	2.75541(-07)	4.52259(-11)	0.0	0.0	0.0	0.0	0.0
32	1.42258(-07)	3.58053(-07)	7.40863(-11)	0.0	0.0	0.0	0.0	0.0
33	3.17445(-08)	6.96700(-08)	2.17139(-11)	0.0	0.0	0.0	0.0	0.0
34	9.74989(-09)	2.01109(-08)	6.69196(-12)	0.0	0.0	0.0	0.0	0.0
35	6.13543(-09)	1.50933(-08)	4.52632(-12)	0.0	0.0	0.0	0.0	0.0

Table XII (Cont'd.)

Energy Group	Activity (reactions/sec/source neutron)							
	A_f^{235U}	A_f^{239Pu}	A_f^{237Np}	A_f^{238U}	$A^{S}_{(n,p)}$	$A^{Mg}_{(n,p)}$	$A^{A\ell}_{(n,\alpha)}$	$A^{Zr}_{(n,2n')}$
36	3.60790(-09)	6.87729(-09)	2.75717(-12)	0.0	0.0	0.0	0.0	0.0
37	4.48765(-09)	8.89777(-09)	3.60428(-12)	0.0	0.0	0.0	0.0	0.0
38	2.15936(-09)	6.42366(-09)	1.78788(-12)	0.0	0.0	0.0	0.0	0.0
39	1.54285(-09)	4.28802(-09)	1.33101(-12)	0.0	0.0	0.0	0.0	0.0
40	2.54134(-09)	6.53979(-09)	2.19347(-12)	0.0	0.0	0.0	0.0	0.0
41	1.00356(-09)	2.83367(-09)	9.31795(-13)	0.0	0.0	0.0	0.0	0.0
42	3.81880(-10)	1.24103(-09)	3.92469(-13)	0.0	0.0	0.0	0.0	0.0
43	1.63765(-10)	8.29691(-10)	2.06489(-13)	0.0	0.0	0.0	0.0	0.0
44	9.00743(-11)	1.17174(-10)	5.59963(-14)	0.0	0.0	0.0	0.0	0.0
45	1.93307(-11)	9.25986(-11)	3.49010(-21)	0.0	0.0	0.0	0.0	0.0
46	4.94529(-12)	1.17395(-11)	5.92272(-21)	0.0	0.0	0.0	0.0	0.0
47	1.10976(-12)	2.64708(-12)	4.83880(-19)	0.0	0.0	0.0	0.0	0.0
48	6.38398(-13)	2.10597(-12)	1.41712(-17)	0.0	0.0	0.0	0.0	0.0
49	4.43944(-13)	1.58240(-12)	2.38584(-18)	0.0	0.0	0.0	0.0	0.0
50	1.11772(-15)	4.88053(-15)	2.81668(-20)	0.0	0.0	0.0	0.0	0.0
SUM	6.49361(-04)	2.81382(-03)	3.71947(-05)	1.99943(-05)	0.0	0.0	0.0	0.0

*Read ad 5.04975×10^{-4}

Table XIII. Activities in the Threshold Foils for 1.01 MeV Beam Incident at 180°

Energy Group	Activity (reactions/sec/source neutron)							
	A_f^{235U}	A_f^{239Pu}	A_f^{237Np}	A_f^{238U}	$A^{S}_{(n,p)}$	$A^{Mg}_{(n,p)}$	$A^{A\ell}_{(n,\alpha)}$	$A^{Zr}_{(n,2n')}$
1	0.0	0.0	0.0	0.0	0.0	0.0	0.0	0.0
2	0.0	0.0	0.0	0.0	0.0	0.0	0.0	0.0
3	0.0	0.0	0.0	0.0	0.0	0.0	0.0	0.0
4	0.0	0.0	0.0	0.0	0.0	0.0	0.0	0.0
5	0.0	0.0	0.0	0.0	0.0	0.0	0.0	0.0
6	0.0	0.0	0.0	0.0	0.0	0.0	0.0	0.0
7	0.0	0.0	0.0	0.0	0.0	0.0	0.0	0.0
8	0.0	0.0	0.0	0.0	0.0	0.0	0.0	0.0
9	0.0	0.0	0.0	0.0	0.0	0.0	0.0	0.0
10	0.0	0.0	0.0	0.0	0.0	0.0	0.0	0.0
11	0.0	0.0	0.0	0.0	0.0	0.0	0.0	0.0
12	0.0	0.0	0.0	0.0	0.0	0.0	0.0	0.0
13	0.0	0.0	0.0	0.0	0.0	0.0	0.0	0.0
14	4.27656(-04)*	1.98145(-03)	3.01093(-05)	1.92241(-05)	0.0	0.0	0.0	0.0
15	5.37813(-05)	2.59239(-04)	3.41124(-06)	8.65682(-07)	0.0	0.0	0.0	0.0
16	2.83416(-05)	1.28822(-04)	1.25425(-06)	1.04617(-07)	0.0	0.0	0.0	0.0
17	1.28436(-05)	5.70741(-05)	3.58663(-07)	2.12010(-08)	0.0	0.0	0.0	0.0
18	8.08156(-06)	3.41720(-05)	8.77242(-08)	0.0	0.0	0.0	0.0	0.0
19	4.97775(-06)	2.01212(-05)	2.21281(-08)	0.0	0.0	0.0	0.0	0.0
20	3.12894(-06)	1.24255(-05)	9.32231(-09)	0.0	0.0	0.0	0.0	0.0
21	2.13282(-06)	8.48039(-06)	5.03276(-09)	0.0	0.0	0.0	0.0	0.0
22	1.30435(-06)	4.95494(-06)	2.21971(-09)	0.0	0.0	0.0	0.0	0.0
23	8.72693(-07)	3.17306(-06)	1.16389(-09)	0.0	0.0	0.0	0.0	0.0
24	6.37074(-07)	2.25392(-06)	7.39021(-10)	0.0	0.0	0.0	0.0	0.0
25	8.52354(-07)	2.90968(-06)	8.13569(-10)	0.0	0.0	0.0	0.0	0.0
26	6.86217(-07)	2.18016(-06)	4.66947(-10)	0.0	0.0	0.0	0.0	0.0
27	2.23629(-07)	6.73590(-07)	1.20914(-10)	0.0	0.0	0.0	0.0	0.0
28	1.64957(-07)	4.75475(-07)	7.60892(-11)	0.0	0.0	0.0	0.0	0.0
29	1.28810(-07)	3.58548(-07)	5.49370(-11)	0.0	0.0	0.0	0.0	0.0
30	1.36113(-07)	3.84979(-07)	5.60827(-11)	0.0	0.0	0.0	0.0	0.0
31	9.52865(-08)	2.61045(-07)	4.36998(-11)	0.0	0.0	0.0	0.0	0.0
32	1.31862(-07)	3.39114(-07)	7.15484(-11)	0.0	0.0	0.0	0.0	0.0
33	2.92976(-08)	6.58486(-08)	2.09421(-11)	0.0	0.0	0.0	0.0	0.0
34	8.99301(-09)	1.89910(-08)	6.44669(-12)	0.0	0.0	0.0	0.0	0.0
35	5.64994(-09)	1.42423(-08)	4.36115(-12)	0.0	0.0	0.0	0.0	0.0

Table XIII. (Cont'd.)

Energy Group	Activity (reactions/sec/source neutron)							
	A_f^{235U}	A_f^{239Pu}	A_f^{237Np}	A_f^{238U}	$A^{S}_{(n,p)}$	$A^{Mg}_{(n,p)}$	$A^{A\ell}_{(n,\alpha)}$	$A^{Zr}_{(n,2n')}$
36	3.29514(-09)	6.45217(-09)	2.64838(-12)	0.0	0.0	0.0	0.0	0.0
37	4.12487(-09)	8.33762(-09)	3.43056(-12)	0.0	0.0	0.0	0.0	0.0
38	1.98403(-09)	6.04535(-09)	1.71550(-12)	0.0	0.0	0.0	0.0	0.0
39	1.41475(-09)	4.02947(-09)	1.27498(-12)	0.0	0.0	0.0	0.0	0.0
40	2.31988(-09)	6.12578(-09)	2.09466(-12)	0.0	0.0	0.0	0.0	0.0
41	9.08416(-10)	2.63153(-09)	8.80967(-13)	0.0	0.0	0.0	0.0	0.0
42	3.42161(-10)	1.14270(-09)	3.68305(-13)	0.0	0.0	0.0	0.0	0.0
43	1.45846(-10)	7.67863(-10)	1.95260(-13)	0.0	0.0	0.0	0.0	0.0
44	8.02639(-11)	1.08080(-10)	5.28058(-14)	0.0	0.0	0.0	0.0	0.0
45	1.70505(-11)	8.49848(-11)	3.28156(-21)	0.0	0.0	0.0	0.0	0.0
46	4.49042(-12)	1.07183(-11)	5.44628(-21)	0.0	0.0	0.0	0.0	0.0
47	1.00371(-12)	2.39662(-12)	4.37573(-19)	0.0	0.0	0.0	0.0	0.0
48	5.77477(-13)	1.90564(-12)	1.28090(-17)	0.0	0.0	0.0	0.0	0.0
49	4.02925(-13)	1.43939(-12)	2.16912(-18)	0.0	0.0	0.0	0.0	0.0
50	1.01527(-15)	4.42310(-15)	2.54747(-20)	0.0	0.0	0.0	0.0	0.0
SUM	5.46232(-04)	2.51988(-03)	3.52634(-05)	2.02156(-05)	0.0	0.0	0.0	0.0

*Read as 4.27656×10^{-4}

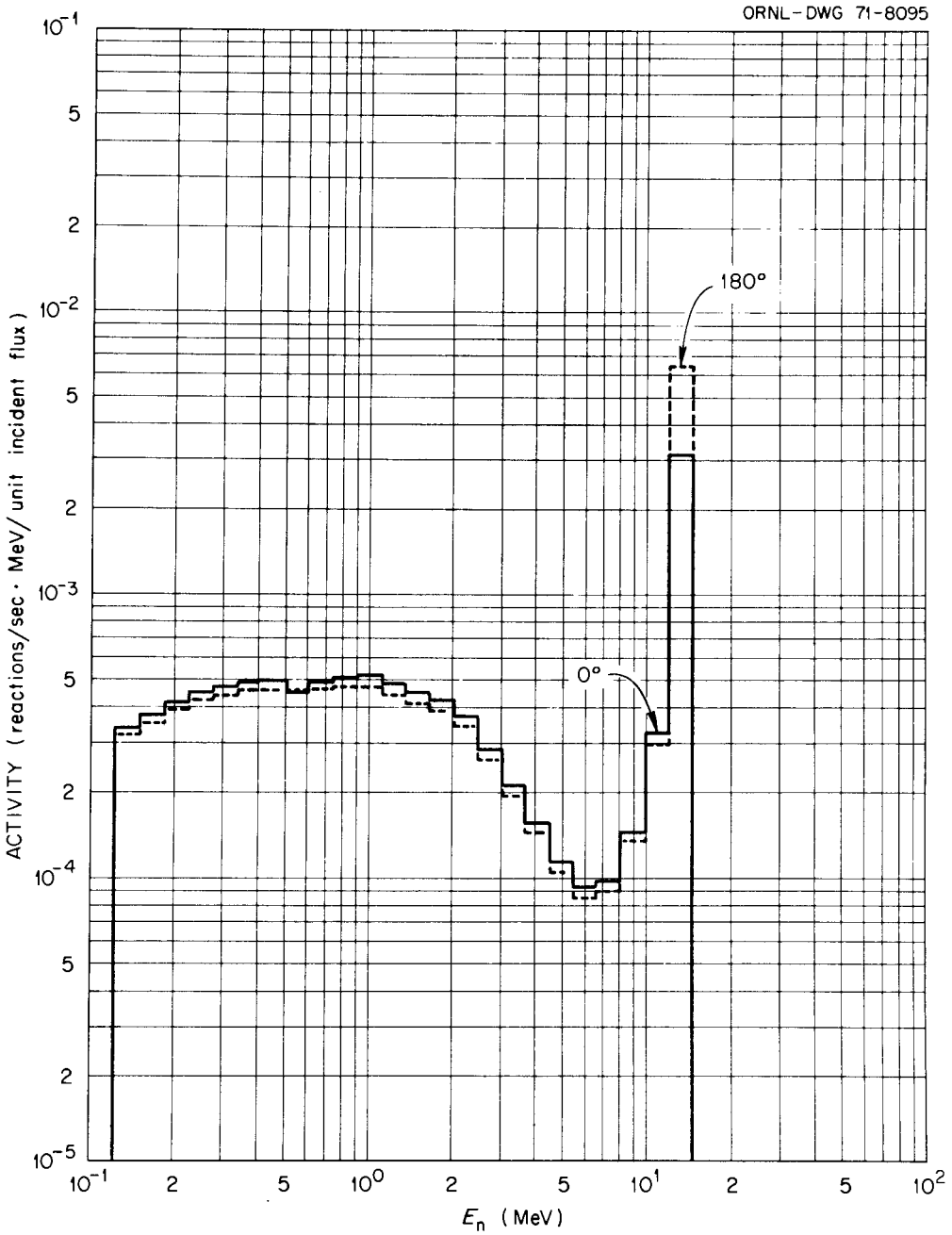

Figure 22. Fission Activity in ^{235}U Foil due to 13.57 MeV Beam

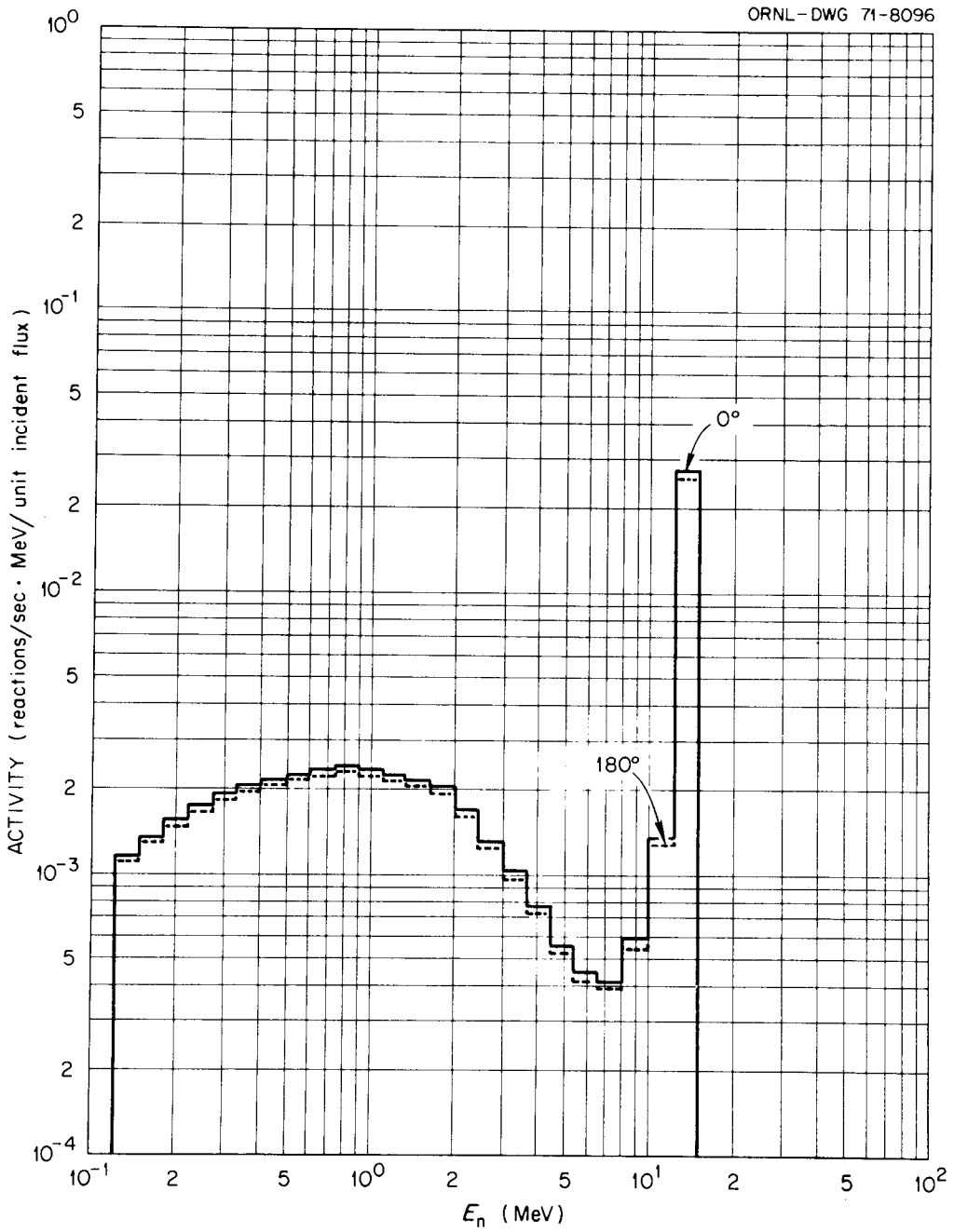

Figure 23. Fission Activity in ^{239}Pu Foil due to 13.57 MeV Beam

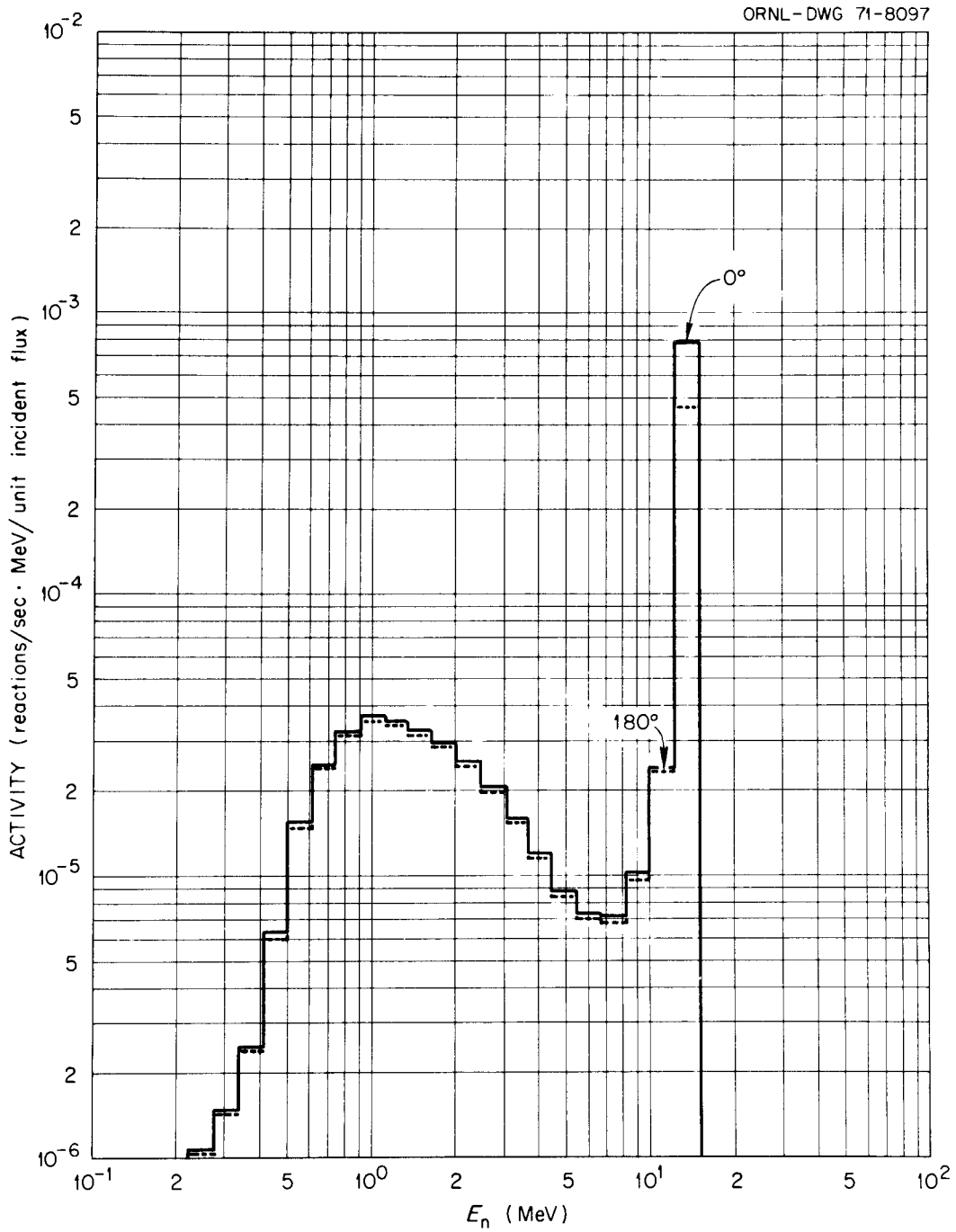

Figure 24. Fission Activity in ^{237}Np Foil due to 13.57 MeV Beam

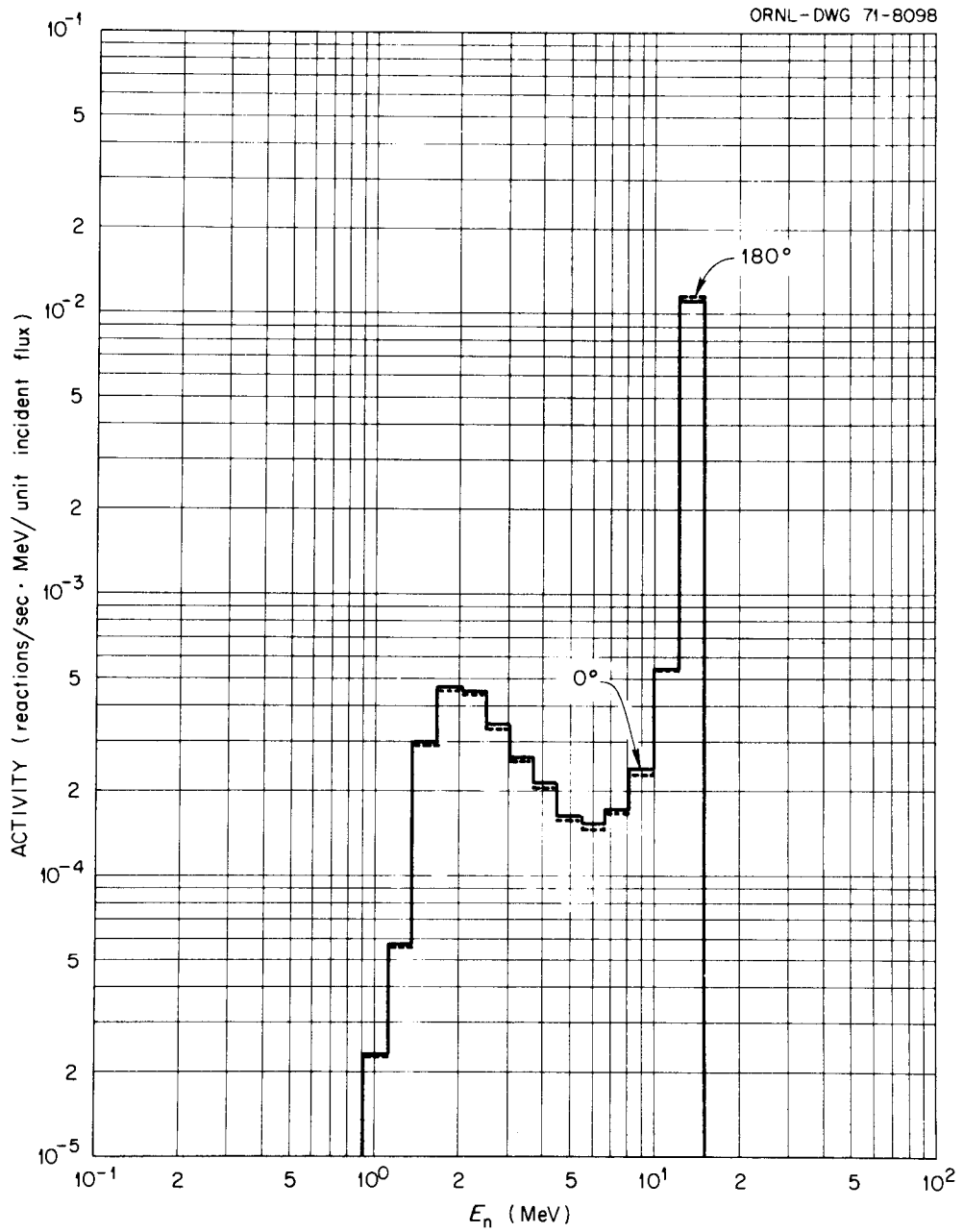

Figure 25. Fission Activity in ^{238}U Foil due to 13.57 MeV Beam

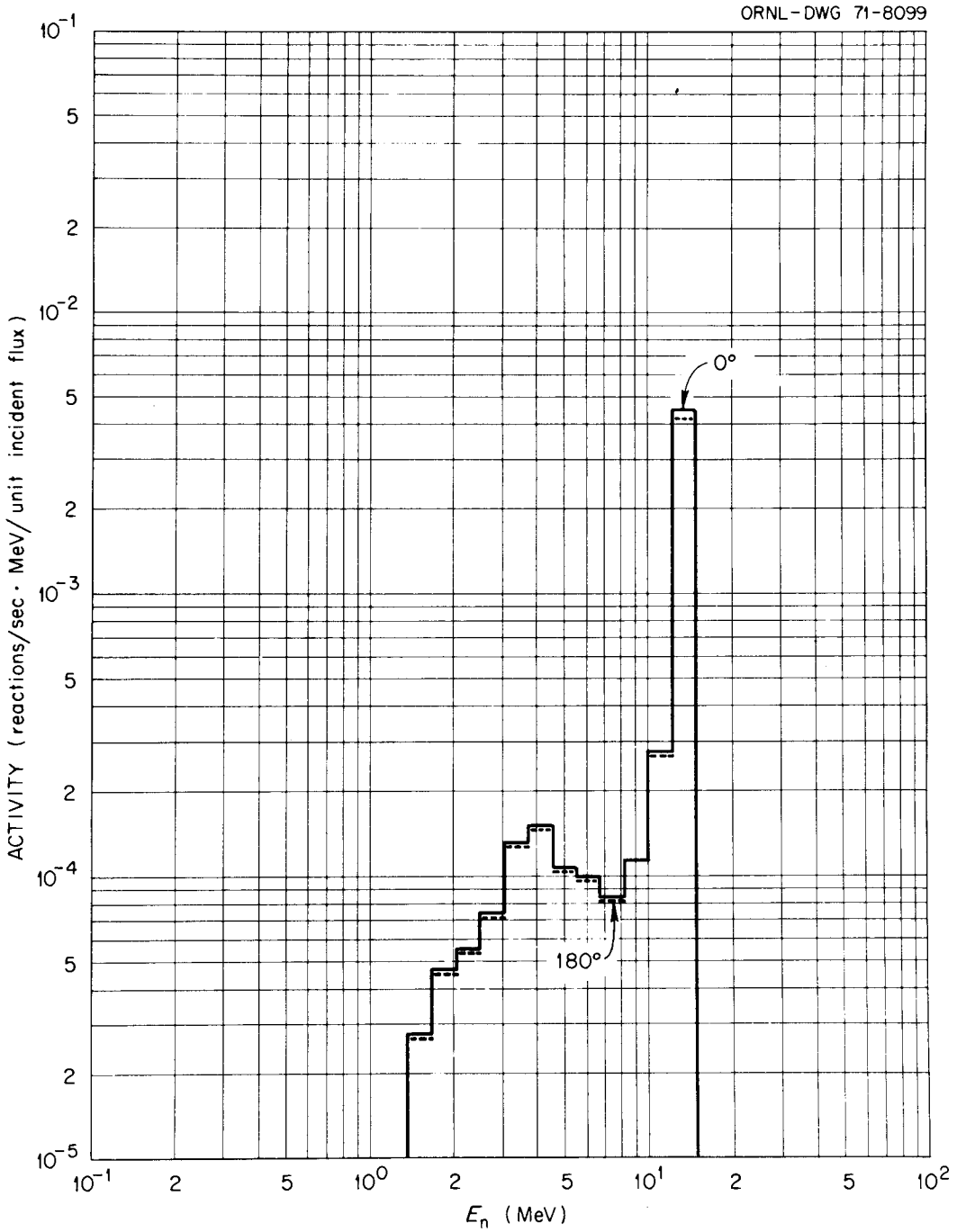

Figure 26. (n,p) Activity in S Foil due to 13.57 MeV Beam

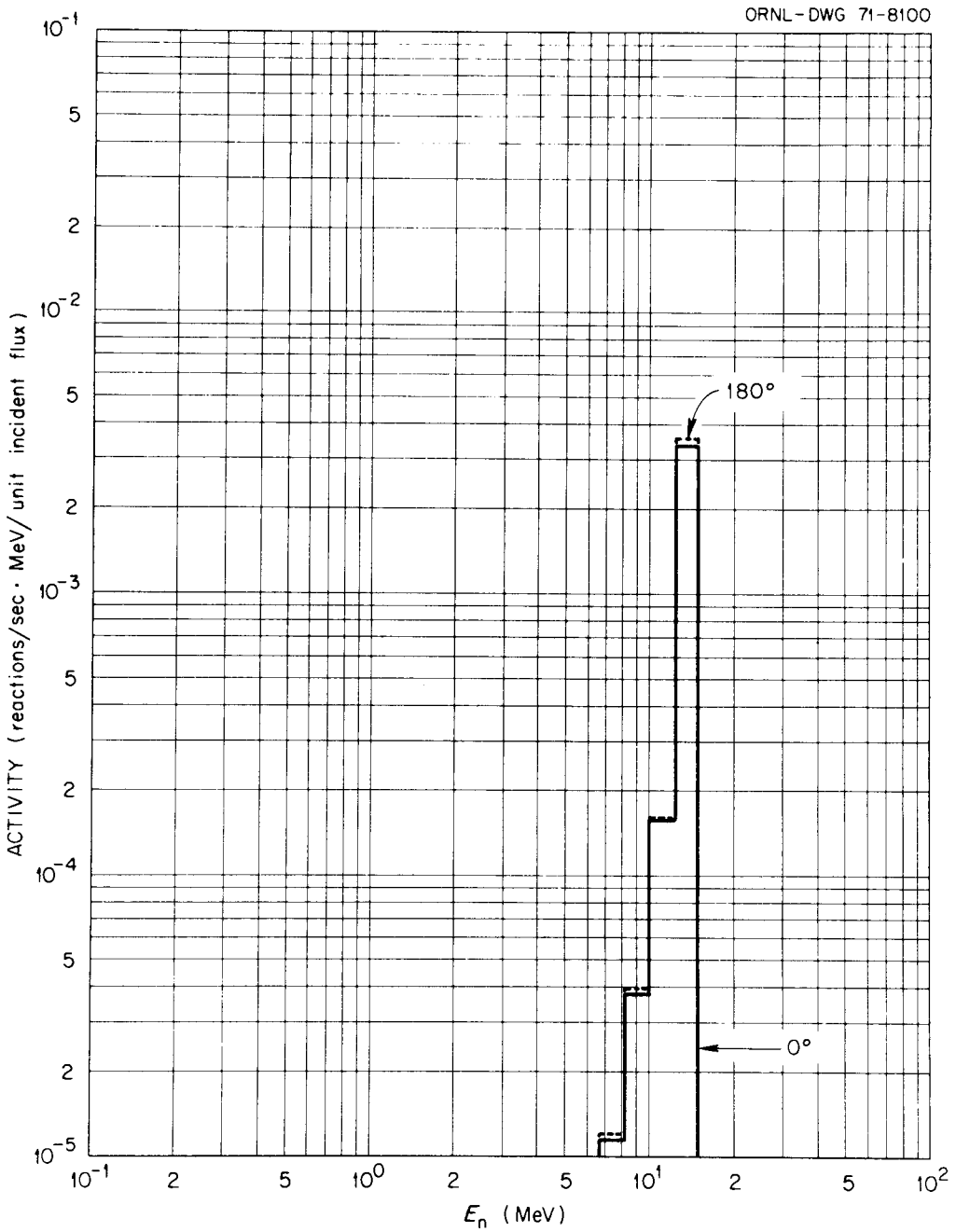

Figure 27. (n,p) Activity in Mg Foil due to 13.57 MeV Beam

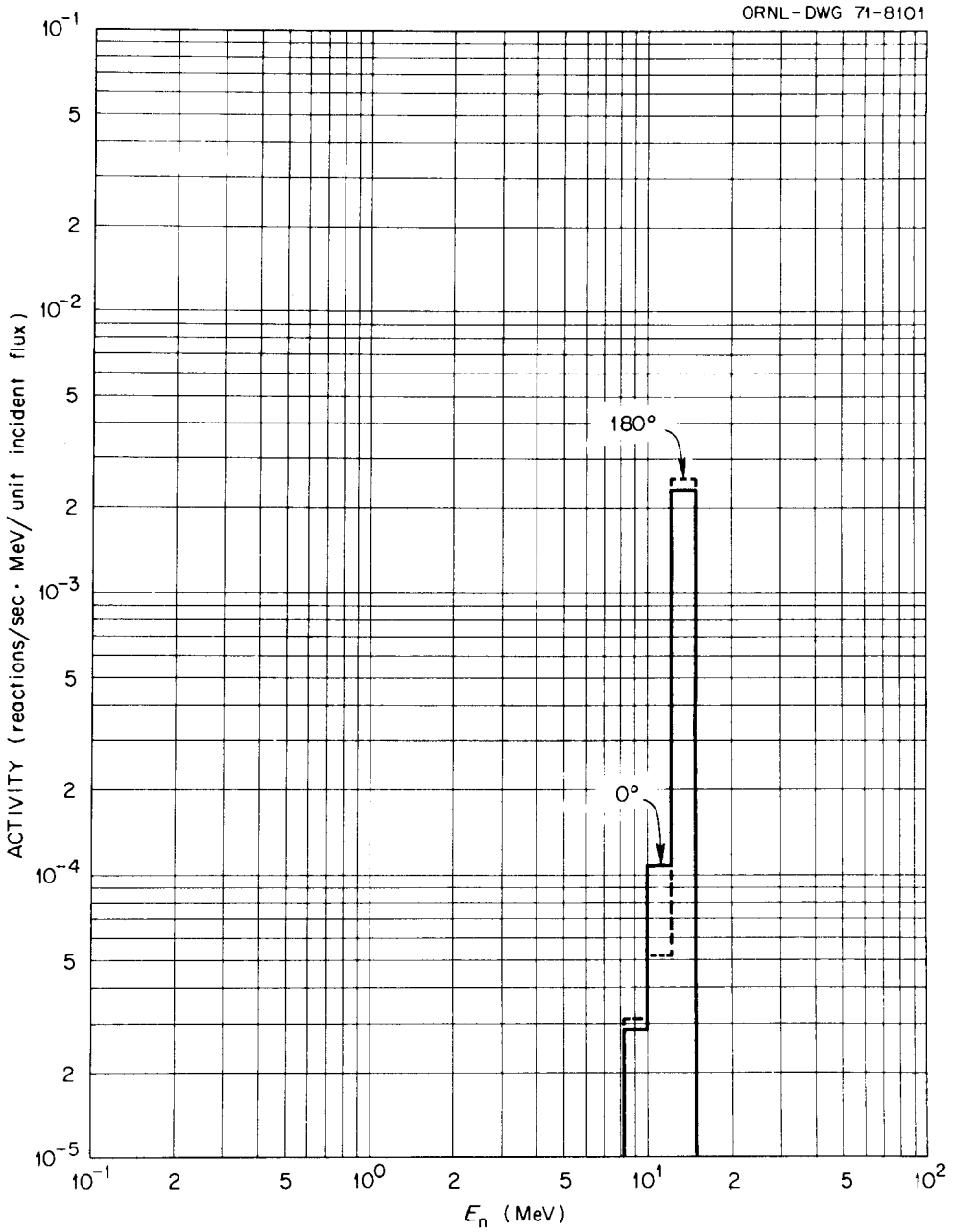

Figure 28. (n,α) Activity in Aℓ Foil due to 13.57 MeV Beam

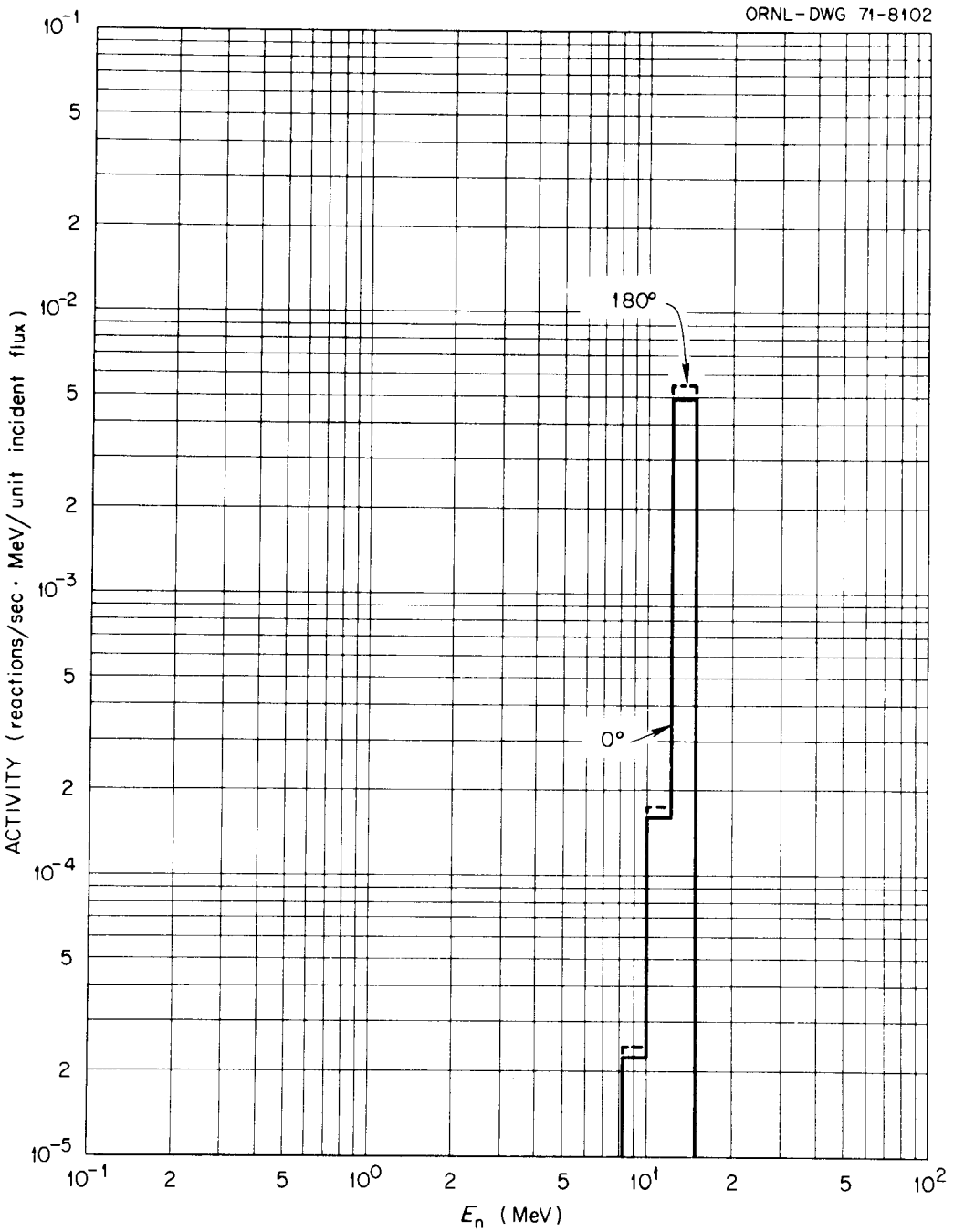

Figure 29. (n,2n') Activity in Zr Foil due to 13.57 MeV Beam

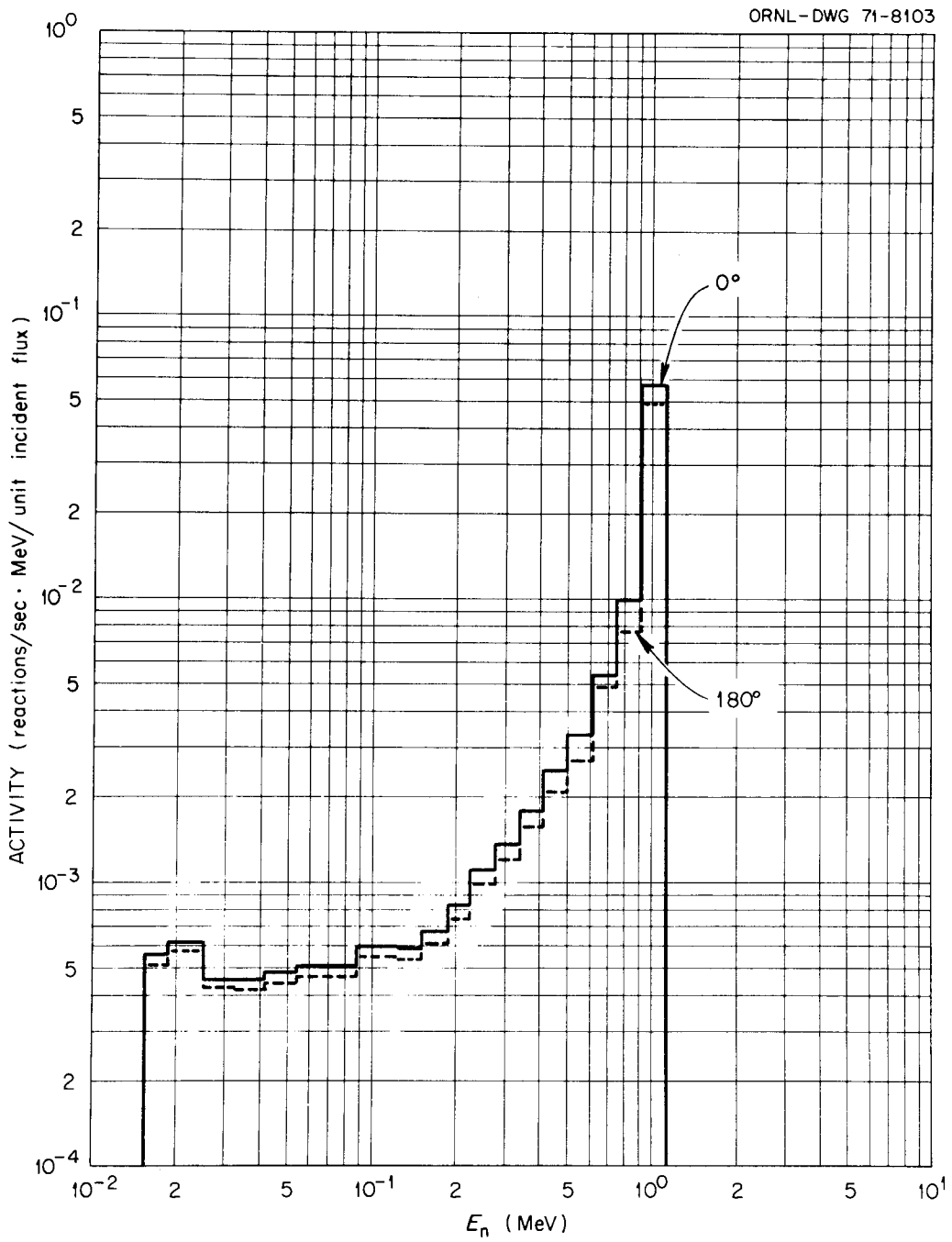

Figure 30. Fission Activity in ^{235}U Foil due to 1.01 MeV Beam

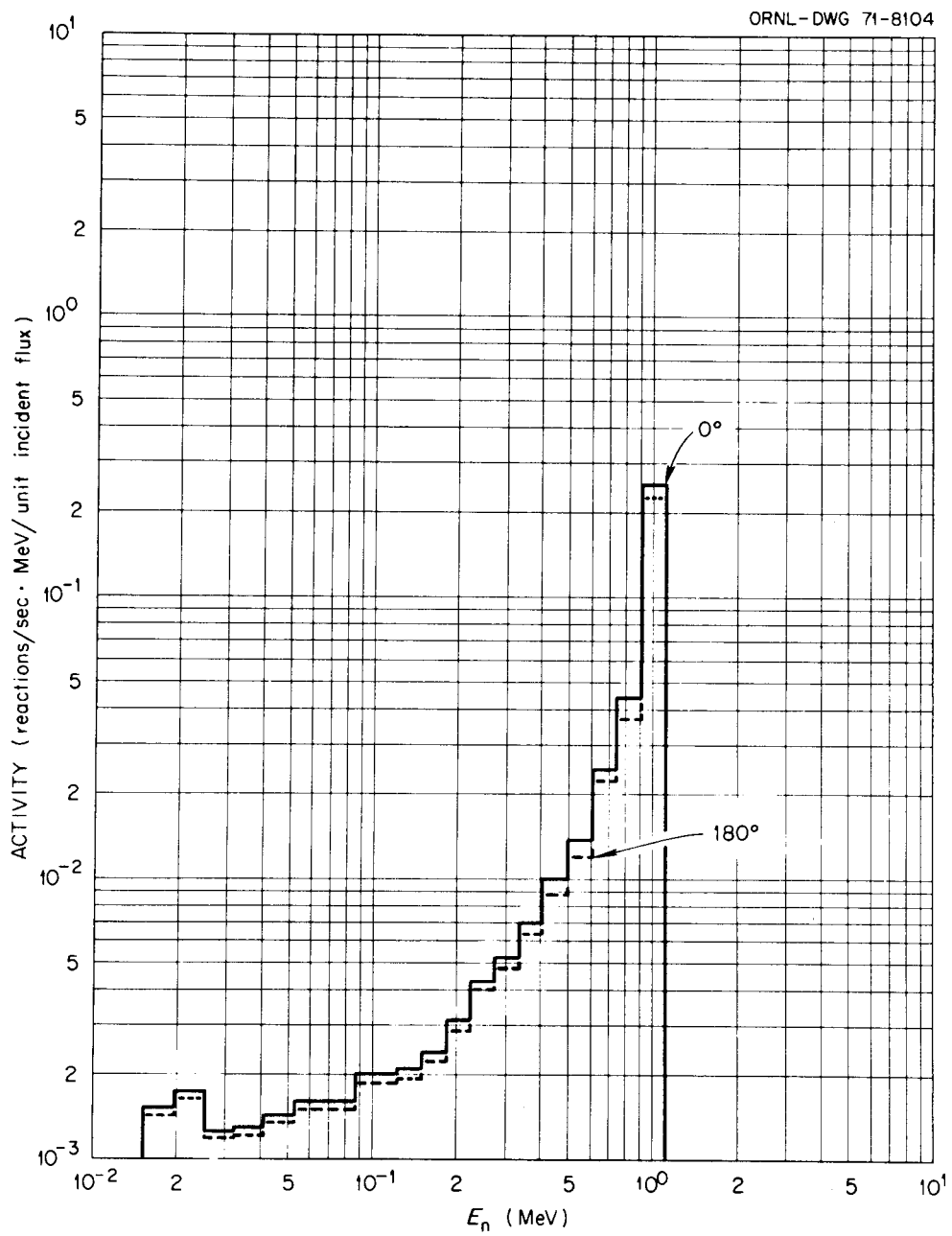

Figure 31. Fission Activity in ^{239}Pu Foil due to 1.01 MeV Beam

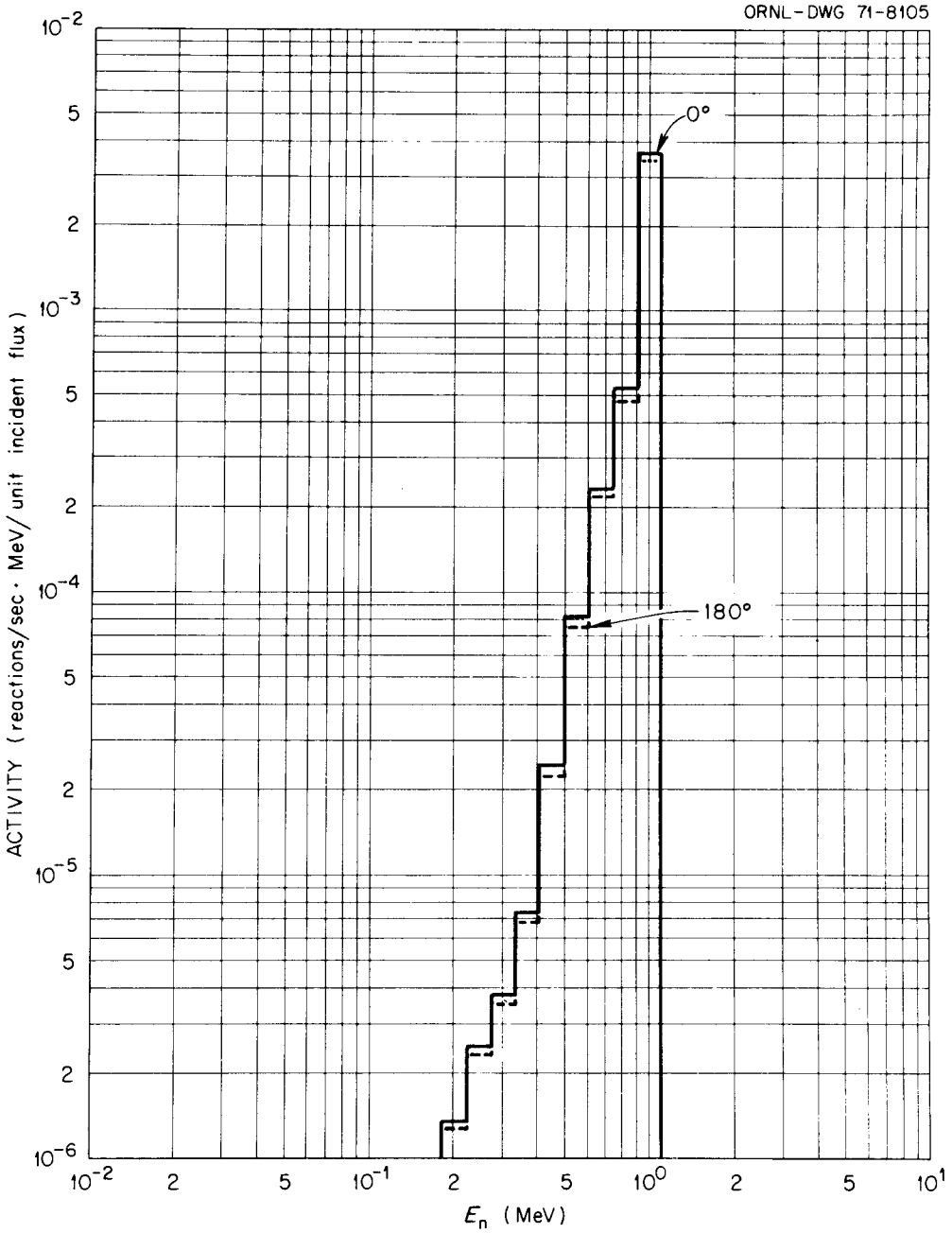

Figure 32. Fission Activity in ^{237}Np Foil due to 1.01 MeV Beam

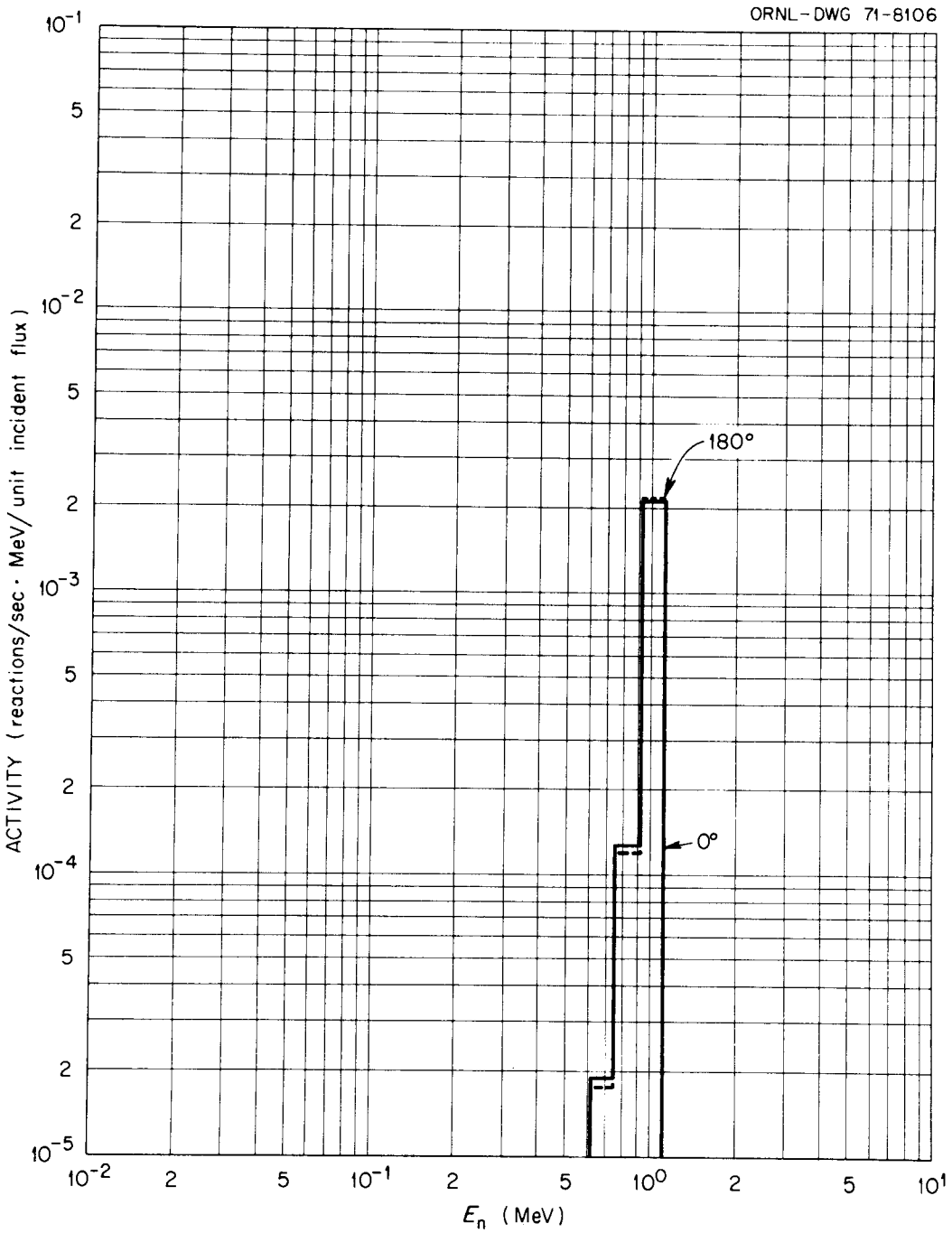

Figure 33. Fission Activity in ^{238}U Foil due to 1.0. MeV Beam

References

1. Glower, D. D., Experiment Reactor Analysis and Radiation Measurements, McGraw-Hill Book Company (1965), pp. 58-68.

2. Freestone, R. M., Jr., "Monte Carlo Calculations of the Neutron Flux within a $^{10}B_4C$ Shell," USAEC Report ORNL-TM-1816 (June 9, 1967).

3. Mynatt, F. R., "A User's Manual for DOT," USAEC Report K-1694 (to be published).

4. Joanou, G. D., and J. S. Dudels, "GAM-II - A B_3 Code for the Calculation of Fast Neutron Spectra and Associated Multigroup Constants," Gulf General Atomic Report GA-4265 (1963).

5. Stehn, J. R., M. D. Goldberg, B. A. Magurno, and R. Wiener-Chasman, "Neutron Cross Sections, z = 1-20," Vol. I, USAEC Report BNL-325 (May, 1964).

6. Goldberg, M. D., S. F. Mughabghab, B. A. Magurno, and V. M. May, "Neutron Cross Sections, z = 21-40," Vol. IIA, USAEC Report BNL-325 (February, 1966).

7. Goldberg, M. D., S. F. Mughabghab, S. N. Purohit, B. A. Magurno, and V. M. May, "Neutron Cross Sections, z = 41-60," Vol. IIB, USAEC Report BNL-325 (May, 1966).

8. Stehn, J. R., M. D. Goldberg, R. Wiener-Chasman, S. F. Mughabghab, V. A. Magurno, and V. M. May, "Neutron Cross Sections, z = 88-98," Vol. III, USAEC Report BNL-325 (February, 1965).

9. Westcott, C. H., "The Specification of Neutron Flux and Effective Cross Sections in Reactor Calculations," Atomic Energy of Canada Limited Report CRRP-662 (Aug. 15, 1956).

Internal Distribution

1-3. L. S. Abbott
4. R. G. Alsmiller, Jr.
5. A. A. Brooks
6-10. C. E. Clifford
11. C. E. Burgart
12-13. W. E. Ford, III
14. R. M. Freestone, Jr.
15. J. S. Gillen
16. T. A. Love
17. J. L. Lucius
18. F. C. Maienschein
19. B. F. Maskewitz
20. G. L. Morgan
21. F. R. Mynatt
22. R. W. Peelle
23. F. G. Perey
24. R. W. Roussin
25. D. Sundberg
26. G. E. Whitesides
27. L. R. Williams
28. E. R. Cohen (consultant)
29. H. Feshbach (consultant)
30. H. Goldstein (consultant)
31. C. R. Mehl (consultant)
32. H. T. Motz (consultant)
33-34. Central Research Library
35. ORNL Y-12 Technical Library
36-38. Laboratory Records
39. Laboratory Records, ORNL RC
40. ORNL Patent Office

External Distribution

41. P. B. Hemmig, Division of Reactor Development & Technology, U. S. Atomic Energy Commission, Washington, D. C.
42. W. H. Hannum, Division of Reactor Development & Technology, U. S. Atomic Energy Commission, Washington, D. C.
43. K. O. Laughon, AEC Site Representative, ORNL
44-45. Director, Defense Nuclear Agency; Attn: RARP, RAEV; Washington, D. C.
46. Director, Ballistic Research Laboratories; Attn: Radiation Division, Dr. Kazi; Aberdeen Proving Ground, Md. 21005
47-48. Commanding Officer, Harry Diamond Laboratories; Attn: DORF for D. McGarry and NEWPO for F. Wimenitz; Washington, D. C. 20438
49. Los Alamos Scientific Laboratory, P. O. Box 1663; Attn: W. Biggers; Los Alamos, New Mexico 87544
50. Sandia Laboratories, P. O. Box 5800; Attn: Organization 5200 for V. V. Walker; Albuquerque, New Mexico 87155
51-52. Division of Technical Information Extension (DTIE)
53. Laboratory and University Division (ORO)
54-63. J. H. McNeilly, Army Nuclear Defense Laboratory, Edgewood Arsenal, Maryland